Characterization of Tumor Infiltrating Lymphocytes in Pediatric Cancers and the Development of Novel Immunotherapies

by Clifford Grant Morgan

B.S. in Microbiology, May 2009, Michigan State University

A Dissertation submitted to

The Faculty of
Columbian College of Arts and Sciences
of the George Washington University
in partial fulfillment of the requirements
for the degree of Doctor of Philosophy

August 31, 2015

Dissertation directed by

Anthony Sandler
Professor of Surgery

The Columbian College of Arts and Sciences of The George Washington University certifies that Clifford Grant Morgan has passed the Final Examination for the degree of Doctor of Philosophy as of May 13th, 2015. This is the final and approved form of the dissertation.

Characterization of Tumor Infiltrating Lymphocytes in Pediatric Cancers and the Development of Novel Immunotherapies

Clifford Grant Morgan

Dissertation Research Committee:

Anthony Sandler, Professor of Surgery, Dissertation Director

David Leitenberg, Associate Professor of Pediatrics and Microbiology, Immunology, and Tropical Medicine, Committee Member

Conrad Russell Y. Cruz, Assistant Professor of Pediatrics, Committee Member

Dedication

To my grandfather, Monte H. Morgan, who would never let me quit,

To my wife, Emily Hathaway, who would have let me quit,

And to Nicholas Kenyon, who frequently encouraged me to quit.

Acknowledgements

I would foremost like to thank Dr. Sasa Radoja, who brought me into this journey, personally teaching me every technique he could, and who delved deep with me into new worlds of immunology to explore, with a more patient and comforting attitude than a young graduate student could ever hope for; and Dr. Anthony Sandler, who allowed me to finish this journey, through his ever optimistic encouragement and faith in my ability to succeed in the face of adversity.

I would like to thank all the members of my committee, Dr. David Leitenberg, Dr. C. Russell Y. Cruz, Dr. Kanneboyina Nagaraju, and Dr. Stanislav Vukmanovic, for their guidance, knowledge, and direction. I would also like to thank Dr. Jennifer Ma, Dr. Lina Chakrabarti, and Dr. Priya Srinivasan, for all of their help along the way.

To my family and friends who have supported me from the beginning, and the new ones I have made along the way, you are the ones I share this achievement with.

To all, thank you.

Abstract of Dissertation

Characterization of Tumor Infiltrating Lymphocytes in Pediatric Cancers and the Development of Novel Immunotherapies

Cytotoxic T lymphocytes (CTLs) are the primary component of the adaptive immune system responsible for clearance of virally infected and tumorigenic cells. In cancer however, this tumor-specific immune response is often impaired. The impairment is multifactorial; some cancers utilize mechanisms to evade the immune system through downregulation of Major Histocompatability Complex I or lack of tumor-specific antigens, while others use methods to actively inhibit local function of tumor-induced immune responses via production of immunosuppressive cytokines, Fas-mediated apoptosis, or recruitment of T regulatory cells (Tregs). These Tregs function to further immune regulate and inhibit CTLs, using methods such as suppressive cytokines, and cytotoxic killing. All of these components lead to an "on/off" phenotype, where CTL effector function is shut down within the Tumor Immunosuppressive Microenvironment (TIM), but can be recovered quickly upon removal of CTLs from the TIM. The transient impairment of Tumor Infiltrating Lymphocytes (TIL) has been described in mouse models, but is poorly characterized in humans.

In this dissertation, we examined infiltration of CTLs across several types of human pediatric cancers, taken from patients who had not undergone prior treatment. We found tumors associated with favorable prognoses, including Wilms' Tumor and Neuroblastoma (NB), had higher levels of CTL infiltration than those with less favorable prognoses, e.g. Ependymoma, which possessed no observable infiltration. Additionally,

we demonstrate the TIL "on/off" phenotype in a case of Pilocytic Astrocytoma, demonstrating significant recovery of TIL effector function.

We proposed that the poor infiltration and impaired effector function in these pediatric tumors was a direct result of the TIM, and sought to improve this immune response by developing an attenuated live cell vaccine, utilizing a murine NB model, Neuro2a, to create a NB line with knock down (KD) of Inhibitor of Differentiation 2 (Id2), which impaired their ability to form tumors *in vivo*. In prophylactic and therapeutic models, introduction of Id2-KD cells in combination with the immune checkpoint blockade inhibitor anti-CTLA-4, induced an increase in CTLs capable of homing to the tumor, that were also able to employ effector function within the TIM, resulting in clearance of wild-type Neuro2a tumors.

A separate emerging immunotherapeutic approach is to express a Chimeric Antigen Receptor (CAR) on CTLs that allows them to be activated to kill cells expressing the CAR-specific protein, bypassing MHC presentation. Using a murine Rhabdomyosarcoma model, we demonstrate that tumor infiltrating Tregs express lytic molecules, encouraging us to develop a method of successfully transducing Tregs with a CAR (DC101), rather than CTLs, thereby exploiting characteristics of the Treg in the TIM, specifically their cytotoxic capability and their unique recruitment and ability to thrive in that environment. We demonstrate *in vitro* CAR-mediated redirection of lytic effector function using DC101-expressing CTLs against tumor cell lines, though attempting to increase Treg cytotoxicity *in vitro* via known inducers of CTL cytotoxicity (IFNα or IL-12) or known inducers of Tregs within the TIM (TGF-β1) showed no increase in Treg cytotoxicity.

Table of Contents

List of Figures

List of Tables

List of Abbreviations

°C	Degrees Celsius
Ab	Antibody
ACT	Adoptive Cell Therapy
AD	Anchorage Dependent
AI	Anchorage Independent
Akt	Protein Kinase B
AP-1	Activator Protein 1
APC	Antigen Presenting Cell
APC	Allophycocyanin
BBB	Blood Brain Barrier
Bcl2	B-cell lymphoma 2
Ca^{2+}	Calcium
CAR	Chimeric Antigen Receptor
CCL	C-C motif chemokine
CD	Cluster of Differentiation
CFSE	carboxyfluorescein succinimidyl ester
cm	centimeter
CNMC	Children's National Medical Center
Cr	Chromium
CTL	Cytotoxic T Lymphocyte
CTLA-4	Cytotoxic T-Lymphocyte-Associated protein 4

CREB	cyclic adenosine monophosphate Response Element-Binding protein
Cy	Cyanine
DAG	Diacyl Glycerol
EGF	Epidermal Growth Factor
EGFRvIII	Epidermal Growth Factor Receptor variant III
EMT	Epithelial to Mesenchymal Transition
E:T	Effector to Target Ratio
Erk	Extracellular regulator kinase
FBS	Fetal Bovine Serum
FcR	Fc (fragment crystallizable) Receptor
FGF	Fibroblast Growth Factor
FITC	Fluorescein Isothyocyanate
Foxp3	Forkhead box 3
g	gravity
HLA	Human Leukocyte Antigen
hrs	hours
Id	Inhibitor of Differentiation
ITAM	Immunoreceptor Tyrosine-based Activation Motif
IFNα	Interferon α
IL	Interleukin
i.p.	intra peritoneal
IP_3	Inositol 1, 4, 5-triphosphate

i.v.	intra venous
KD	Knock Down
Lat	Linker of Activated T cells
Lck	Lymphocyte-specific protein tyrosine kinase
LFA-1	Lymphocyte Function-associated Antigen 1
m	minute
MAP2	Microtubule-associated protein 2
mCi	millicurie
MHC	Major Histocompatibility Complex
min	minute
MIP-1α	Macrophage Inflammatory Protein
mL	milliliter
mm	millimeter
Mθ	Macrophage
MTOC	Microtubule Organizing Center
µg	microgram
µL	microliter
N2a	Neuro2a cells
Na	Sodium
NB	Neuroblastoma
NFAT	Nuclear Factor of Activated T cells
NK-κB	Nuclear Factor κ B
NK	Natural Killer

OMS	Opsoclonus Myoclonus Syndrome
PD-1	Programmed cell Death protein 1
PDGFRβ	beta-type Platelet Derived Growth Factor Receptor
PD-L1	Programmed Death Ligand 1
PE	R-phycoerythrin
PerCP	Peridinin Chlorophyll
PI3K	Phosphatidylinositol 3-Kinase
PIP_2	Phosphatidylinositol 4, 5-bisphosphate
PKC	Protein Kinase C
PLC-γ	Phospholipase C γ
PMA	Phorbol 12-Myristate 13-Acetate
RANTES	Regulated upon Activation, Normal T-cell Expressed, and Secreted
RAP	Reversible Adaptive Plasticity
Rb	Retinoblastoma protein
s.c.	subcutaneous
SCID	Severe Combined Immunodeficiency
scFv	Single Chain Variable Fragmemt
SDS-PAGE	sodium dodecyl sulfate polyacrylamide gel electrophoresis
shRNA	short hairpin Ribonucleic Acid
Slp-76	Synaptotagmin-like proteins 76
SMAD	Similar to Mothers Against Decapentaplegic
TAA	Tumor Associated Antigen
TAP	Transporter associated with Antigen Processing

TCR	T Cell Receptor
TDL	Tumor Draining Lymph node
TGF-β	Transforming Growth Factor β1
TIL	Tumor Infiltrating Lymphocyte
TIM	Tumor Immunosuppressive Microenvironment
Tregs	T Regulatory Cells
TSA	Tumor Specific Antigen
VEGFR-2	Vascular Endothelial Growth Factor Receptor 2
v/v	volume to volume
WT	Wild Type
WT1	Wilms' Tumor Protein
Zap-70	Zeta-chain-associated protein kinase 70

CHAPTER 1: BACKGROUND

1.1 Cytotoxic T Cell Function

Cytotoxic T lymphocytes (CTLs) are the primary component of the adaptive immune system responsible for clearance of virally infected and tumorigenic cells. CTL priming begins with the presentation of antigens to naïve CD8+ T cells in primary lymphoid organs via antigen presenting cells (APCs). This activation involves three main steps, beginning with recognition of antigen presented via Major Histocompatibility Complex (MHC) I on the APCs, directly to the CD3/T cell receptor complex (TCR) on the T cell (1-3). The second signal of activation comes from the B7 ligand on APCs stimulating CD28 on the T cell (4-6). Finally, the third signal to induce potent T cell activation is cytokine mediated, primarily dependent upon Interleukin (IL)-2 for proliferation and production of cytotoxic granules (7, 8).

Upon activation of the TCR, the intracellular ζ chain of the CD3 complex, a homodimer, becomes phosphorylated on its immunoreceptor tyrosine-based activation motif (ITAM) regions by Lck, which recruits Zap-70 (9-11) (Figure 1). Zap-70 phosphorylates LAT, which recruits Slp-76 to phosphorylate it as well (12). Slp-76 is able to then recruit Phospholipase C-γ (PLC-γ), which cleaves PIP_2 into IP_3 and DAG leading to increases in intracellular Ca^{2+} and recruitment of PKCθ (13). PKCθ activates transcription factors such as NFAT, CREB, NF-κB and AP-1, essential for CTL differentiation (14). These primed CTLs are then released into circulation and peripheral tissues, where they engage their specific target for destruction.

CTL effector function can be executed in several ways, the primary methods being cytokine release, or cytotoxicity. The latter method can be further divided into Fas-mediated apoptosis, or cytotoxic granule exocytosis. Fas-mediated apoptosis occurs when the Fas-Ligand (FasL) crosslinks to Fas on the surface of target cells (15, 16). Alternatively, granule mediated exocytosis occurs by the targeted release of granules containing Perforin, a pore-forming complex, and several Granzymes, serine proteases, which cleave pro-caspases to initiate apoptosis, primarily via Granzyme B (15-17).

Granule mediated exocytosis is triggered by TCR recognition of their target via MHC I presentation in the periphery, CTL activation, again directed by Lck, Zap-70, LAT, and Slp-76, begins with actin reorganization, and relocation of the microtubule organizing center (MTOC) (18, 19) (Figure 2B). The MTOC polarizes towards the immunological synapse, inducing the traversing of lytic granules towards the MTOC, the regulation of which is thought to be controlled by an accumulation of DAG, which recruits the motor protein Dynein (20) (Figure 2C). These granules are then moved towards the immune synapse for release, a process mediated by PKCδ (21, 22) (Figure 2D). Perforin from lytic granules creates pores in the membrane of the target cell, allowing for Granzyme entry into the cell, inducing caspase-mediated apoptosis (23-25).

Figure 1. Schematic representation of CTL activation. Professional antigen presenting cells, including dendritic cells, macrophages, and B cells, introduce peptides to naïve CTLs through MHC I, received through the CD3 complex and CD8 coreceptor. This signaling leads to the recruitment of Lck, which phosphorylates the immunoreceptor tyrosine-based activation motif (ITAM) on the CD3ζ chains, resulting in the recruitment of Zap-70. This in turn phosphorylates LAT, which recruits in Slp-76 to further phosphorylate LAT, resulting in the recruitment of PLC-γ, which cleaves PIP_2 into IP_3 and DAG. IP_3 induces an increase in the levels of intracellular calcium, while DAG recruits PKCθ, to activate transcription factors for T cell priming, such as NFAT, CREB, NF-κB, and AP-1.

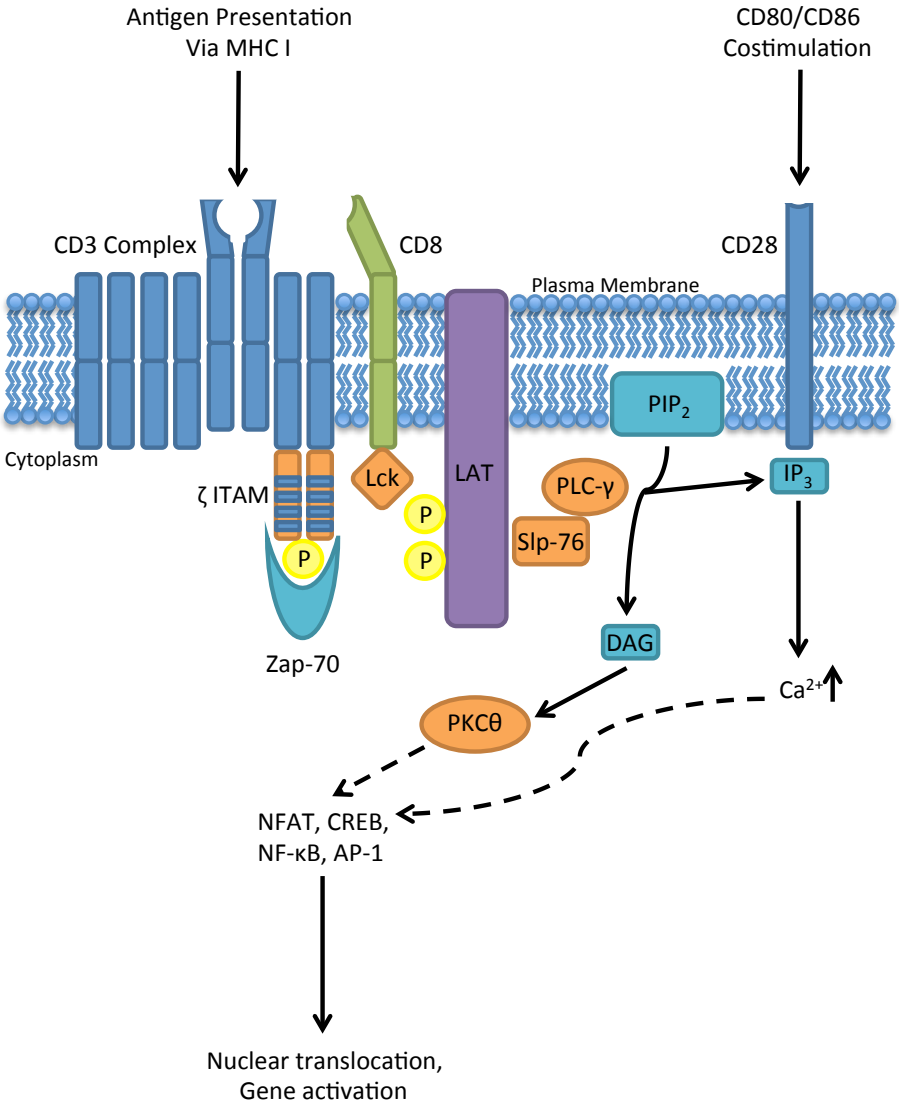
Antigen Presentation
Via MHC I
CD80/CD86
Costimulation
CD3 Complex
CD8
CD28
Plasma Membrane
PIP2
Cytoplasm
ζ ITAM
Lck
LAT
PLC-γ
IP3
P
P
P
Slp-76
DAG
Zap-70
Ca2+
PKCθ
NFAT, CREB,
NF-κB, AP-1
Nuclear translocation,
Gene activation

Figure 2. Schematic representation of Granule Mediated Cytotoxicity. After antigen presentation though MHC I, naïve CTLs become primed, and undergo a stage of proliferation and induction of lytic granules (A). Upon recognition of their target, the CTL cytoskeleton reorganizes, moving the microtubule organizing center (MTOC) towards the newly formed immune synapse (B). Lytic granules then begin to travel towards the MTOC, and fuse with the plasma membrane (C), where they release their contents towards the target cell, using Perforin to create pores in the target cell, allowing entry of granzymes to activate apoptosis in the target cell (D). Figure reproduced from (17).

A

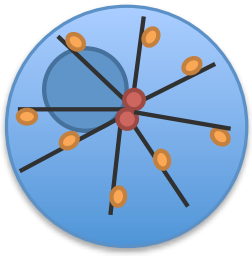

B

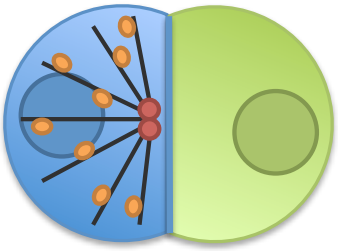

C

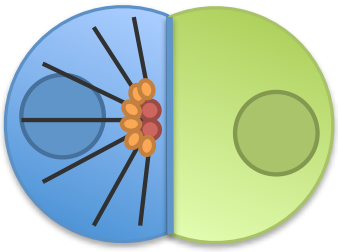

D

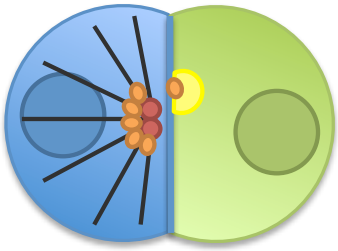

1.2 Tumor Immunosuppressive Microenvironment

The ability of the immune system to specifically target and clear cells within the host is often impaired in the context of cancer. Immune suppressive or evasion is mediated by several mechanisms employed by tumors, described in detail below. However research has demonstrated that within mouse models, this tumor immunosuppressive microenvironment is transient, and can be overcome *ex vivo*, leading to an "On/Off" phenotype for tumor infiltrating lymphocytes (26, 27). The details of these mechanisms are presented below.

1.2.1 Tumor Infiltrating Lymphocytes

CTLs are the primary cell type responsible for the clearance of cancer, as they are able to home to the tumor site in a host, and specifically kill cancerous cells. The specificity of these tumor infiltrating lymphocytes (TIL) has led them to become a primary target in cancer immunotherapy (28, 29). One well established method, adoptive cell therapy (ACT), begins with the removal of TIL from patients, and the subsequent *ex vivo* culturing of those TIL (29, 30). The goal of this culturing is to expand the TIL to a much greater number than a naturally developed immune response would generate. The primary component responsible for this expansion is IL-2 (31, 32), which induces proliferation in CTLs, however other modifications to the TIL, such as the use of additional cytokines (33, 34), or transduction with chimeric antigen receptors, discussed here later, can be used to better regulate the expansion and effector function of these TIL. This expansion phase can take weeks to months, depending upon the rate at which the patient's cells proliferate *ex vivo* (28, 30). When enough CTLs have been generated, they

are reintroduced to the patient in higher than natural numbers, where they are able to home to the sites of tumors, and destroy them (28, 30, 35, 36).

Clinical trials of ACT have proven to be an effective method of tumor clearance across several types of solid and liquid tumors, including melanoma, sarcoma, adenocarcinoma, and leukemia (28, 29, 37, 38). Unfortunately, not all cancers induce the development of a potent, specific immune response. Often, CTLs are either impaired in their ability to home to the tumor site, or inhibited in their function upon arrival to the tumor. These mechanisms through which tumors evade or suppress CTL effector function are discussed below.

1.2.2 Immune Evasion and Suppression Mechanisms

Tumors possess several mechanisms to avoid immune destruction, and most are employed across a broad range of cancers. One of these mechanisms is a down regulation of MHC I (39, 40). MHC I is the major antigen presenting protein, which is recognized by CD3/CD8 on CTLs, and is required to activate CTL effector function. Methods of this downregulation include mutations in the β-2 microglobulin gene, loss of MHC alleles, or decreased expression of MHC (39) (Figure 3). While changes in MHC expression levels result in tumor susceptibility to killing by NK cells, tumors employ many additional ways to evade destruction.

There are some cancers that have Tumor Associated Antigens (TAAs), which are proteins expressed in higher levels in cancer, compared to that of the normal cell state (39, 41). However, these TAAs are often found in other parts of the body and carry out

different functions. As a result, the immune system recognizes them as self-antigens, and fails to mount an appropriate immune response.

Tumor cells can also express negative costimulatory molecules, such as PD-L1s, which interact with PD-1 on T cells to inhibit activation (39). Tumor cells can also stimulate the cytotoxic T-lymphocyte-associated protein 4 (CTLA-4) receptor on CTLs, which when bound by B7, the same signal that is transduced through CD28 upon T cell activation, an inhibitory signal is transduced that impairs the activation/maturation of the CTLs (39, 42).

It has also been shown that within the TIM, TIL are inhibited in their granule release despite TCR activation (26, 27). Activation of CTLs results in production of Protocadherin-18, leading to the failure to activate signal transduction proteins downstream of the TCR, such as PLCγ-1, LAT, and ZAP70, as well as LFA-1. This is because the protein that activates LFA-1, $p56^{lck}$, is rapidly dephosphorylated by Protocadherin-18 upon contact with tumor cells, resulting in a failure to signal for cytoskeletal rearrangement and subsequent granule release (26, 43).

Additionally, cells within the TIM can secrete immunosuppressive cytokines, primarily Transforming Growth Factor-β (TGF-β) and IL-10 (44, 45). TGF-β acts to inhibit activation, proliferation, and differentiation in T cells. The mechanism for TGF-β works through receptor mediated phosphorylation of Smad proteins, which leads to the decreased expression of c-myc, and at the same time increases the production of cyclin-dependent kinase inhibitors, like p15 and p21 (46). IL-10 is known to impair dendritic cell function, inhibit antigen peptide transporters TAP1 and TAP2, and effector T cell functions (39). Interestingly, these two cytokines, TGF-β and IL-10, also are the primary

driving force behind the T Regulatory cell (Treg) differentiation pathway, and act to convert classical $CD4^+$ T helper cells into $CD4^+$ $CD25^+$ $FoxP3^+$ Tregs (39, 47). Tumors can also recruit Tregs via the chemokine CCL22, which aid in further suppressing the specific lysis of tumor cells by CTLs (48, 49). Taken together, these conditions allow Tregs to function and thrive within the TIM, unlike most other TIL subsets (50).

Figure 3. Schematic representation of tumor mediated immune-evasive and immunosuppressive mechanisms. Tumor cells can secrete several cytokines themselves which lead to the inhibition of an effector immune response, including TGF-β, IL-10, Galectin-1, Gangliosides, PGE_2 and Kynurenines. They can also secrete chemokines like CCL22, which serves to recruit Tregs to the TIM, in turn further secreting TGF-β and IL-10. In addition to shutting down a tumor directed effector response, TGF-β and IL-10 induce conversion of T helper cells into Tregs. Tregs can also travel into tumor draining lymph nodes where they specifically kill dendritic cells, thereby preventing tumor antigen presentation to naive CTLs. Tumors can also employ contact mediated forms of suppression, through a catalog of molecules including B7 molecules, which bind to negative costimulatory receptors on the surface of CTLs, such as CTLA-4 and PD-1. Tumor cells can also induce CTL apoptosis via the ligands TRAIL, RCAS1, and Fas. Additional methods of immune evasion employed by tumor cells include mutations in the genes for LMPs and TAP, which respectively play a role in antigen processing and shuttling antigens into the endoplasmic reticulum, for assembly into MHC I molecules. Mutations can also occur in the genes for MHC I itself, or the β_2 microglobulin, required for proper MHC I assembly and membrane translocation. Figure reproduced and modified from (39).

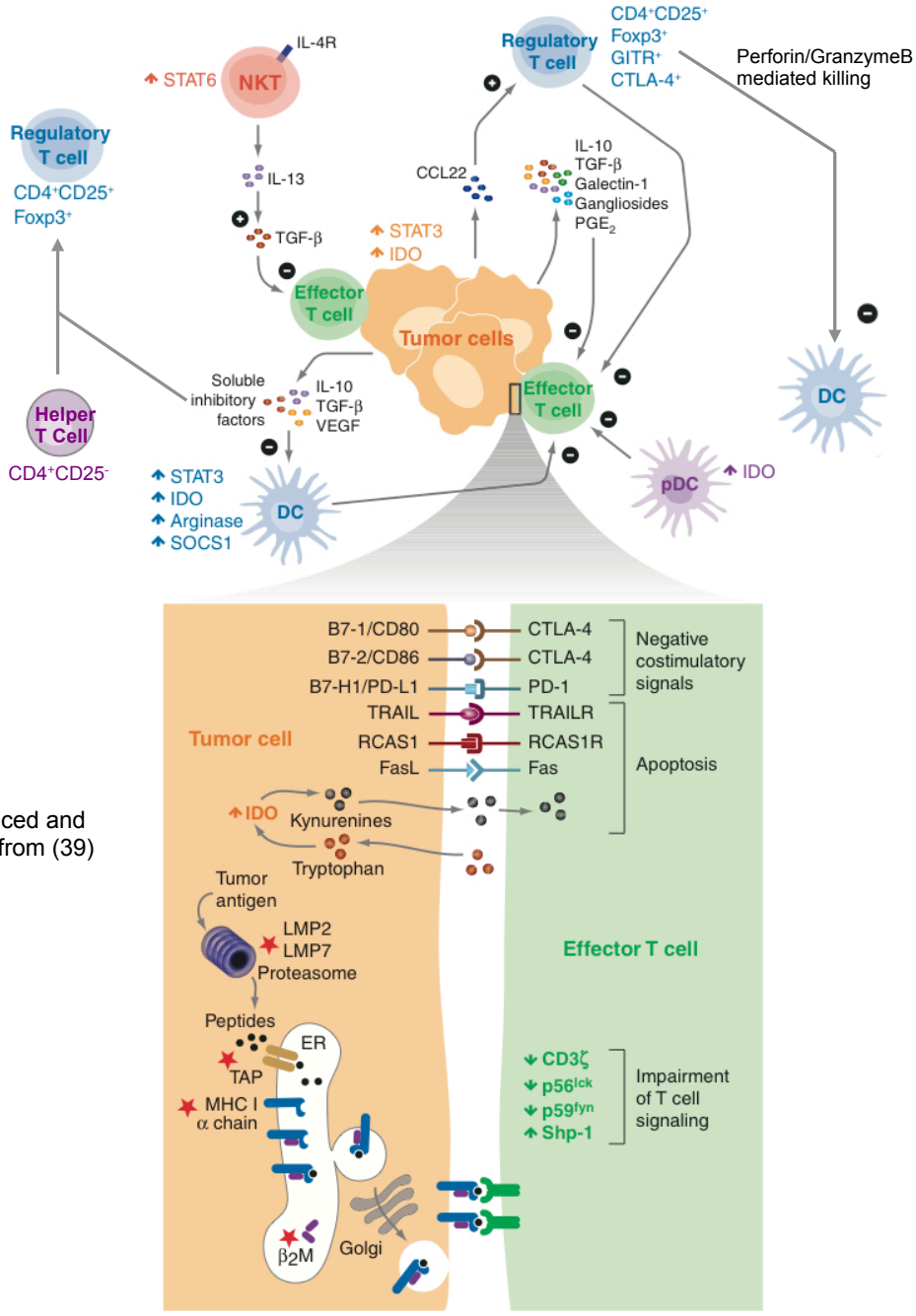

Reproduced and modified from (39)

1.2.3 T Regulatory Cells

Tregs themselves have several methods of inhibiting and regulating immune responses. They can produce TGF-β and IL-10, which can both directly inhibit CTLs, and as previously mentioned, convert other $CD4^+$ T cells into Tregs (51-54). These factors also suppress MHC expression, and induce B7-H4 expression on APCs, which in turn inhibit the activation of CTLs within the TIM via negative costimulation (42, 55). Additionally, Tregs express CTLA-4, which competes with CD28 on CTLs for the B7 ligand, described in 1.1. Tregs also express high levels of CD25, commonly known as the high affinity IL-2α receptor. In doing so, they act as an "IL-2 sink", draining the environment of available IL-2, which is critical for CTL proliferation and activation (56).

Recent studies have demonstrated another mechanism of Treg immunosuppression: lytic targeting and degradation (57-61). This process has long been thought exclusive to CTLs and Natural Killer cells, another lytic, though non-specific, immune responder cell. One study demonstrated that Tregs from tumor bearing mice express high levels of lytic molecules, compared to tumor free mice. These Tregs travel to the tumor draining lymph nodes (TDLs), where they use a perforin-mediated contact dependent method to specifically lyse dendritic cells (DCs). This killing was proven to be antigen specific, using an ovalbumin OTII system (57).

Natural expression of Perforin and Granzyme B within Tregs seems to be dependent upon the host animal or patient actually bearing a tumor (58, 62). The exact mechanism of this stimulation is not known *in vivo*, however it has been repeatedly shown that Granzyme B can be expressed in Tregs *in vitro* via anti-CD3 and IL-2 stimulation (59, 61, 63). These *in vitro* stimulated Tregs can be used to kill targets in an

antigen specific manner. One group demonstrated that murine Tregs activated and induced to express Granzyme B *in vitro* are able to kill CD4+ T helper cells in a Granzyme B-dependent, Perforin-independent, contact mediated manner (59). Additionally, human Tregs, which are *in vitro* activated, are able to kill activated CD4+ and CD8+ cells, as well as CD14+ monocytes, and both immature and mature DCs, in a Perforin-dependent contact mediated. This contact mechanism is mediated by CD18, and Treg cytotoxicity was inhibited upon antibody blockade of CD18 in cytotoxic assays (60). Whether this same contact mechanism is involved in murine Treg specific cytotoxicity has not been shown.

1.2.4 Transient Immune Suppression

It has been demonstrated by our laboratory, and others, that purifying CTLs directly from the tumor, and culturing them *in vitro* can overcome the effects of the TIM. Within as little as 6-8 hours, these CTLs can be reintroduced to cells of the cognate tumor *in vitro*, and they kill in a Perforin-dependent, Fas-independent manner (27). This demonstrates that despite all of the immune evasion effects employed by tumors, the successful generation of a tumor immune response does occur. However, the TIM transiently inhibits this response. Simply removing CTLs from their environment restores their ability to kill. This has been demonstrated across several tumor models (26, 27).

Within these models, it is known that Tregs produce high levels, and many different types of immuno-suppressive factors within the TIM (39, 41, 56, 64). As a method to overcome suppression of CTL effector function, studies have been done to try

to ablate Tregs from the host, and while this works, it almost always leads to autoimmunity, as the lack of Tregs throughout the host prevents necessary immune regulation from being carried out.

Other ways to overcome suppression of CTL effector function include inducing T cells to degranulate (exert perforin-mediated cytotoxicity) in a TCR-independent manner. For example, Phorbol 12-Myristate 13-Acetate (PMA) used in conjunction with Ionomycin, induces degranulation within a T cell, by activating DAG effectors like PKC, and Ras GRP, and increasing intracellular calcium, respectively (65, 66). Chemokines, such as Macrophage Inflammatory Protein (MIP-1α) and Regulated upon Activation, Normal T-cell Expressed, and Secreted (RANTES), also known as CCL5, have also been shown to induce lytic granule release (67, 68). Another encouraging method is that of bispecific antibodies, antibodies that wield two distinct scFv domains, which target both the tumor ligand and the CTL TCR to induce exocytosis-mediated killing of tumor cells (69-73). Separately, work has also been done with CARs, which allow for a bypassing of the MHC/TCR interaction required for classical targeted degranulation, which is discussed in greater detail below.

1.3 Chimeric Antigen Receptors

An emerging immunotherapy for the treatment of cancers, CARs have been shown to be effective in treating cancer not only in several mouse models, but also in clinical human trials (37, 74). The success of the CAR comes from its genetically engineered structure, and the method through which it induces specific T cell function,

while not requiring MHC I presentation to the TCR on CTLs (75). Their structure, function, and success are explained here in brief.

1.3.1 Structure and Advantages

The evolution of the CAR has gone through several generations, resulting in what is generally referred to as the "third generation" used now. The first generation of CARs were a genetically engineered receptor which uses the scFv specific portion of an antibody linked via the CD8 transmembrane domain to the ζ-chain of the CD3 complex, or the intracellular portion of the FcεRIγ, to induce specific killing in CTLs against native form proteins expressed on the surface of the target cell (41, 76-78). The second generation took this design and improved upon it, by adding a costimulation domain, either from the CD28 or 4-1BB coreceptors, to enhance stimulation, resulting in increased proliferation and survival (79). The third generation then included a second coreceptor, usually from a catalog of proteins like OX40, or CD27, which serve anti-apoptotically, to increase survival of T cells and the duration for which they function (80, 81) (Figure 4).

The advantage of the CAR is two fold, in that it has high affinity for surface ligands, rather than being dependent upon MHC presentation of antigen, and secondly that it conveys the same natural intracellular signal as the TCR complex (75). While cancer specific or associated antigens are often intracellular proteins, CARs can be used to target stages of tumor development such as angiogenesis, where markers of neovascularization like vascular endothelial growth factor receptor-2 (VEGFR-2) or epidermal growth factor receptor variant III (EGFRvIII) are used (81-83). Targeting

tumor development essentially suffocates tumor growth, and can result in tumor clearance.

Figure 4. Chimeric antigen receptor structure and function. Chimeric antigen receptors (CARs), much like a transgenic T cell receptor (tTCR), allow for the generation of target specific lymphoctyes. Unlike a tTCR however, CARs bypass the requirement for antigen presentation via MHC I. The basic structure of a car is composed of a protein-specific portion, linked to the ITAM of the CD3ζ chain. This allows for native cell surface proteins to induce the same natural signaling cascade of activation that MHC I presentation to a TCR would. The 3rd generation of CARs use the scFv domain of an antibody, specifically the Variable Heavy and Light chains, as their protein-specific component. This is then linked to the transmembrane domain of the CD8 coreceptor, and followed by the subsurface domain of the CD28 costimulation receptor, both of which contribute to a more potent activation of the T cell. This is often added onto through an additional motif for proliferation or antiapoptotic signals, from molecules like 4-1BB or OX40, respectively, before finally transmitting the signal through the ITAMs of the CD3ζ chain.

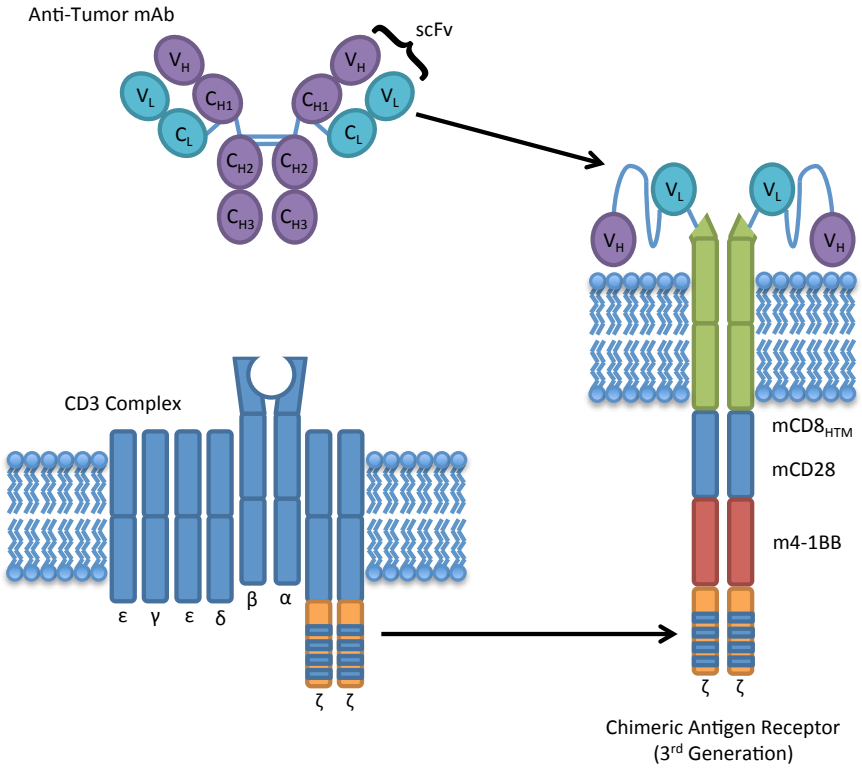
Anti-Tumor mAb
scFv
V_H
V_L
C_{H1}
C_L
C_{H2}
C_{H3}
CD3 Complex
ε γ ε δ β α
ζ ζ
$mCD8_{HTM}$
mCD28
m4-1BB
Chimeric Antigen Receptor
(3rd Generation)

1.3.2 Application in Cancer Immunotherapy

CARs have demonstrated great success in several mouse models of cancer, including lymphoma, melanoma, pancreatic, ovarian and prostate cancer, and brain cancers like glioblastoma (79, 84-87). These models target either tumor specific ligands, or angiogenesis related ligands. In human clinical trials, CARs have also demonstrated success in acute and chronic lymphoid leukemias, specifically with CARs against the B cell marker CD19 (88-90). In general, these patients undergo an ACT, as described previously, where their own T cells are removed, and transduced in culture *ex vivo* to express the CAR of interest. The autologous CTLs are then transfused back into the patient after immune depletion, where they expand further while targeting and destroying the cancer cells (29, 82, 91).

While these CAR-based ACTs have shown great success, there are a few drawbacks and safety concerns related to their use. One of these concerns comes from the nature of the CAR's specificity, where the CAR-bearing T cells are specific for proteins that are tumor associated, and not tumor specific. This leads to a phenomenon of "on-target, off-tumor" specific destruction of normal tissues by CAR-bearing ACT cells (92). This phenomenon is commonly seen in anti-CD19 CAR ACTs, which results in B cell aplasia, though the use of intravenous immunoglobulin can be used to effectively manage this non-cancerous tissue destruction (77, 92-94). This phenomenon does not always occur, as CAR-based ACTs for tumor-associated antigens, such as PSMA and ROR1 have not yet been reported on immune destruction of non-cancerous tissue, while antigens such as her2, MART-1, and carbonic anhydrase IX have all demonstrated effective T cell killing of antigen expressing normal tissue (95-99).

Another complication commonly associated with CAR-based ACTs is that of the induction of massive cytokine storms. High levels of activated T cells results in the release of several inflammatory cytokines, including IL-6, TNF and IFN-γ, which lead to high fever, hypotension, and potentially, organ failure (92, 94). The effects of IL-6 can be managed through the use of tocilizumab, a monoclonal antibody drug commonly used in the treatment of rheumatoid arthritis, while other symptoms may rely upon steroids, vasopressors, and/or supportive therapy delivered in an intensive care unit (92). The treatment of these side effects is complicated, because the therapy itself is not drug-based, but rather cell-based. The adoptively transferred T cells continue to proliferate within the patient, and cannot be reduced, as a drug-based therapy would be.

Potential solutions for these risks include the introduction of genetically engineered suicide genes along with the CAR during transduction, or a reduced number of initially adoptively transferred cells, potentially administered instead in a staggered, dosing timeline (100-102). It has also been demonstrated in anti-CD19 ACTs that stronger T cell responses result in patients with larger tumor burdens, than in those with residual disease (103). This finding suggests that CAR-based ACTs may be best used for the treatment of residual disease, after initial therapies and interventions.

1.4 Pediatric Tumor Immunology

Pediatric cancers are generally less understood than adult cancers, in the context of tumor immunity. This is in part due to the limited used of primary resection and the challenge of acquiring corresponding lymphocyte and tumor samples for study (104). This limitation on acquiring patient samples has led to a small number of directly

identified T cell based antigens in pediatric cancers. However, many adult tumors poses tumor associated antigens also found in pediatric cancers. Commonly found among these antigens is Survivin, which is widely expressed in cancers including leukemias, sarcomas, several brain tumors, and neuroblastoma (NB) (105-107). Furthermore, in cases of NB, it has been demonstrated that immune responses specific for Survivn have been generated (108).

Beyond Survivin, cancer-testis antigens are highly expressed across many pediatric tumors. These antigens are expressed in normal tissue only in the testis, whose germ cells lack class I expression, and are generally immune privileged. As a result, immune responses directed against cancers that express cancer-testis antigens do not target normal tissue in the rest of the body, which does not express these antigens (109). For instance, G antigen (GAGE)-1 is identified in 82% of all NB cases, and seen in nearly 100% of stage 4 NB and Ewing's sarcoma cases (110, 111). Other GAGE family members are expressed in high percentages among pediatric cancers including sarcomas, glioblastomas, and medulloblastomas (112, 113). Another cancer-testis family, named melanoma associated antigen (MAGE), expresses at least one of the four identified MAGE subfamily forms in 50-80% of all NB cases, and is also found in cases of osteosarcomas, glioblastomas, and medulloblastomas (110, 114-116).

Despite the identification of several pediatric tumor associated antigens, there is little evidence of tumor clearance due to naturally induced immune response in these patients. However, there is emerging evidence that these pediatric tumors can be immunogenic, and are capable of being recognized by the immune system. The most promising demonstration of a tumor specific immune response is demonstrated in cases

of NB patients who present with Opsoclonus Myoclonus Syndrome (OMS). OMS, which presents with random eye movements, myoclonus, and ataxia, is present in 2-3% of all NB patients, while its incidence rate in NB free population is 1 in 10^7 per year, though around half of all OMS cases are in patients with NB (117, 118). These NB patients with OMS have a much more favorable three-year survival rate, around 100%, compared to standard NB patients. This syndrome is shown to be associated with the generation of circulating antibodies, which bind to cerebellar tissue (118, 119). These patients also have demonstrated increased lymphocyte infiltration within their tumor mass, and a much more favorable prognosis than NB patients without OMS (120, 121).

Given the display in NB patients of several tumor-associated antigens and a partially characterized immune response developed in the face of tumor development, NB appears to be an excellent candidate to further explore the generation of tumor-specific immune responses to cancer. To better understand NB, its clinical prognosis and therapeutic evasion methods are described below.

1.4.1 Neuroblastoma

NB is the most common extra-cranial solid pediatric tumor type, developing from neural crest progenitor cells (122). It exhibits a wide range of clinical outcomes, ranging between spontaneous regression, to lethal disease (123). It is a heterogeneous tumor, composed of cells in undifferentiated states and those displaying neural crest-derived phenotypes (124). This heterogeneity is common in many tumor types, deriving from several sources, including genetic/epigenetic changes, microenvironmental pressure, anoikis resistance, and cancer stem cell populations (124). These phenotypic changes can

also occur in response to cancer treatment, such as radio and chemotherapy. The ability of cancer cells to survive and adapt depending upon their condition is termed "Reversible Adaptive Plasticity," and has been well characterized in NB (124, 125).

1.4.1.1 Clinical Prognosis and Treatment

Neuroblastoma develops from the tissues making up the sympathetic nervous system, resulting in tumors forming within the adrenal medulla and paraspinal ganglia, presenting in the neck, chest, abdomen, or pelvis. NB can also metastasize into organs local to the original tumor cell origin, lymph nodes and bone marrow. Patients that do not receive therapy often have their tumors mature into benign ganglioneuroma.

Existing genetic markers of unfavorable neuroblastoma prognosis include MYCN amplification and TrkB/NTRK2 upregulation, while conversely TrkA/NTRK1 upregulation is indicative of a favorable outcome (123). NB also follows an autosomal dominant pattern of inheritance, related to activating function mutations in anaplastic lymphoma kinase (ALK) and loss of function mutations in PHOX2B, with up to a hypothesized 22% of patients having their cancer develop from a germinal mutation (123, 126-128). Additionally, NB also exhibits triploidy in several partial to whole chromosome gains (129, 130).

Treatment of NB almost always involves surgery, usually in conjunction with moderate to intense amounts of chemotherapy. Under these therapies, low and intermediate risk patients, i.e. those with localized tumor or lymph node metastasis, have an >98% to 95% survival rate, respectively (131). However, patients classified as high risk, with metastasis to bone and bone marrow, undergo surgery, dose-intensive

chemotherapy, and radiotherapy, occasionally with immunotherapy, still only reach a survival rate of 40-50% (132-135). The exceptions to this pattern, as mentioned previously, are those diagnosed as stage 4S. NB is commonly found in the liver, in patients displaying a stage 4S diagnosis, though these cases typically display complete regression with no to minimal clinical intervention (131), beyond occasional chemo- and/or radiotherapy in the event of life threatening liver disease from the tumors. The survival rate of these patients is >90% (131).

1.4.1.2 Reversible Adaptive Plasticity and Id2

One of the more challenging factors for treating tumors is based upon their ability to transition into different cell phenotypes, due in part to a heterogeneity of cell types within the tumor mass. One form of tumor cell transition, dubbed epithelial to mesenchymal transition (EMT), allows tumor cells to be aggressive, and treatment resistant. EMT occurs when epithelial cells detach from their basement membrane, and acquire mesenchymal characteristics, allowing them to migrate through the body, until they seed in a new location (136-138). This is the primary mechanism by which many tumors undergo metastasis. Markers of this transition include a loss of E-cadherin, in conjunction with up-regulation of β-catenin, vimentin, and SNAIL (124).

Another mechanism by which tumors transition phenotypes, occurs in response either to genetic instability, or environmental stimulus, such as chemo- or radiotherapy. In these cases, cells that do not adapt to their environmental challenges die off, but those which do survive the selective pressure, may gain increased aggressiveness, or metastatic potential, in addition to their apparent resistance to therapeutic agents (139). Some have

dubbed these highly adaptive, self-renewing cells as “cancer stem cells,” though their existence is still debatable (140, 141).

This is in part because cancer cells under survival challenge do not always de-differentiate. It has been demonstrated in models of NB, glioblastoma, and melanoma that cells in conditions of hypoxia transition from their adherent phenotype, to that of a more invasive, migratory phenotype (142-146). NB in particular, has shown the ability to convert back and forth from adherent and migratory invasive phenotypes. This reversible adaptive plasticity (RAP) displays many qualities similar to EMT or selective pressure transitions, but many unique characteristics as well. In the NB line Neuro2a (N2A), adherent, or anchorage dependent (AD) cells, when grown in vitro under serum starvation, but in the presence of EGF and FGF, detached and formed free-floating anchorage independent (AI) tumorspheres. These cells transitioned back to an AD phenotype when returned to normal serum growth conditions. While able to detach and reattach, AI cells demonstrated no changes in their levels of the classic markers for EMT previously mentioned, when compared to AD cells. These cells also displayed some stem-like qualities, with cells from both AD and AI phenotypes able to differentiate into neuronal, oligodendrocyte, and astrocyte lineages. However when assessed for stem cell markers nestin, Sox2, CD133 and CD44, AD and AI cells again demonstrated no significant difference in expression (124).

N2A AD cells are characterized by high expression of MAP2 and Id2, and are highly proliferative, while AI cells are characterized as MAP2 negative, while showing an upregulation in PDGFRβ, slow growth rate and anoikis resistance, evidenced by their upregulation of PI3K/Akt, Erk, Bcl2, and several integrins. These changes are also

observed in several human NB lines, while anoikis-resistant cancers such as melanoma, rhabdomyosarcoma, rhabdoid tumors and pancreatic adenocarcinoma also utilize these changes. The role of Id2 in RAP has been demonstrated as the primary regulator of transition for AD to and from AI. Id2 is an MYCN regulator, and it also competitively binds the Rb protein. In highly proliferative states, Id2 binds to Rb, thus preventing Rb from binding E2F, a known S-phase checkpoint. However in states where Id2 is downregulated, Rb is free to bind E2F, thus inhibiting proliferation. Id2 also functions as a negative regulator of the TGFβ/Smad pathway in NB cells, of which activation is required for the AD to AI transition (125) (Figure 5). These functions correlate with the twenty-fold increase in Id2 expression, in AD cells versus AI cells. Chemotherapeutic mouse models targeting the mechanisms behind RAP have shown dramatic slowing in tumor growth, as well as an overall 50% inhibition of tumor formation (125).

Given the importance of Id2 in aiding NB to escape traditional chemotherapeutic treatment, we sought to target Id2 directly *in vivo*. Using lentiviral transduction, Id2 was knocked down in Neuro2a cells, *in vitro*, and then mice were challenged with these Neuro2a-Id2-knockdown cells. The results of these experiments are presented in the aims below.

Figure 5. Schematic representation of intracellular Id2 signaling pathway. Neuro2a AI cells lose their proliferative potential due to decreases in n-myc and Id2, under conditions of challenge, such as loss of cell-matrix anchorage, or serum starvation. This occurs through competitive binding of retinoblastoma protein (Rb) and TGF-β, as decreases in Id2 allow for Rb to bind to E2F, thereby blocking progression of cells into S-phase. These cells must either undergo apoptosis, or develop anoikis resistance, which occurs when Id2 expression is decreased, as TGF-β is able to activate the pathways needed for anoikis resistance. Figure reproduced from (125).

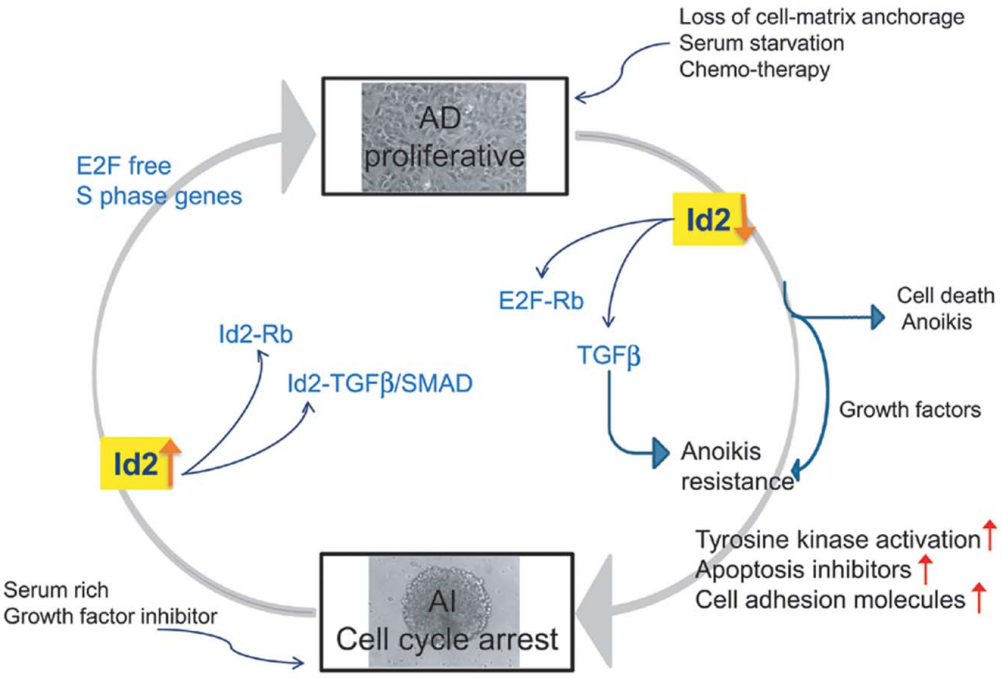

Reproduced from (125)

CHAPTER 2: SPECIFIC AIMS

CD8+ Cytotoxic T Lymphocytes (CTLs) are members of the adaptive immune response, and the primary cell type responsible for the clearance of virally infected and tumorigenic cells in the body. In cancer however, CTLs, which are programed to recognize specific antigens, are often unable to effectively target tumor cells. While some tumors evade immune surveillance via down-regulation of the Major Histocompatibility Complex I and lack of tumor-specific antigens, others generate a Tumor Immunosuppressive Microenvironment (TIM). The TIM can shut down the tumor-specific immune response via production of immunosuppressive cytokines, Fas-mediated apoptosis, negative costimulation, and recruitment of T Regulatory Cells (Tregs). This leads to an "on/off switch" phenotype for CTLs, where CTL function is inhibited within the TIM, but lytic activity is restored upon removal of CTL from the environment. This transient inhibition of CTL function has been proven and established in mouse models, but is not well characterized in humans.

In this dissertation, we investigate whether the "on/off switch" phenotype exists in humans, proving the clinical relevancy of mouse models, and develop methods to circumvent this immune shutdown *in vivo*.

AIM 1: Characterization of CD8+ T Cells Infiltrating Pediatric Tumors

Summary: Mouse models demonstrate that the body develops an immune response to cancerous cells, which becomes functionally suppressed at the site of the tumor. Whether this phenomenon occurs in humans however, has never been demonstrated. We

characterize here the levels of CTL infiltration within untreated childhood tumor samples, and demonstrate that Tumor Infiltrating Lymphocytes (TIL) removed from the TIM are non functional immediately, but regain cytotoxic function upon brief *ex vivo* culture.

AIM 2: Generation of a Specific Cytotoxic T-Cell Response from a Tumor Vaccine Against a Murine Neuroblastoma Model

Summary: Neuroblastoma (NB) is the most common extra-cranial solid pediatric cancer. NB demonstrates a mechanism of *in vivo* phenotype switching, mediated by Id2, which allows it to evade standard chemotherapy. We show here in a Neuro2a (N2) model, that stably knocking down Id2 via lentiviral transduction results in tumor cell growth attenuation, and that when introduced to mice, in conjunction with anti-CTLA-4, result in the induction of a T cell mediated immune response, capable of clearing wild type (WT) N2A cells from the host.

AIM 3: Development of CAR-Expressing Tregs Possessing Anti-Tumor Activity

Summary: Tregs are actively recruited to the TIM, where the immunosuppressive cytokines found within the tumor environment drive their function, and can even convert CD4+ T Helper cells into Tregs. Their role within the TIM is to prevent autoimmunity, by inhibiting CTL function through several pathways, including targeted cytotoxicity. Using Chimeric Antigen Receptors (CARs), we propose to redirect this activity towards the tumor itself. We show here that T cells expressing CARs are able to kill their targets *in vitro,* and additionally, we demonstrate CAR transduction in Tregs, but lower cytotoxicity of Tregs compared to CTLs *in vitro*.

CHAPTER 3: METHODS

3.1 Animals

C57BL/6, A/J, NOD.CB17-Prkdc<scid>/J (HOM) and Nude mice were purchased from The Jackson Laboratory. The animals were acclimated for 4–5 days prior to tumor challenge. All procedures involving animals were approved by the Institutional Animal Care and Use Committee of Children's National Medical Center (CNMC), Washington DC.

3.2 Human Tumor Samples

De-identified fresh human tumor samples were obtained from the Pathology department of CNMC. Written informed consents were obtained from the parents or guardians of the patients in accordance with the Declaration of Helsinki. All procedures involving the use of human tumor specimens were approved by the Institutional Review Board of CNMC.

3.3 Cell Lines

2C11 hybridoma, P815, L1210 cells (ATCC Manassas, VA), IL-2 producing cell line IL2P (obtained from Dr. S Vukmanovic, CNMC) and M-3-9M Rhabdomyosarcoma (obtained from Dr. Crystal L Mackall, National Cancer Institute) were cultured in RPMI 1640 containing 10% fetal bovine serum (FBS, Gibco Carlsbad, CA). Platinum-E cells (obtained from Dr. N Restifo, National Institutes of Health) were cultured in High Glucose DMEM (Gibco), containing 10% FBS, 1% Sodium Pyruvate, 1% MEM Non-

essential amino-acids, 2mM Glutamine, 1% penicillin/streptomycin, 0.1% gentamicin, 10μg/mL puromycin, and 10μg/mL blasticidin. MS1 (ATCC) were cultured in High Glucose, +L-Glutamine DMEM (ATCC), containing 5% FBS. B16:F0 Melanoma from C57BL/6 background and Neuro2a (ATCC), the murine neuroblastoma cell line derived from A/J mice, were cultured as follows. Anchorage Dependent (AD) cells were grown in DMEM (Gibco) containing 10% FBS, 0.5% penicillin/streptomycin (Sigma, St. Louis, MO) and 10% L-glutamine (Sigma). Anchorage independent tumorspheres (AI) from the Neuro2a cells were grown in NeuroCult complete media consisting of NeuroCult Neural Stem Cell (NSC) Basal medium, 1/10 NeuroCult NSC Proliferation supplements, 20 ng/ml EGF, 10 ng/ml bFGF and 2 μg/ml Heparin. NeuroCult media, supplements and growth factors were all purchased from Stem Cell Technologies (Vancouver, BC, Canada).

3.4 Antibodies (Ab) and Reagents

Antibodies used for flow cytometry staining of mouse lymphocytes surface markers included PE-anti-CD45, PE-anti-CD25, FITC-anti-CD49b, FITC-anti-CD4, FITC-anti-CD11b, FITC-anti-CD11c, and their respective isotype controls (all from eBiosciences, San Diego, CA). Additional mouse lymphocyte surface staining antibodies include PE-anti-CD4, PE-anti-CD11c, FITC-anti-CD3, FITC-anti-NK1.1, FITC-anti-CD90.1, FITC-anti-CD8α, PerCP-Cy5.5-anti-CD8α, APC-anti-CD4, and their respective isotype controls (all from BD Biosciences, Palo Alto, CA). Mouse intracellular flow cytometry staining antibodies used were PE-Cy5-anti-Foxp3, and APC-anti-granzyme B, and their respective isotype controls (from eBiosciences and Invitrogen, Carlsbad, CA

respectively). Flow cytometry analysis of murine VEGFR-2/FLK-1 on cell lines was carried out using PE-anti-FLK-1 (BD Biosciences). Antibodies used in the flow cytrometric analysis of human tumor infiltrating lymphocytes were APC-anti-CD4, FITC-anti-CD8, PerCP-Cy5.5-anti-CD16, PE-anti-CD19, and their respective isotype controls (all from BD Biosciences). Flow cytometric analysis of transduced lymphocytes was carried out using rmVEGF R2/Fc Chimera (R&D Systems, Minneapolis, MN) to label DC101, followed by secondary antibody staining of PE-anti-IgG Fcγ (eBiosciences). All cases of flow cytometry used FcR Block anti-CD16/CD32 (eBiosciences). Western blot antibodies used include rabbit-polyclonal-anti-Id1, rabbit-polyclonal-anti-Id2, rabbit-polyclonal-anti-Id3, (all from Santa Cruz Biotechnology, Santa Cruz, CA), and goat-anti-rabbit-HRP conjugated (Jackson Immunoresearch, West Grove, PA).

3.5 Tumor Digestion

Upon removal, tumors were weighed, and then minced in 2mL of serum free RPMI. Minced tumors were then placed in a 50mL tube, and filled to a final volume of 5mL serum free RPMI per 1g of tumor. To enzymatically digest the tumor to a single cell suspension, Collagenase I (Sigma), Dispase II (Roche, Basel, Switzerland) and DNase I (Roche) were added at a final concentration of 1500U/mL, 4.8mg/mL, and 3000U/mL, respectively. The tumor was allowed to digest in a 37°C shaker bath for 20 minutes, swirling the tube by hand every 5 minutes, and then placed on ice for 1-2 minutes, allowing the remaining undigested pellet to settle. The supernatant containing the single cell suspension was then collected and passed through a 40μm strainer, before

being centrifuged at 250 x g for 5 minutes, and resuspended at the desired volume. This procedure was based on and modified from (147).

3.6 Chromium Release Assay

CTL activity of *in vitro* stimulated T cells or TIL was determined in standard ^{51}Cr release assays, described previously in (148). In brief, 10^6 target cells, cognate tumor cells, or syngeneic but non cross-reactive L1210 tumor cells were incubated with 0.2 mCi $Na[^{51}]CrO_4$ in RPMI 1640 medium for 45 min at 37°C. Cells were washed twice with complete medium and transferred to round-bottom 96-well plates at $5x10^3$ cells/well. Effector *in vitro* stimulated T cells were prepared as mentioned previously. Effector TIL were prepared by *in vitro* culture of TIL in complete RPMI 1640 medium overnight in the presence of 2% v/v supernatants containing IL-2. Cells were added to target cells at varying numbers in a final volume of 0.2 ml to give the E:T ratios as indicated in the figure legends. After a 4-h incubation at 37°C, 0.1 ml of supernatants were harvested, and released radiolabel was determined by scintillation counting. Maximal release from target cells was determined by treatment of cells with 1% Triton X-100, spontaneous release was determined from cultures of labeled target cells incubated with medium only, and the formula used for determination of specific lysis was: [(experimental release − spontaneous release)/(maximal release − spontaneous release)] × 100.

3.7 Stimulation of T Cells *in vitro* and *ex vivo* T Cell Purification

To generate T cell blasts from full splenic population, $4x10^6$ total splenocytes in 4 ml of complete RPMI 1640 per well of a 6-well plate were cultured for 36–40 h in the

presence of 2% v/v of supernatants containing anti-CD3 Ab produced by 2C11 hybridoma. Where indicated, the cells were additionally cultured in the presence of 2% v/v of supernatants containing IL-2 (149). To generate T cell blasts from purified populations, CD8+ T cells or CD4+/CD25+ cells were purified using the magnetic bead-coupled Ab MACS system (Miltenyi Biotec, Auburn, CA). These cells were then plated in 1mL of complete RPMI 1640 per well of a 24-well plate, coated with 10μg/mL anti-CD3ε (2C11, BD Biosciences) and anti-CD28 (37.51, eBiosciences). CD8+ and CD4+/CD25+ cells were then cultured for 36-40 h, or 72-96 h, respectively, in the presence of 2% v/v of supernatants containing IL-2.

3.8 Lentiviral Transduction of Tumor Cell Lines

Lentiviral shRNA particles and Luciferase were obtained from Santa Cruz Biotechnology. Briefly, $1x10^5$ target cells were seeded in a 12 well plate, in respective culture media mentioned previously, kept at 37°C overnight. 24 hrs later, the media was removed, and replaced with new media, additionally containing Polybrene (Santa Cruz Biotechnology) at 5 μg/mL. Lentiviral particles were then added to the wells and incubated at 37°C for 24 hrs. The media was then removed and new culture media without Polybrene was added to the wells. 24hrs following this, cells were removed from the plate and split in a 1:5 ratio, to continue growing at 37°C for 48 hrs. To select for stably transduced cells, Puromycin (Invitrogen) was added to the wells at a concentration of 2-10 μg /mL. This media was replaced every 3 days, until remaining cells were confluent enough to passage (>80%). Transduction efficiency of Luciferase expression was assessed via Luciferase Assay (Promega, Madison, WI). Cell lines transduced with

Luciferase containing lentivirus were rinsed while plated on 100mm culture dish in 1X PBS. To this 900 μL of 1X Lysis reagent was added to the dish. Cells were then scraped from the dish, collected into a microcentrifuge tube (Eppendorf, Hamburg, Germany), and briefly spun down. Lysate was transferred to a new tube, then 20 μL of the lysate was added to 100 μL of Luciferase Assay Reagent, and measured via photometer. Cell lines transduced with shRNA lentivirus were assessed for transduction efficiency via Western Blot.

3.9 Western Blot Analysis

Western blots were performed as previously described in (124). Briefly, cell lysates were prepared on ice by incubating $1x10^7$ cells/mL Cytobuster (EMD Millipore, Billerica, MA) containing Benzonase, Phosphotase, and Protease inhibitor for 20 min. Proteins were separated by SDS-PAGE using Criterion XT 4-12% Bis-Tris polyacrylamide (Bio-Rad Laboratories Inc., Hercules, CA) and transferred to polyvinylidene fluoride membranes (EMD Millipore). Membranes were incubated with blocking buffer (0.1% Tween 20, 5% BSA in 1X TBS) for 30 min at room temperature. Membranes were then incubated with primary and secondary antibodies were individually diluted in blocking buffer, and incubated with the membrane at 4°C overnight and 60 min at room temperature, respectively. Membranes were rinsed 4 times with washing buffer (0.1% Tween 20 in 1X TBS) between incubations. Finally, membranes were reacted with WesternBright ECL HRP substrate (Advansta, Menlo Park, CA) for 2 minutes, and developed using the Omega Lum G system (Aplegen, Inc, Pleasanton, CA).

3.10 Tumor Models and Adoptive Transfer

Mice had their fur removed on their hind leg via shaving or Nair, at the injection site prior to injection. They were then subcutaneously inoculated with $1x10^6$ syngeneic tumor cells, in 100μL 1X PBS. Mice were then treated 7-8 days later with i.v. adoptive transfer of $5x10^6$ syngeneic T cells from stimulation groups indicated. Starting tumor volumes ranged from 8-12mm in diameter. All animals were sacrificed when tumor diameters reached 20mm.

3.11 Neuro2a-Id2-KD Vaccination Studies

Mice were vaccinated with either 3-day post tumor inoculation, or 5-day-established post tumor inoculation models. The timeline for vaccination begins with IP injection of 150 μg anti-CTLA-4 antibody (9D9) or IgG2b isotype control (BioXCell, Kuala Lumpur, Malaysia) and subcutaneous injection of $1x10^6$ Neuro2a-Id2-KD cells on the opposite hind leg as the original tumor injection site. Anti-CTLA-4 injections were repeated twice more every 72 hrs, and a second boost of $1x10^6$ Neuro2a-Id2-KD cells were given subcutaneously at the same site 7 days after the first injection.

3.12 Macrophage Harvest and Phagocytosis Assay

Macrophages were harvested from the bone marrow of 6-week-old A/J mice, and cultured in D10 with 30% L929 cell condition medium (LCCM) for 10 days, replacing media every 72 hrs. They were then collected and plated at a density of $5x10^4$ in a 24-well tissue-culture plate. Neuro2a or Neuro2a-Id2-KD cells were labeled with

carboxyfluorescein succinimidyl ester (CFSE) according to protocol (Invitrogen). After 2 hrs, $2x10^4$ CFSE-labeled target cells were added to the macrophage seeded wells, with 10 μg/mL of anti-CD47 antibody and incubated for 2 hrs. Cells were collected and labeled with anti-CD11b-Cy5.5 conjugated antibody, and assessed for phagocytosis via flow cytometry for CD11b+/CFSE+ events. This procedure was based on and modified from (150).

3.13 Live Imaging of Mice

Mice injected with luciferase expressing tumor cells were imaged using IVIS Lumina Series III (PerkinElmer, Waltham, MA). To image, mice were injected IP with D-Luciferin, and were anesthetized 15 minutes later using isoflurane inhalation (Butler Schein, Dublin, Ohio). Using the Living Image program, mice were imaged with a 60 second exposure for all images.

3.14 NK1.1, CD4, and CD8 T Cell Depletion

Starting 1 day before tumor inoculation, Anti-NK1.1 (PK136, eBioscience), Anti-CD4 (GK1.5, eBioscience) and Anti-CD8 (53-6.7 eBioscience) depleting antibodies were injected at concentrations of 300μg, 100 μg and 100 μg, respectively. The depletion injections were repeated every 96 hrs on days 3, 7, and 11 post tumor injection. Depletion of NK1.1, CD4, and CD8 T cells were validated using peripheral blood, and analyzed via flow cytometry (>95% depletion). Mice in depletion studies were vaccinated using a 5-day post tumor inoculation model.

3.15 CAR-Bearing Retrovirus Production

Platinum-E cells were plated at $5x10^6$ cells in 10mL per $10cm^2$ on Poly-D-Lysine Biocoat plates (Corning, Tewksbury, MA) and incubated overnight at 37°C. 16-18hrs post plating, media was removed and cells were rinsed with 1X PBS. Culture media without selective antibiotics was added to the plate, and they were returned to 37°C for 1hr, before adding a mixture containing 9µg CAR plasmid, 6.3µg pCL-Eco, and 60µL Lipofectamine 2000 (Invitrogen) in 6mL OptiMEM (Gibco) to each $10cm^2$ plate. The plates were then incubated at 37°C for 6-8hrs. Transfection media was then aspirated off, and culture media without puromycin or blasticidin was then added to the plates, which were incubated for 48hrs at 37°C. After 48hrs, viral supernatant was collected, and centrifuged at 1000 x g for 5 mintues, before passing through a 40 µm strainer to remove any remaining cell debris. Viral supernatant not used immediately for transduction was stored at -80°C. This procedure was based on and modified from (151).

3.16 CAR-Bearing Retroviral Transduction of T Cells

CD8+ or CD4+/CD25+ T cell populations were obtained and stimulated for 24 or 72 hrs, respectively, under conditions previously mentioned. They were then collected and expanded for 12 hrs in complete RPMI containing 2% v/v of supernatants containing IL-2. During this time, Non Tissue Culture Treated 24 well plates (BD Biosciences) were coated with 300µL of Retronectin (Takara) in 1X PBS at 25µg/mL at 4°C. 30 minutes prior to use, these plates were blocked with 2mL/well 2% BSA in 1X PBS at 37°C, and washed with 1X PBS. 2mL of viral supernatant was then added to each well, and spun at 2000 x g for 2hrs at 32°C. Supernatant was then removed from the plates, and

10^6 T cells were added to the wells at $1x10^6$/1.5mL in complete RPMI containing 2% v/v of supernatants containing IL-2. Plates were spun at 600 x g at 32°C for 10 minutes, and incubated at 37°C. This procedure was based on and modified from (151).

CHAPTER 4: CHARACTERIZATION OF CD8+ T CELLS INFILTRATING PEDIATRIC TUMORS

4.1 Introduction

Several mouse models of cancer have been used to demonstrate the generation of a tumor specific immune response, which becomes reversibly inhibited within the TIM. This inhibition comes from several factors employed by tumors, including inhibitory cytokines such as TGFβ and IL-10, Fas-mediated induction of apoptosis, and recruitment of T regulatory cells. While these mouse models have demonstrated that CTL function is recoverable upon removal of TIL from the TIM, this recovery of T cells isolated from human tumors has not been assessed. We show here an analysis of CD8+ T cell infiltration within several human pediatric tumor samples, and furthermore, the recovery of cytotoxic T cell function from purified TIL.

4.2 Results

4.2.1 Characterization of Tumor Infiltrating Lymphocytes within Human Patient Samples

To investigate whether or not human tumors display infiltration by CTLs, samples were obtained from biopsies and resections of solid tumors, over the span of two years, from patients at Children's National Medical Center (CNMC) in Washington, D.C. To study the natural tumor induced immune response, it was critical to obtain samples from untreated patients, as chemo- and radiotherapy can weaken, alter, or destroy components of the immune system, as well as change the morphology of the tumor.

Tumor samples were enzymatically digested into a single cell suspension, and total cellular events were analyzed via flow cytometry for expression of CD8, the classical surface marker for CTLs. In cases where enough tissue was provided, samples were assessed for additional markers. While some tumor types displayed no detectable levels of CD8+ cells (Ependymoma, Embryonal Rhabdomyosarcoma, Synovial Sarcoma, Gliofibroma), other types exhibited low levels of infiltration (Wilms' Tumor, Pilocytic Astrocytoma, Neuroblastoma) (Table 1). The percentages shown in all lymphocytes populations were determined by gating on all positive events within the total tumor digestion, compared to isotype control for their respective antibodies. For tumors types that were examined more than once, infiltration levels remained consistent (Figure 6).

Of note, NB samples displayed either little to no evidence of CD8+ T cells, with the exception of Patients 2 and 5 (Figure 7A). These findings for NB patients are consistent with T cell infiltration in our pediatric NB cell line, Neuro2a, which display infiltration of CD4+/CD45+ and CD8+/CD45+ cells at 2.53% and 1.65%, respectively (mean n=4 tumors). (Figure 7B). Patients 2 and 5 presented with OMS, the characteristics of which are discussed previously. These two OMS-NB patients displayed a substantial infiltration level of CD8+ cells, (Figure 7C), with Patient 2 having 17.3% of all TIL CD8+ cells and Patient 5 having of all TIL 15.2% CD8+ cells, which to our knowledge, is the first time this has been shown. The high levels of CD8+ T cells found within OMS-NB patient samples provide strong evidence towards the autoimmune hypothesis of OMS, but also suggesting that TILs are associated with the more favorable outcome of OMS-NB patients compared to non-OMS NB patients.

Table 1. Catalog of CD8 infiltration in human tumor samples. Levels of all evaluated TIL from human tumor samples, as assessed via flow cytometry, after isotype correction. Positive gating events were analyzed from the entire tumor cell collection after enzymatic digestion.

Tumor Type/Date	% of CD8 in total tumor	% of CD4 in total tumor	% of CD16 in total tumor	% of CD19 in total tumor
Wilms'				
1/14/11	0.196			
4/12/12	0.406			
9/11/12	0.106	0.056		
Ependymoma				
3/11/11	0			
4/25/12	0			
Embryonal Rhabdomyosarcoma				
3/17/11	0			
Synovial Sarcoma				
10/17/11	0			
Pilocytic Astrocytoma				
11/7/11	1			
Neuroblastoma				
1/23/12	0			
4/27/12	7.49	0.35		
10/25/12	0	0		0
1/17/13	1.056	0.604	0	0
1/29/15	2.12	4.38	0.048	0.496
Gliofibroma				
1/7/13	0			

Figure 6. Flow cytometric analysis of human Wilms' Tumor CD8+ infiltration. (A) Wilms' Tumor patient samples were enzymatically digested immediately after surgery, and analyzed for their infiltration of CD8+ T cells. Following whole tumor digestion, identification of CD8+ gate from the entire cellular collection was established from comparison with isotype control. (B) Graphical representation of TIL levels from (A) after correction for isotype control.

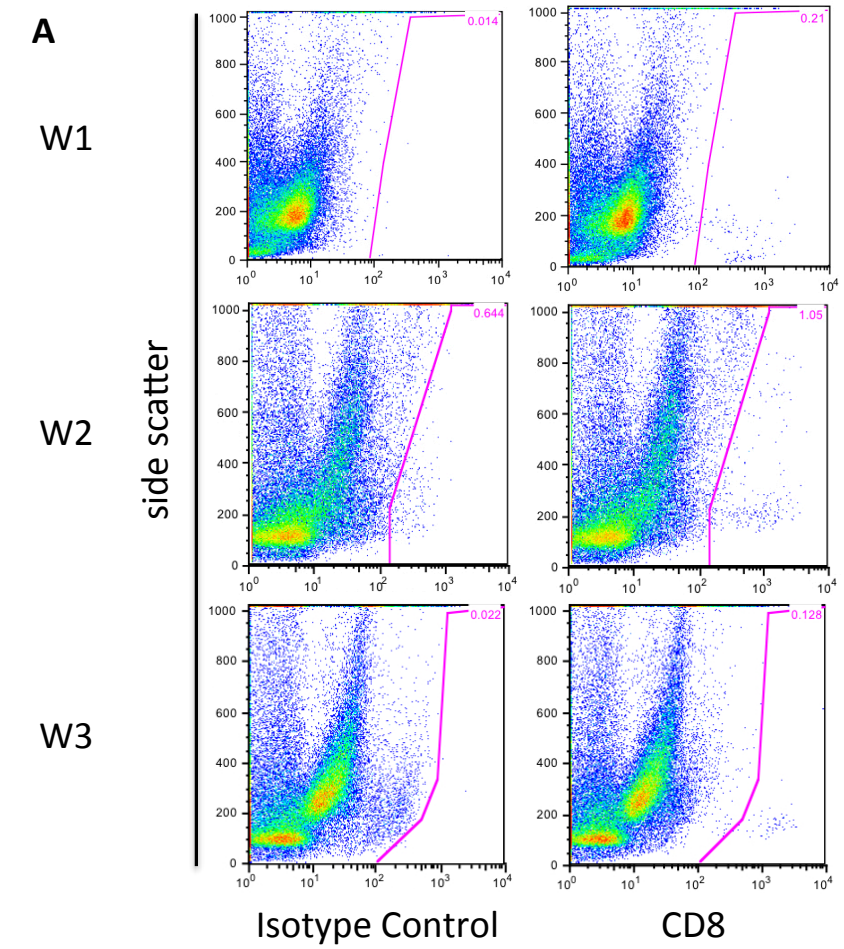
A
W1
W2
W3
side scatter
0.014
0.21
0.644
1.05
0.022
0.128
Isotype Control
CD8

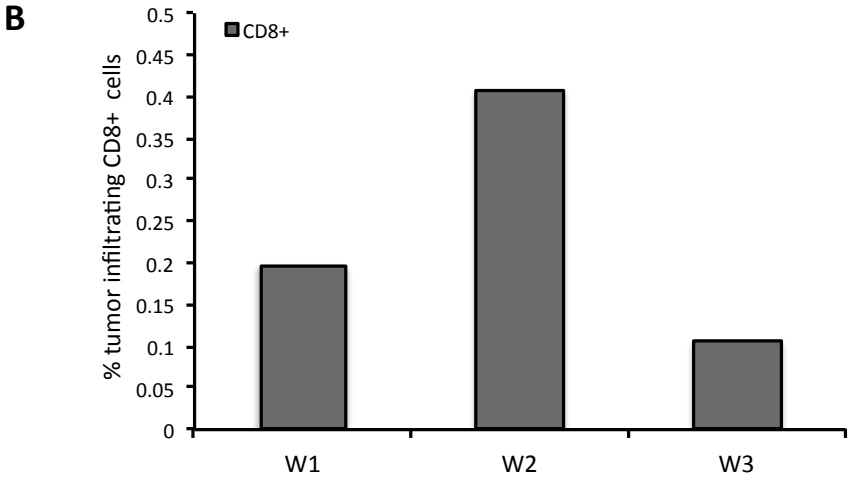
B
CD8+
% tumor infiltrating CD8+ cells
0.5
0.45
0.4
0.35
0.3
0.25
0.2
0.15
0.1
0.05
0
W1
W2
W3

Figure 7. Human normal Neuroblastoma infiltration compared with Opsoclonus Myoclonus patient. Neuroblastoma (NB) tumor samples from patients, two with Opsoclonus Myoclonus syndrome, were enzymatically digested and assessed for TIL. (A) Representative flow cytometry for CD4+ and CD8+ T cells in NB samples. Tumor lymphocyte gating was established via FSC vs low angle-SSC events from the entire cellular collection, following tumor digestion. Identification of CD4+ and CD8+ events within this tumor lymphocyte population were established from comparison to respective isotype controls. (B) Graphical representation of CD4+ and CD8+ cells from murine NB cell line, Neuro2a. CD45+ cells within full tumor digestion were used to establish tumor lymphocyte gating. CD4+ and CD8+ events were established from comparison with their respective istotype controls. Mean infiltration values were generated from the 4 corresponding samples, error bars represent SD. (C) Graphical representation of TIL levels from (A), indicating an increase of CD8+ T cell infiltration within the OMS patient samples, compared to other NB patient specimens.

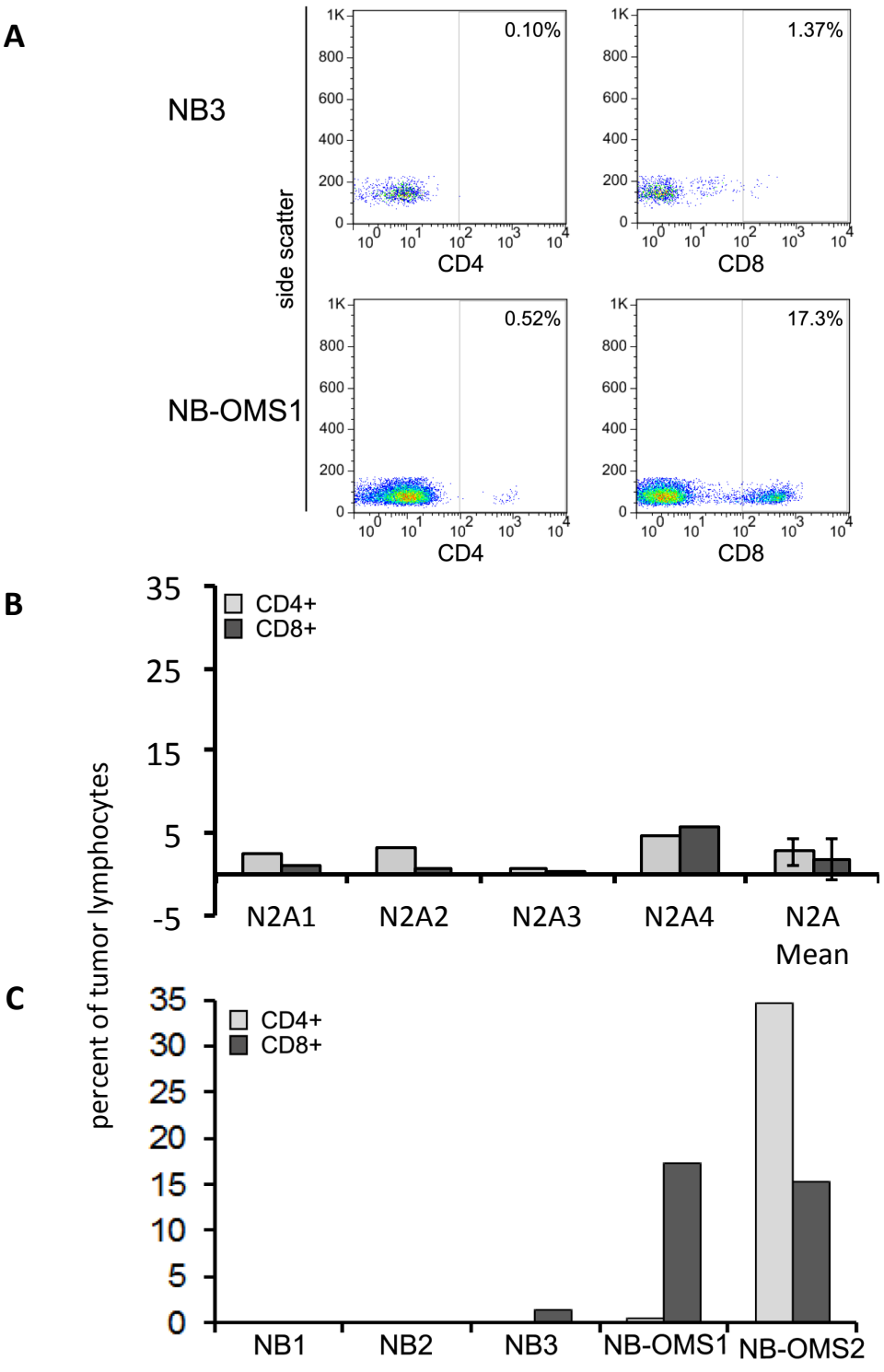
A
NB3
NB-OMS1
side scatter
CD4
CD8
0.10%
1.37%
0.52%
17.3%
B
CD4+
CD8+
percent of tumor lymphocytes
N2A1
N2A2
N2A3
N2A4
N2A Mean
C
NB1
NB2
NB3
NB-OMS1
NB-OMS2

4.2.2 Human Tumor Infiltrating Lymphocytes are Functionally Inhibited at the Tumor Site

To investigate the transient inhibition phenotype of TIL, Neuro2a could not be used due to its poor immune response, as indicated by negligible lymphocyte infiltration. Due to the few available murine NB cell lines available being of A/J mouse background, we instead, utilized the previously unexplored mouse model rhabdomyosarcoma M3-9-M, which come from a C57BL/6 mouse background, as C57BL/6 typically generate stronger cytotoxic T cell responses than those of our A/J mice used in Neuro2a work. Flow cytometric analysis of whole tumor cellular digestion (n=5 mice) revealed infiltration of M3-9-M tumors by CD8+ (1.52%) and CD4+ (0.44%) T cells (Figure 8A). To investigate the functional ability of these cells, TIL were purified from the tumor mass, and assessed for their specific cytotoxicity. These TIL were found to be impaired in their ability to specifically kill target cells of the cognate origin as their tumor upon immediate removal from the TIM. However upon 10 hr *ex vivo* culture, the TIL demonstrated a recovery of their specific cytotoxic ability (Figure 8B). These findings are consistent with other models of transient tumor induced immune suppression (27, 152).

To explore this "on/off" phenotype in a humanized model, a human-mouse xenograft model of neuroblastoma was used. Briefly, NOD/scid/IL2Rγ^{null} mice were engrafted with $5*10^6$ NLF cells, a human neuroblastoma cell line, and 1 week later injected through the lateral tail vein with $50*10^6$ human CD3+ T cells, and tumors were harvested upon reaching a diameter of 20mm (153). Flow cytometry of the tumor digest revealed a small percentage of CD8+ T cell infiltration (Figure 9A), consistent with our Neuro2a and human neuroblastoma samples. These cells were purified from the tumor

digest, and tested for their cytotoxic potential immediately *ex vivo*. Upon removal, TIL demonstrated limited cytotoxicity toward targets of cognate tumor origin, but upon 10 hr *ex vivo* culture, increased their specific cytotoxic functionality (Figure 9B). This data is from a single experiment, and limited cell numbers prevented the standard chromium dose response analysis.

Since preliminary data demonstrated the transient inhibition of TIL in mouse and human-mouse xenograft models, we sought to test for this "on/off" phenotype in TIL purified from human tissue. The previously mentioned case of Pilocytic Astrocytoma provided enough TIL to purify (Figure 10A), and investigate their cytotoxic activity. TIL purified from this tumor displayed no initial cytotoxicity when conjugated via OKT3 to L1210 cells, which are Fas-deficient. These TIL were cultured *ex vivo* for 11 hours, and again assessed for their ability to kill, with a significant ($P=0.044$) increase in cytotoxicity, analyzed via a Student's T Test (Figure 10B).

Figure 8. TIL infiltration and cytotoxicity in M3-9-M Rhabdomyosarcoma. Tumors were enzymatically digested immediately *ex vivo*. (A) Graphical representation of CD4+ and CD8+ T cell infiltration observed in M3-9-M tumors. Analysis was performed on total cells following digestion of tumor samples. CD4+ and CD8+ gating established from respective isotype controls. Values displayed are mean of n=5 tumors, error bars represent SD. (B) CD8+ T cells harvested from M3-9-M tumors display low levels of specific cytotoxicity assessed via standard 4 hr chromium release assay against cognate tumor cells when freshly isolated from their tumor mass. This cytotoxicity is significantly increased upon 8 hr recovery of TIL *ex vivo* at 37°C in tissue culture media, without introduction of additional cytokines. E:T ratios run in triplicate. Representatives of three independent experiments giving similar results are shown. Error bars represent SD.

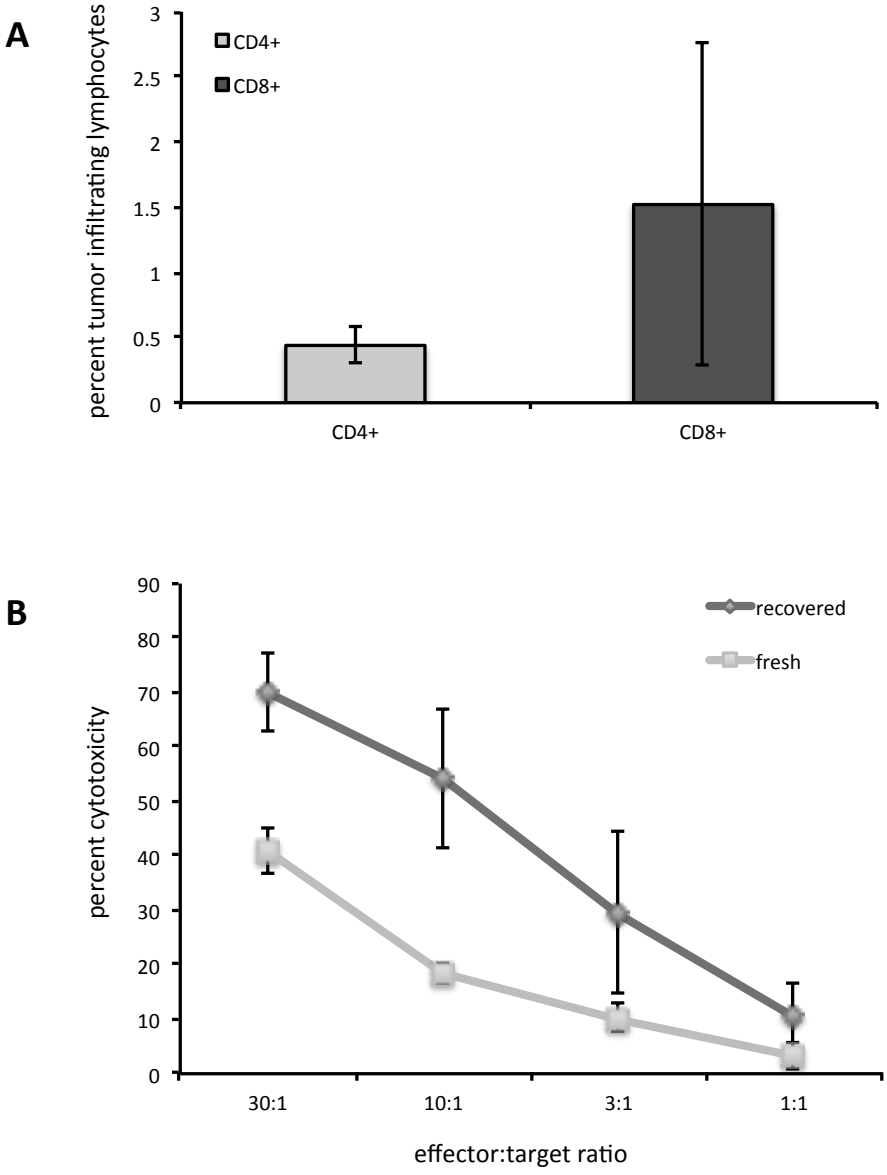
A
percent tumor infiltrating lymphocytes
3
2.5
2
1.5
1
0.5
0
CD4+
CD8+
CD4+
CD8+
B
percent cytotoxicity
90
80
70
60
50
40
30
20
10
0
recovered
fresh
30:1
10:1
3:1
1:1
effector:target ratio

Figure 9. Xenograft CD8+ infiltration and recovery of TIL cytotoxic function. (A) Flow cytometric analysis of CD8+ T cell infiltration in NLF xenograft human-mouse model (described in Results). Following enzymatic digestion of tumor, CD8+ events from the entire cellular collection were established from comparison with isotype control. After purification of CD8+ cells from the tumor digestion, the purity of isolated cells was analyzed using the same gating strategy described above. (B) Purified lymphocytes from NLF tumor re-directed in 4 hr standard chromium release assay against L1210 cells display partial cytotoxicity upon removal from tumor environment. When these cells were recovered for 10 hrs *ex vivo* at 37°C in tissue culture media, without additional cytokines, they showed an increase in their cytotoxic effector function. E:T ratios run in triplicate samples. Data are representative of one mouse.

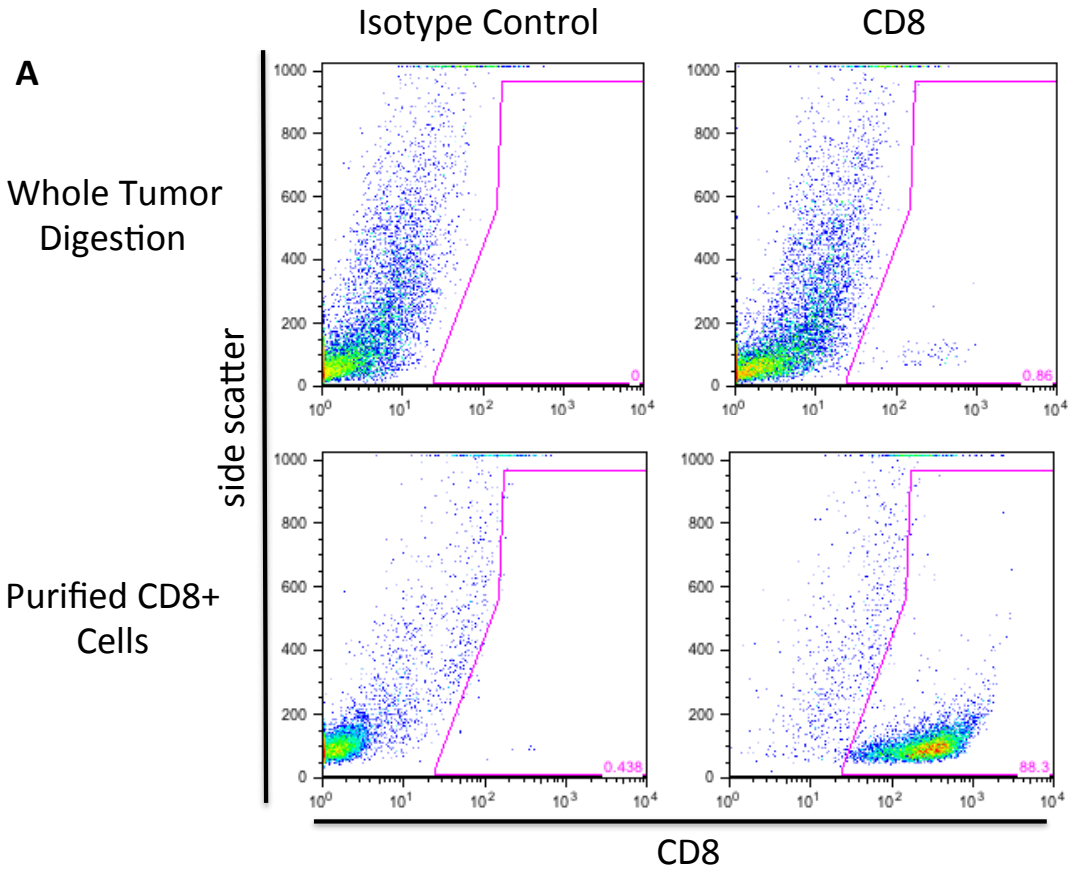
A
Isotype Control
CD8
Whole Tumor Digestion
Purified CD8+ Cells
side scatter
CD8
0
0.86
0.438
88.3

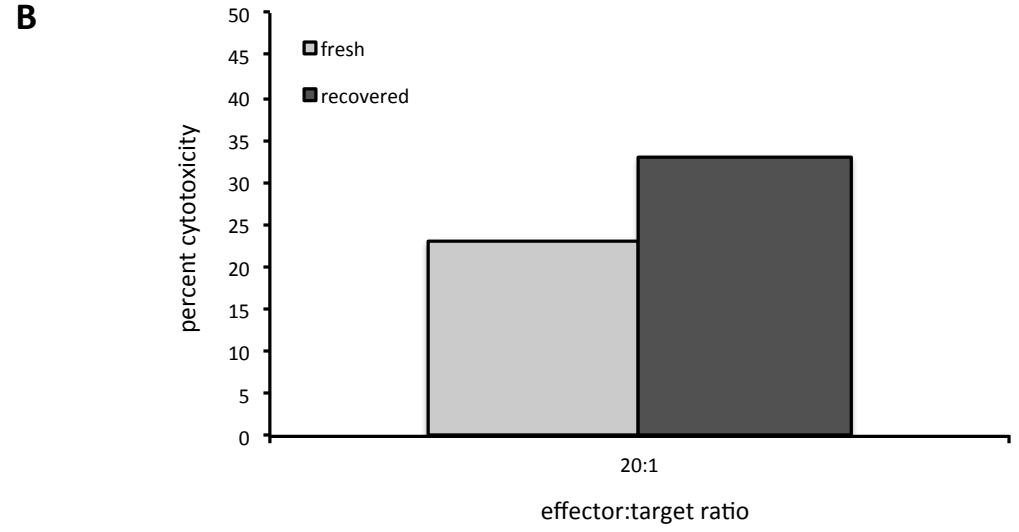
B
fresh
recovered
percent cytotoxicity
20:1
effector:target ratio

Figure 10. Pilocytic Astrocytoma CD8+ infiltration and recovery of TIL cytotoxicity. (A) Flow cytometric analysis of CD8+ T cell infiltration in Pilocytic Astrocytoma. Following enzymatic digestion of tumor, CD8+ events from the entire cellular collection were established from comparison with isotype control. After purification of CD8+ cells from the tumor digestion, the purity of isolated cells was analyzed using the same gating strategy described above. (B) CD8+ T cells were purified from the tumor digestion, shown in (A), and assessed for their cytotoxic effector function immediately *ex vivo*, and again after 11 hrs of *ex vivo* recovery at 37°C, in tissue culture media without additional cytokines. Utilizing re-directed 4 hr standard chromium release assay against L1210 cells, TIL are able to significantly increase their cytotoxic effector function (*p=0.044). E:T ratio run in triplicate samples. Error bars represent SD.

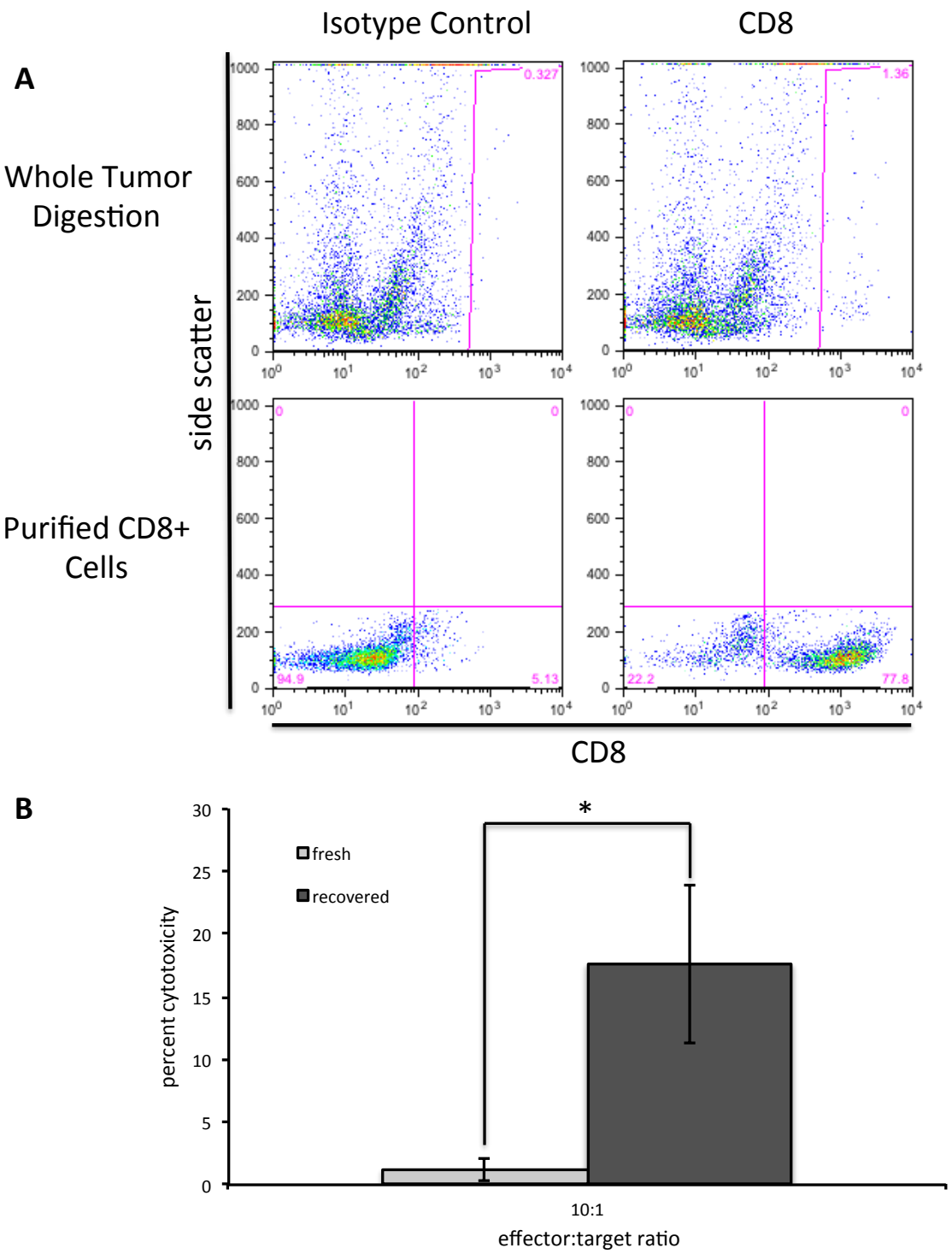
A
Isotype Control
CD8
Whole Tumor Digestion
Purified CD8+ Cells
side scatter
CD8
0.327
1.36
94.9
5.13
22.2
77.8
B
*
fresh
recovered
percent cytotoxicity
10:1
effector:target ratio

4.3 Conclusions

We show here via flow cytometry that several types of human tumors exhibit low levels of natural CD8+ CTL infiltration, in agreement with previous work in the field related to TIL. In two cases of NB, where the patients present with OMS, increased numbers of infiltrating lymphocytes were found, providing potential evidence towards the autoimmune hypothesis of OMS. These finding suggest the potential for developing a tumor specific immune response in humans. Additionally, preliminary data using human-mouse xenograft and human clinical sample studies of TIL cytotoxicity and recovery of function demonstrate a similar "on/off" phenotype present in mouse models of cancer (27, 152, 154). Taken together, these data provide support for the generation of an immune response against human cancers, and the existence of transient immune suppression in human tumors.

CHAPTER 5: GENERATION OF SPECIFIC CYTOTOXIC T-CELL RESPONSE FROM A TUMOR VACCINE AGAINST A MURINE NEUROBLASTOMA MODEL

5.1 Introduction

Despite the ability of the body to generate a tumor specific immune response, this immune response is often shut down or evaded at the site of the tumor. The ability of tumors to shut down these immune responses is multifactorial, including contact, cytokine, and/or immune regulatory cell mediated methods, as discussed previously. As such, cancer has often been best treated with surgery, chemo- and radio-therapeutic methods (134, 135). For NB patients in particular, most low and moderate risk patients do well with chemo- and radiotherapeutic treatment combined with minimal surgical intervention. However, high-risk patients with metastatic NB still have an unfavorable prognosis (123, 131). This leads to the requirement for a better understanding of how NB evades treatment, and the development of new forms of therapy. NB has been shown to poses several tumor associated antigens, as discussed previously, and evidence presented in AIM 1, along with the work of others, shows that NB can induce a powerful immune response, making it an excellent candidate model for the development of new immunotherapies. Our previous work also established that NB is a heterogeneous form of cancer, possessing cells of multiple phenotypes, which are able to freely transition from one to the other (124, 125). This reversible adaptive plasticity (RAP), mediated via Inhibitor of Differentiation 2 (Id2), enables NB to enter an anoikis and chemo-resistant phenotype, making it harder to treat through conventional therapeutic methods, as

observed in patients with a high-risk tumor and poor prognosis. Taking these factors together, we show here the development of a tumor vaccination model that uses Id2-knockdown Neuro2a cells in combination with the immune checkpoint blockade inhibitor anti-CTLA-4, to target and prevent RAP, and induce a potent immune response towards NB.

5.2 Results

5.2.1 Neuro2a-Id2-KD cells protect mice from WT Neuro2a challenge

To investigate the effects of Id2 KD in Neuro2a cells on RAP *in vivo*, Neuro2a cells were transduced *in vitro* with lentiviral vectors expressing shRNA for Id2. Knock down of Id2 was confirmed via western blot analysis (Figure 11A). Neuro2a-Id2-KD cells demonstrated no difference in growth rate *in vitro*, compared to WT Neruro2a (data not shown). These cells were then implanted sub-cutaneously into the hind legs of mice to observe tumor growth. Surprisingly, Neuro2a-Id2-KD tumors either failed to develop or were rejected in 60% of mice (Figure 11B). Mice that rejected Neuro2a-Id2-KD cells were rechallenged with WT Neuro2a, with 8 of 9 mice further rejecting the WT challenge, compared to mice which had not been challenged previously with Neuro2a-Id2-KD cells, in which 100% of mice develop tumors (Figure 11C). To determine if this growth attenuation of the Id2-KD tumors was immune mediated, SCID and Nude mice were challenged with Neuro2a-Id2-KD cells, and compared tumor gowth with that in WT mice (Figure 11D). Immune compromised mice were unable to reject Neuro2a-Id2-KD cells (Figure 11D), which grew tumors in 100% of mice challenged, and grew

aggressively at the same rate as WT Neuro2a cells (Figure 11B). These findings suggested a potential immune mediated rejection/prophylactic protection phenomenon.

To test if this phenomenon could be used as a therapeutic vaccine for established tumors, naïve mice were implanted with WT Neruro2a on their right hind leg, followed 3 days later by Neuro2a-Id2-KD challenge on their left hind leg (Figure 11E). In this scenario, no mice grew tumors at the site of Neuro2a-Id2-KD injection as seen in Figure 11A. Further, there was a significant delay in tumor development at the site of WT injection (Figure 11E, red line). Comparatively, mice implanted with WT Neuro2a and then challenged 5 days later with WT Neuro2a, instead of the Id2-KD cells (Figure 11E, green line), did not show a delay in tumor development, and grew tumors at both injection sites, demonstrating a lack of concomitant tumor immunity, and further implicating Neuro2a-Id2-KD cells as an immunogenic tumor cell.

Figure 11. Id2 knock down attenuates tumorigenicity and induces host immunity. (A) Id2 knock down in Neuro2a cells is confirmed by western blot, compared to wild type cells, and scrambled shRNA control (SC). Experiment performed by Dr. Lina Chakrabarti. (B) Inoculation of $1x10^6$ Neuro2a-Id2-KD cells in development of tumor in only 60% of mice (n=15), compared to WT (n=20) and SC (n=5) tumor cell challenge. (C) Mice from (B) which failed to develop Neuro2a-Id2-KD tumors (n=9) were rechallenged after 6 weeks with $1x10^6$ WT Neuro2a on the opposite leg (squares), and their tumor growth was compared with naïve mice (n=10) challenged with the same amount of WT Neuro2a cells (diamonds). (D) SCID (n=5) and nude (n=5) mice were challenged with $1x10^6$ Id2-KD cells. In each of these cases, tumors were able to grow uninhibited in 100% of immunodeficient mice, compared to WT mouse control from (B). (E) Following challenge with $1x10^6$ WT Neuro2a cells on the right leg, $1x10^6$ WT Neuro2a (n=5) or Neuro2a-Id2-KD (n=10) cells were inoculated into the left leg of mice, 5 days later. Mice vaccinated with WT died swiftly from multiple tumor burden, whereas mice vaccinate with Neuro2a-Id2-KD cells did not develop secondary tumors, and slowed the growth of the initial WT challenge.

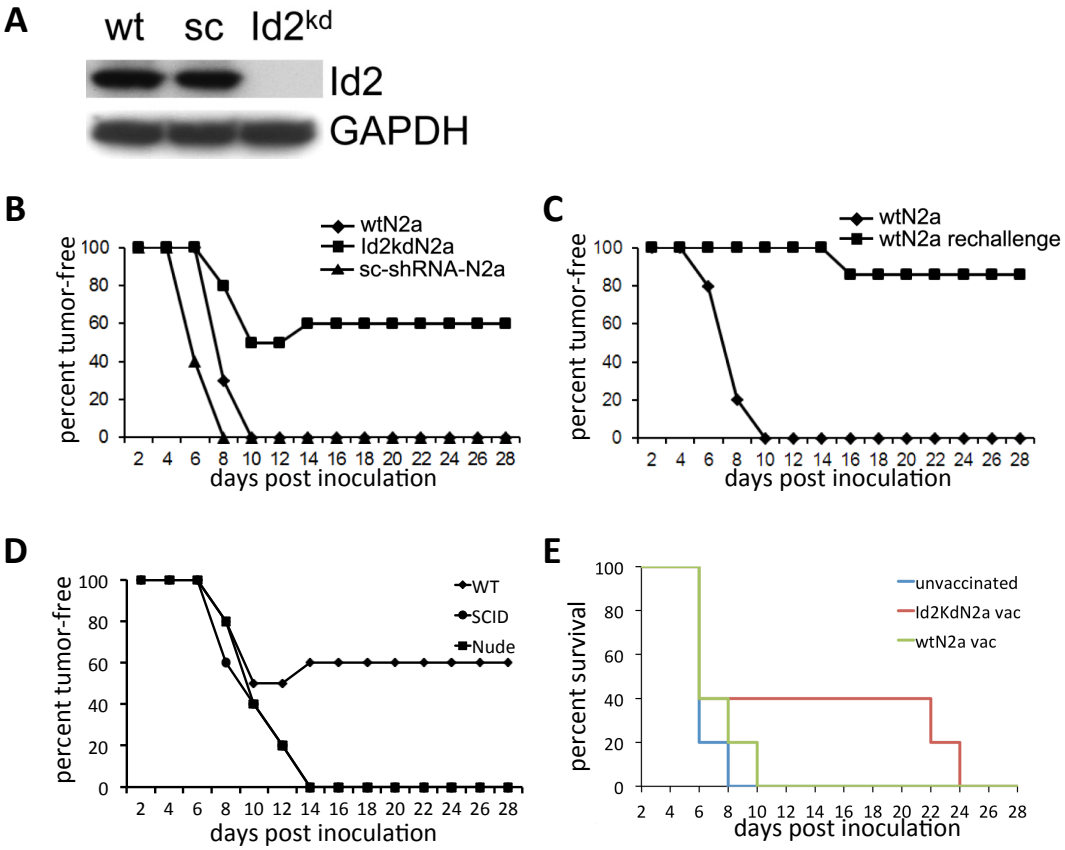
A
wt
sc
Id2kd
Id2
GAPDH
B
wtN2a
Id2kdN2a
sc-shRNA-N2a
percent tumor-free
days post inoculation
C
wtN2a
wtN2a rechallenge
percent tumor-free
days post inoculation
D
WT
SCID
Nude
percent tumor-free
days post inoculation
E
unvaccinated
Id2KdN2a vac
wtN2a vac
percent survival
days post inoculation

5.2.2 Macrophage phagocytosis of Neuro2a-Id2-KD cells is not increased compared to WT Neuro2a

To better characterize the mechanisms behind the immunogenicity of Neuro2a-Id2-KD cells, we sought to find out if enhanced phagocytosis was a contributing factor. To do this, mature bone marrow derived macrophages were cocultured with either WT or Id2-KD Neuro2a cells, previously labeled with CFSE. Flow cytometric analysis for CD11b+/CFSE+ events showed that macrophages did not increase their phagocytosis of Id2-KD cells, compared to WT (Figure 12A).

Antibody-mediated blockade of CD47 on macrophages has been demonstrated to increase their phagocytotic ability, and therefore better induce CD8+ T cell effector responses (155). Seeking to increase phagocytosis of Neuro2a cells, macrophages were cultured in anti-CD47 antibodies before being introduced to target Neuro2a or Neuro2a-Id2-KD cells. However, flow cytometric analysis again showed no increase in phagocytosis of either WT or Id2-KD Neruo2a cells (Figure 12B).

Figure 12. Phagocytosis of Neuro2a-Id2-KD compared to WT. Bone marrow derived macrophages were mixed with either CFSE-labeled WT or Id2-KD Neuro2a cells *in vitro* for 2 hrs at 37°C in tissue culture media at a ratio of (2.5:1), to determine if phagocytosis of Id2-KD cells was increased compared to WT. For experimental groups using αCD47, 10μg/mL of blocking antibodies were introduced to macrophages 2hrs before pooling cellular populations. (A) Macrophages were defined as CD11b+ events within mixed cellular population. Events that were positive for CFSE and CD11b were defined as macrophages that phagocytosed target cells. Gating for CD11b+ events was determined by comparison to isotype control, and CFSE+ events were determined by comparison to non-labeled Neuro2a cells. Flow cytometry plots shown are representative of 3 independent experiments. (B) Graphical representation of data shows no significant increase in phagocytosis of either Neuro2a cell type (n=3 experiments). Errors bars represent standard deviation.

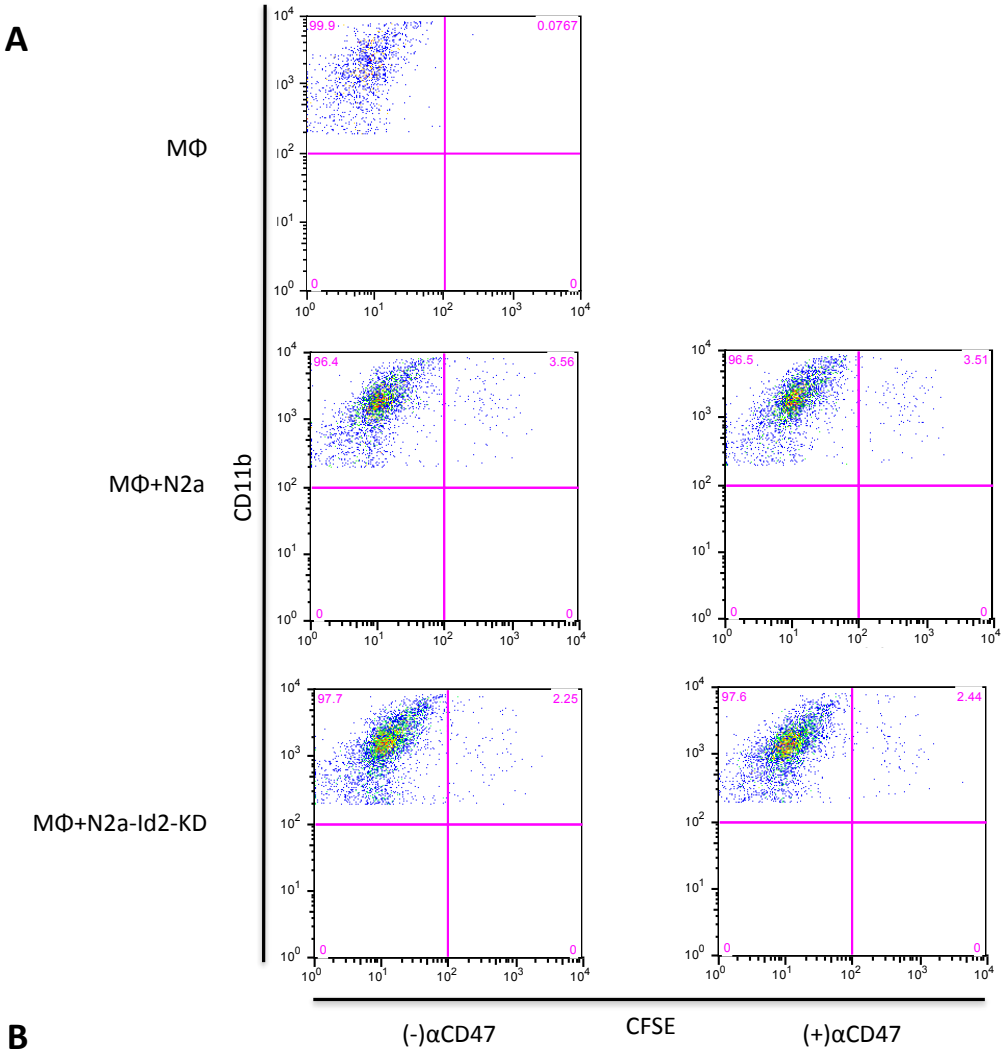
A
MΦ
MΦ+N2a
MΦ+N2a-Id2-KD
CD11b
99.9
0.0767
96.4
3.56
96.5
3.51
97.7
2.25
97.6
2.44
(-)αCD47
CFSE
(+)αCD47

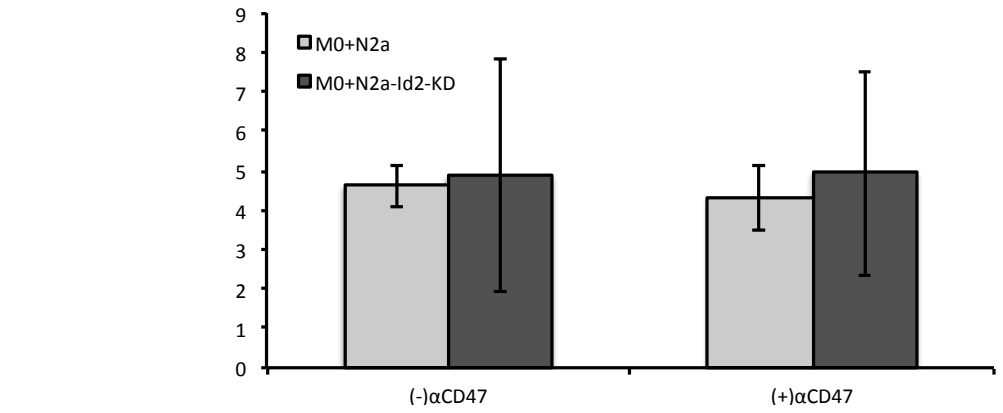
B
M0+N2a
M0+N2a-Id2-KD
(-)αCD47
(+)αCD47

5.2.3 CTLA-4 checkpoint blockade enhances anti-tumor immunity induced by Neuro2a-Id2-KD cells

Seeking to improve the immune response induced by Neuro2a-Id2-KD cells, we chose to combine exposure to Id2-KD cells with introduction of antibodies to block cytotoxic T lymphocyte antigen-4 (CTLA-4), a known inhibitor of T cell activation (156-160) (Figure 13A). Beginning introduction of anti-CTLA-4 5 days after WT Neuro2a inoculation, we observed that anti-CTLA-4 alone was able to induce clearance of tumor in 40% of (n=5) mice (Figure 13B) compared to 0% in the non-vaccinated control mice (n=5), however in combination with Id2-KD cells, we were able to induce clearing of established tumors in 60% of (n=10) mice (Figure 11B).

We decided to test this vaccination effect with a more aggressive form of Neuro2a. Briefly, Neuro2a cells that express luciferase were i.p. implanted into mice, and their growth was tracked via luminescent imaging. After 3 weeks, mice were sacrificed, and their tumors were harvested. These tumors were then homogenized using the tumor digestion protocol explained previously, and the cells were collected and re-implanted into a new mouse. This process of *in vivo* cellular passaging was repeated 3 times, and the cells harvested at the end were named Aggressive-Neuro2a (AgN2a), for their ability to escape or suppress immune clearance in several mice. Utilizing AgN2a tumors implanted in the hind leg, anti-CTLA-4 alone was unable to induce clearance of tumors in any mice, but when combined with Neuro2a-Id2-KD cells, eradicated established tumors in 90% of mice (Figure 13C). In all models, no mice ever developed tumors at the site of Neuro2a-Id2-KD cell implantation. Further evaluation of tumor growth and clearance was monitored via luciferase-bearing Neuro2a cells (Figure 13D). These data

showed that CTLA-4 blockade is able to delay or inhibit tumor growth in a minority of mice, but works more efficiently, able to clear established Neuro2a tumors, when combined with immunization by Neuro2a-Id2-KD cells.

Figure 13. Combination of Neuro2a-Id2-KD and αCTLA-4 antibody as a therapeutic vaccine. (A) Graphical timeline of "5 day vaccination model" in which mice were first administered with $1x10^6$ WT or Ag Neuro2a cells, then 5 days later, vaccinated with 150 μg of αCTLA-4 and/or $1x10^6$ Neuro2a-Id2-KD cells. (B) Using a 5 day post tumor challenge vaccination model from (A), mice treated with αCTLA-4 alone (n=5) resulted in failure of tumor to develop in 40% of mice, with a delay in tumor growth in one mouse. When used in conjunction with Neuro2a-Id2-KD cells, 60% of mice (n=10) either did not develop tumor, or were able to clear their established tumors. (C) In mice challenged with $1x10^6$ AgN2a cells, αCTLA-4 alone was unable to inhibit tumor growth (n=5), however when used in conjunction with Neuro2a-Id2-KD cell vaccine, 90% of mice either did not develop tumors, or were able to clear established tumor mass (n=10). (D) IVIS bioluminescent imaging of mice vaccinated as in (B) shows the presence of established tumor cells as early as 3 days post challenge, with clearance of large tumor burden in 40% of αCTLA-4 alone group and 60% of combined vaccinated group.

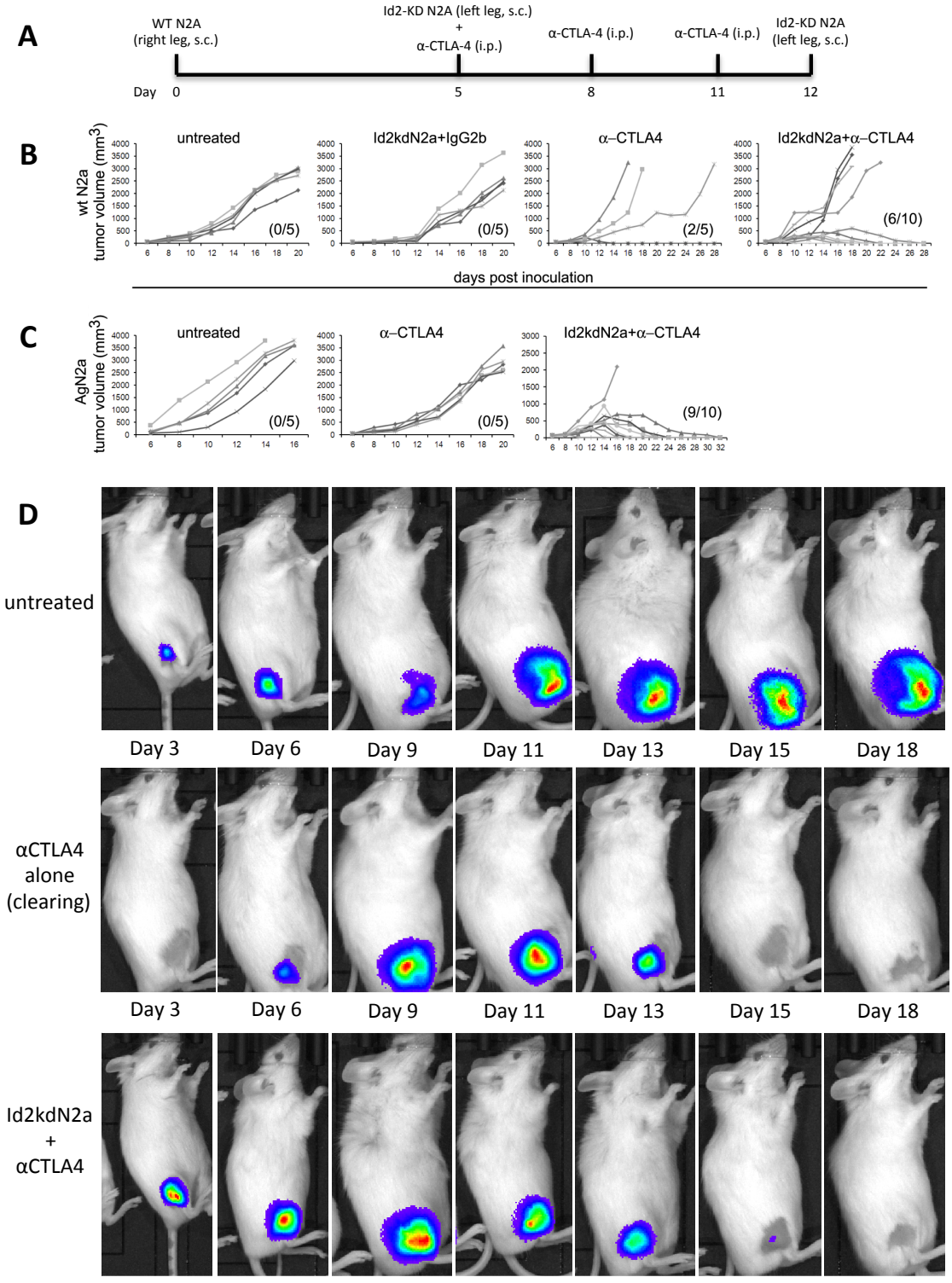
A
WT N2A
(right leg, s.c.)
Id2-KD N2A (left leg, s.c.)
+
α-CTLA-4 (i.p.)
α-CTLA-4 (i.p.)
α-CTLA-4 (i.p.)
Id2-KD N2A
(left leg, s.c.)
Day 0 5 8 11 12
B
wt N2a
tumor volume (mm3)
untreated
Id2kdN2a+IgG2b
α–CTLA4
Id2kdN2a+α–CTLA4
(0/5)
(0/5)
(2/5)
(6/10)
days post inoculation
C
AgN2a
tumor volume (mm3)
untreated
α–CTLA4
Id2kdN2a+α–CTLA4
(0/5)
(0/5)
(9/10)
D
untreated
αCTLA4
alone
(clearing)
Id2kdN2a
+
αCTLA4
Day 3
Day 6
Day 9
Day 11
Day 13
Day 15
Day 18

5.2.4 CD8+ T cells are essential for Neuro2a tumor clearance and depend on CD4+ T Helper cells

From the observation of uninhibited Neuro2a-Id2-KD cell growth in SCID and Nude mice, along with the amplification of vaccination effect when combined with anti-CTLA-4 previously presented, we hypothesized that T cells were primarily responsible for the clearance of Neuro2a tumors in this vaccination model. To test this concept, we depleted mice of individual T cell subsets via systemic introduction of antibodies for CD4, CD8, or NK1.1, before tumor inoculation and vaccination (Figure 14A). Depletion was confirmed via flow cytometric analysis of whole blood sampling. Depletion antibodies were administered every 96hrs during the vaccination process of the experiment. CD8+ T cell depleted mice were completely void of therapeutic effect induced by combined anti-CTLA-4 and Neuro2a-Id2-KD tumor cells, compared to non-depleted mice (Figure 14B). Additionally, 100% of CD8+ T cell depleted mice developed tumors at the site of Neuro2a-Id2-KD cell inoculation (Figure 14C). Mice depleted of NK1.1+ Cells were able to clear their WT tumors after therapy at a rate similar to non-depleted mice (Figure 14B). CD4+ T cell depleted mice initially showed no adverse reaction in their response to vaccination compared to non-depleted, with clearance of tumor in 75% of mice (Figure 14B). However all CD4 depleted mice developed WT Neuro2a tumors 4 weeks after inoculation.

To investigate whether this effect was from a resurgence of T regulatory cells upon completion of depletion, we harvested the tumors of CD4+ T cell depleted mice, and examined the TIL within. Flow cytometric analysis of TIL for CD45, CD4, and Foxp3 demonstrated no evidence of Foxp3+ cells (Figure 14D), indicating that delayed

tumor onset was not due to infiltration of Tregs at the site of the tumor. Taken together, this data proves CD8+ T cells as the primary immune responders responsible for clearance of Neuro2a tumors, but are dependent upon CD4+ T helper cells during the activation stage for a complete, robust response and clearance of Neuro2a.

Figure 14. T cell immunity required for tumor eradication following combination therapy. (A) Timeline of depletion and vaccination methods. Mice were systemically depleted of CD4, CD8, or NK1.1 cells before tumor challenge, and subjected to combination αCTLA-4 and Neuro2a-Id2-KD cell 5 day post tumor challenge vaccination model (n=5 in all groups). Depletion confirmed by flow cytometry of whole blood. (data not shown) (B) All groups of mice began depletion of immune cell subsets 1 day prior to administration of $1x10^6$ WT Neuro2a cells. Depletion antibodies were administered 3 more times, every 96 hrs. Vaccination was carried out as detailed in Figure 13, using a combination of αCTLA-4 and $1x10^6$ Neuro2a-Id2-KD cells, starting 5 days after tumor challenge. (C). Growth of Neuro2a-Id2-KD cells in immune depleted mice from (B). All CD8 depleted mice developed Neuro2a-Id2-KD cells at the site of vaccination. (D) TIL from delayed tumors of the CD4 depleted mice were evaluated via flow cytometry for CD45, CD4, and Foxp3.

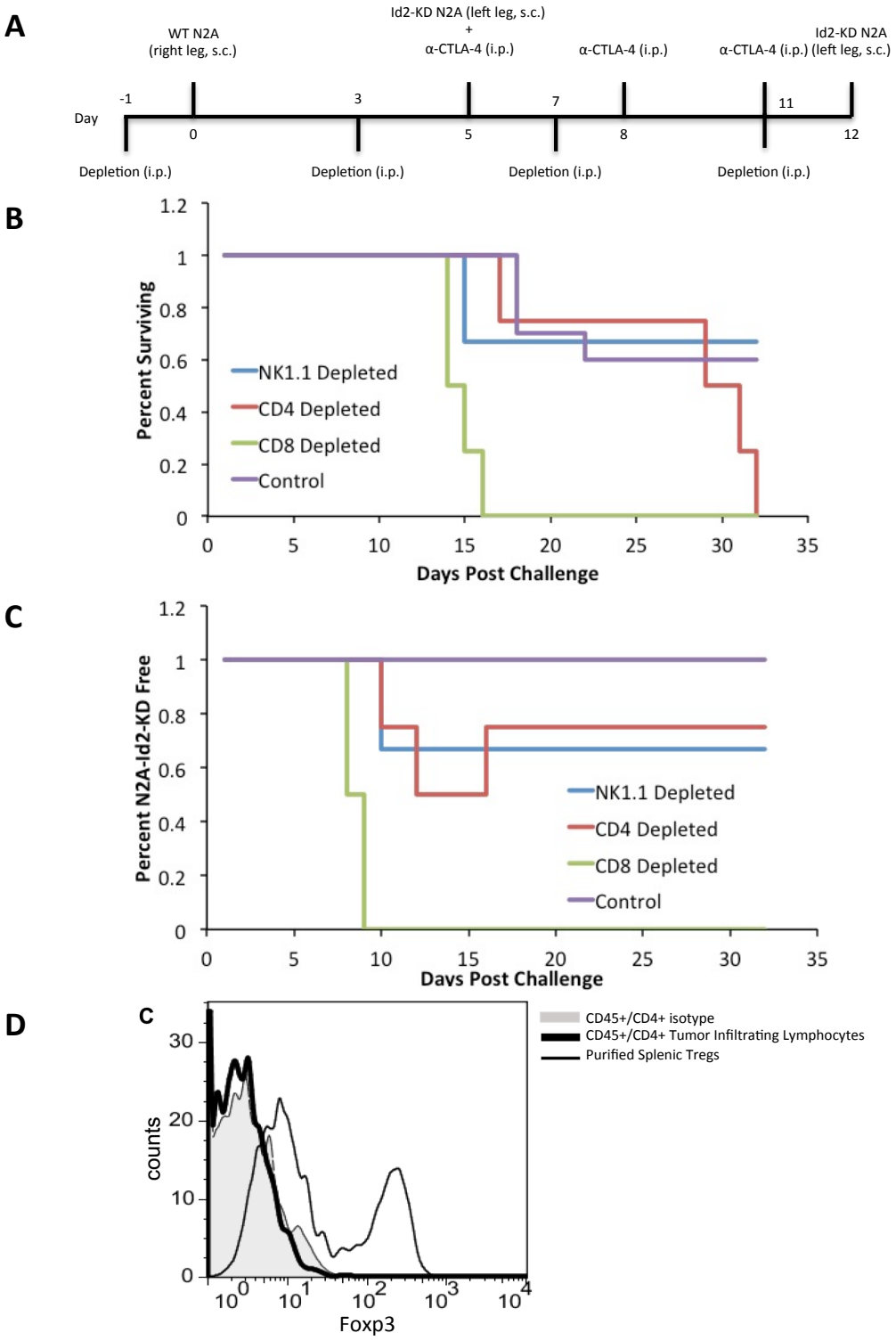
A
WT N2A
(right leg, s.c.)
Id2-KD N2A (left leg, s.c.)
+
α-CTLA-4 (i.p.)
α-CTLA-4 (i.p.)
Id2-KD N2A
α-CTLA-4 (i.p.) (left leg, s.c.)
Day
-1
0
3
5
7
8
11
12
Depletion (i.p.)
Depletion (i.p.)
Depletion (i.p.)
Depletion (i.p.)
B
Percent Surviving
NK1.1 Depleted
CD4 Depleted
CD8 Depleted
Control
Days Post Challenge
C
Percent N2A-Id2-KD Free
NK1.1 Depleted
CD4 Depleted
CD8 Depleted
Control
Days Post Challenge
D
C
CD45+/CD4+ isotype
CD45+/CD4+ Tumor Infiltrating Lymphocytes
Purified Splenic Tregs
counts
Foxp3

5.2.5 CD8+ T Cells within tumor mass of vaccinated mice are functional and infiltrate in high numbers

Having demonstrated the role of CD8+ T cells in our attenuated therapeutic tumor vaccine model (Figure 14), we sought to analyze their role within the TIM. Comparing levels of lymphocyte infiltration in WT non-vaccinated tumors with those that underwent Neuro2a-Id2-KD cell and anti-CTLA-4 vaccination (Figure 15A), we found a significant increase in CD8+ T cell infiltration in vaccinated mice (Figure 15B). CD4+ T cells levels also increased, though not statistically significantly (Figure 15C). Previous studies using similar mouse models show that CD8+ T cells within the TIM are nonfunctional, or suppressed in their effector function, but can regain their function within hours of *ex vivo* recovery (27). To test if CD8+ TIL from shrinking tumors in vaccinated mice demonstrated uninhibited CTL effector function, tumors were harvested and CD8+ T cells were purified from the tumor digestion. These TIL were then assessed for their specific cytotoxic function immediately *ex vivo* by chromium^{51} release assay. The cells purified from mice having undergone combination-vaccination displayed significantly higher levels of cytotoxicity against WT Neuro2a cells, immediately *ex vivo* (Figure 15D), compared to TIL pooled from tumors of non-vaccinated mice, which displayed no level of cytotoxicity (30:1 *p=0.028, 10:1 **p=0.007, 3:1 **p=0.003). The high functionality of these cells and increased infiltration within the TIM further emphasizes the role of CD8+ T cells in the clearance of Neuro2a tumors in our combined-vaccination model.

Figure 15. Enhanced *in vivo* immune response mediates tumor clearance. (A) Flow cytometric gating strategy used to define CD45+ lymphocytes within whole tumor digestion. Analysis of CD45+ events established by comparison with isotype control. (B) Flow cytometric analysis of TIL harvested from tumors in non-vaccinated versus vaccinated mice. Gating of CD45+ events, as shown in (A), on total cells from enzymatic tumor digestion. CD4+ and CD8+ gates were established by comparison with respective isotype controls. Results representative of (n=5) mice. (C) Quantification of infiltration from non-vaccinated and vaccinated mouse tumors shows a significantly (n=5 mice per group, * $p<0.02$) larger CD8+ T cell influx in vaccinated mouse tumors compared to non-vaccinated, as well as a large but not significant increase in CD4+ cells. (D) Cytotoxic effector function of CD8+ T cells assessed immediately *ex vivo* via 4 hr chromium release assay against cognate tumor cells demonstrates significantly higher levels of specific cytotoxicity (30:1 * $p=0.028$, 10:1 ** $p=0.007$, 3:1 ** $p=0.003$), without the requirement of recovery time, compared to TIL from non-vaccinated mice. Samples run in triplicate, error bars represent SD.

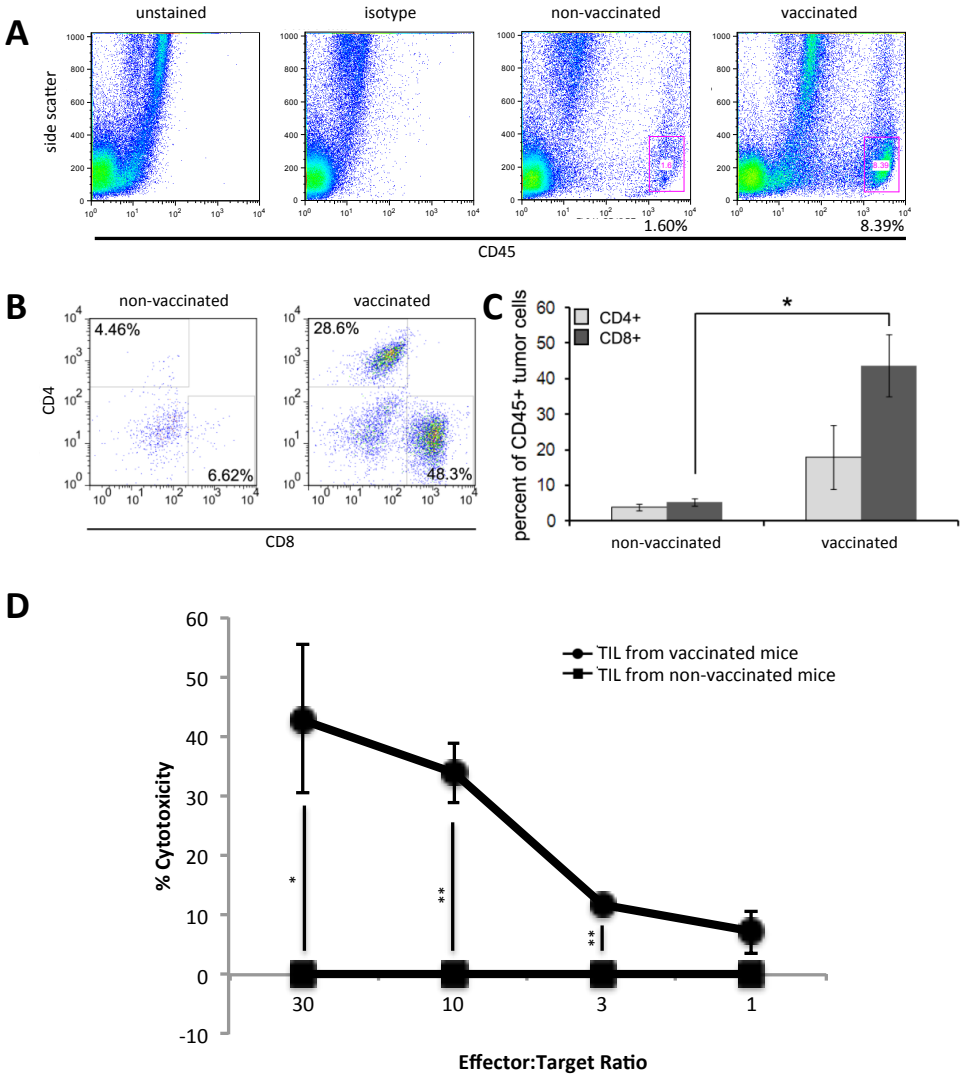
A
unstained
isotype
non-vaccinated
vaccinated
side scatter
1.60%
8.39%
CD45
B
non-vaccinated
vaccinated
4.46%
6.62%
28.6%
48.3%
CD4
CD8
C
CD4+
CD8+
percent of CD45+ tumor cells
non-vaccinated
vaccinated
D
TIL from vaccinated mice
TIL from non-vaccinated mice
% Cytotoxicity
Effector:Target Ratio
30
10
3
1

5.3 Conclusions

Using a combination-vaccine of checkpoint inhibitor blockade via anti-CTLA-4, and attenuated live tumor cells, via lentiviral shRNA knockdown of Id2, we have generated a potent immune response towards Neuro2a, capable of clearing established tumors. While no evidence of increased phagocytosis via macrophages is observed, we show via *in vivo* depletion of independent T cell subsets, this immune response to be dependent upon CD8+ T effector cells, which require the assistance of CD4+ T helper cells during activation of immune response. Using flow cytometry, we demonstrated a significant increase in CD8 infiltration of tumors in vaccinated mice, and through chromium^{51} release assay, demonstrate cytotoxic effector activity toward Neuro2a cells of cognate tumor origin immediately *ex vivo*. Taken together, these data provide compelling evidence of cytotoxic T-cell immunity in a novel tumor cell vaccination strategy against Neuro2a.

CHAPTER 6: DEVELOPMENT OF CAR-EXPRESSING TREGS POSSESING ANTI-TUMOR ACTIVITY

6.1 Introduction

During the development of a tumor-specific immune response, CTLs primed against the tumor travel to the tumor mass and are cytotoxic to the tumor cells. These tumor infiltrating lymphocytes (TIL) however, are often suppressed in their function, once inside the TIM. Factors inducing suppression include cytokine and contact mediated suppression originating from both the tumor cells and Tregs, which are immune regulators recruited to the tumor mass. While these immunosuppressive components inhibit CTLs, Tregs in fact continue to function, and thrive in this environment (39, 56). Previous studies have demonstrated that Tregs inhibit CTLs through several mechanisms, including cytokine mediated suppression, contact and cytotoxic mechanisms (57-61). Previous work by others show that CTLs that display CARs against tumor specific proteins are able to target and overcome some of these immunosuppressive mechanisms, as they no longer require MHC I antigen presentation to their TCR (41, 82). They are most often however, unable to fully overcome the immunosuppressive factors within the TIM, leading to slower tumor growth but not clearance. Seeking to improve upon this concept, we hypothesized that Tregs would be ideal CAR cells for tumor directed therapy as they are both cytotoxic and function in the tumor immune-suppressive environment. We thus proposed to develop tumor targeted CAR bearing Tregs, taking advantage of their ability to function in the TIM, while converting their cytotoxic killing against the tumor mass itself, rather than the TIL.

6.2 Results

6.2.1 Rhabdomyosarcoma Tumor Infiltrating T Regulatory Cells Express Granzyme B

With the evidence from previous literature demonstrating that mice bearing tumors develop Tregs that express lytic molecules, we sought to investigate this phenotype in mice bearing our M3-9-M rhabdomyosarcoma cell line. Tregs of mice bearing M3-9-M tumors were investigated 2 weeks post tumor challenge for their levels of granzyme B in spleens, tumor draining lymph nodes (TDL) and the tumor mass itself. The gating of lymphocytes was determined from TDLs, as shown in Figure 16A. Granzyme B levels were low for CD8+ (3.2%) and Foxp3+ (4.7%) cells in spleens of tumor bearing mice (Figure 16B), as well as in CD8+ (3.5%) and Foxp3+ (7.9%) cells of TDLs, (Figure 16C).

To investigate the levels of granzyme B in Tregs specifically within the tumor digest, we used the MACS Treg splenic purification kit on the tumor digests to remove CD8+, CD11b+, CD45R+, CD49b+ and Ter-119+ cells, thereby leaving only CD4+ cells within the tumor digestion. The remaining cells were then gated on CD25 expression (Figure 17A). Doing this, we found that cells staining positive for Foxp3 were also 84.3%+ for granzyme B (Figure 17B). This finding is consistent with previous work describing the induction of lytic Tregs in tumor bearing mice, and encouraging for the use of CAR-bearing Tregs in an adoptive transfer immunotherapy model.

Figure 16. Tregs do not express Granzyme B *in vivo* within spleen and TDL of tumor bearing mice. Flow cytometric analysis of Granzyme B (GZMB) levels in organs of M3-9-M tumor bearing mice. (A) Representative gating of lymphocytes in TDL, comparing FSC versus SSC. This lymphocyte gate was applied to splenic and TDL groups in (B) and (C). (B) Comparison of CD8+ and Foxp3+ lymphocytes found in spleens of M3-9-M tumor bearing mice. Spleens were excised and homogenized into a single cell suspension before labeling with antibodies. Gating on lymphocytes was determined as shown in (A), CD8+, Foxp3+, and GZMB+ events were determined by comparison with their respective isotype controls. (C) Comparison of CD8+ and Foxp3+ lymphocytes found in TDL of M3-9-M tumor bearing mice. TDLs were excised and homogenized into a single cell suspension before labeling with antibodies. Lymphocyte gating, and positive staining for CD8, Foxp3, and GZMB were determined as described in (A) and (B).

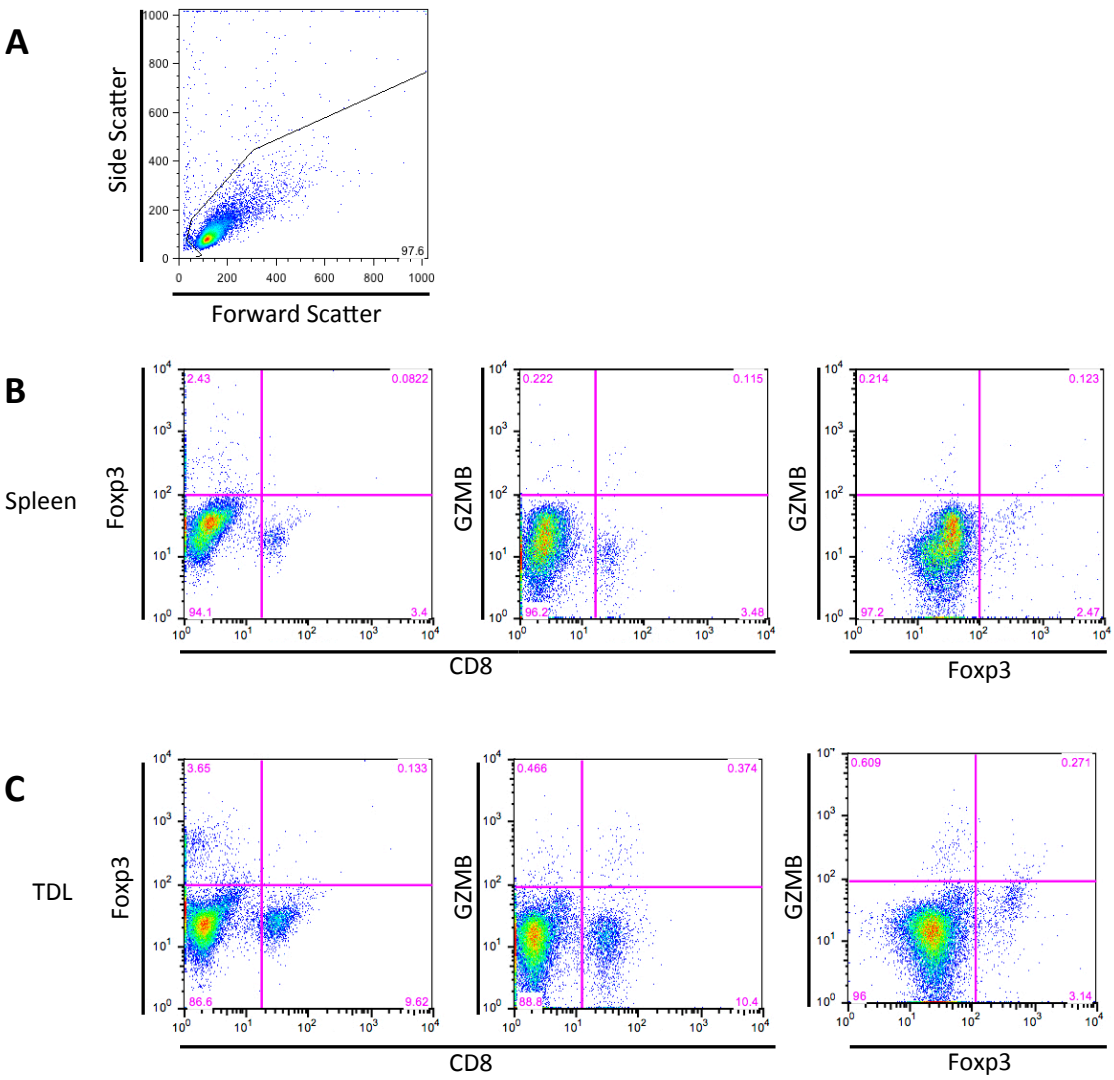
A
Side Scatter
Forward Scatter
97.6
B
Spleen
Foxp3
CD8
2.43
0.0822
94.1
3.4
GZMB
CD8
0.222
0.115
96.2
3.48
GZMB
Foxp3
0.214
0.123
97.2
2.47
C
TDL
Foxp3
CD8
3.65
0.133
86.6
9.62
GZMB
CD8
0.466
0.374
88.6
10.4
GZMB
Foxp3
0.609
0.271
96
3.14

Figure 17. Tregs express Granzyme B *in vivo* within tumor microenvironment. Flow cytometric analysis of Granzyme B (GZMB) levels within M3-9-M tumors. (A) Gating on CD25+ events within tumor digestion, after enzymatic digestion, followed by removal of CD8+, CD11b+, CD45R+, CD49b+, and Ter-119+ cells, then positive selection for CD25+ cells upon remaining tumor digestion. CD25+ gating was determined by comparison to isotype control. (B) Flow cytometric analysis of CD8+, Foxp3+ and GZMB+ events in CD25+ gate from (A). CD8+, Foxp3+, and GZMB+ events were determined by comparison with isotype controls, and splenic populations (Figure 16).

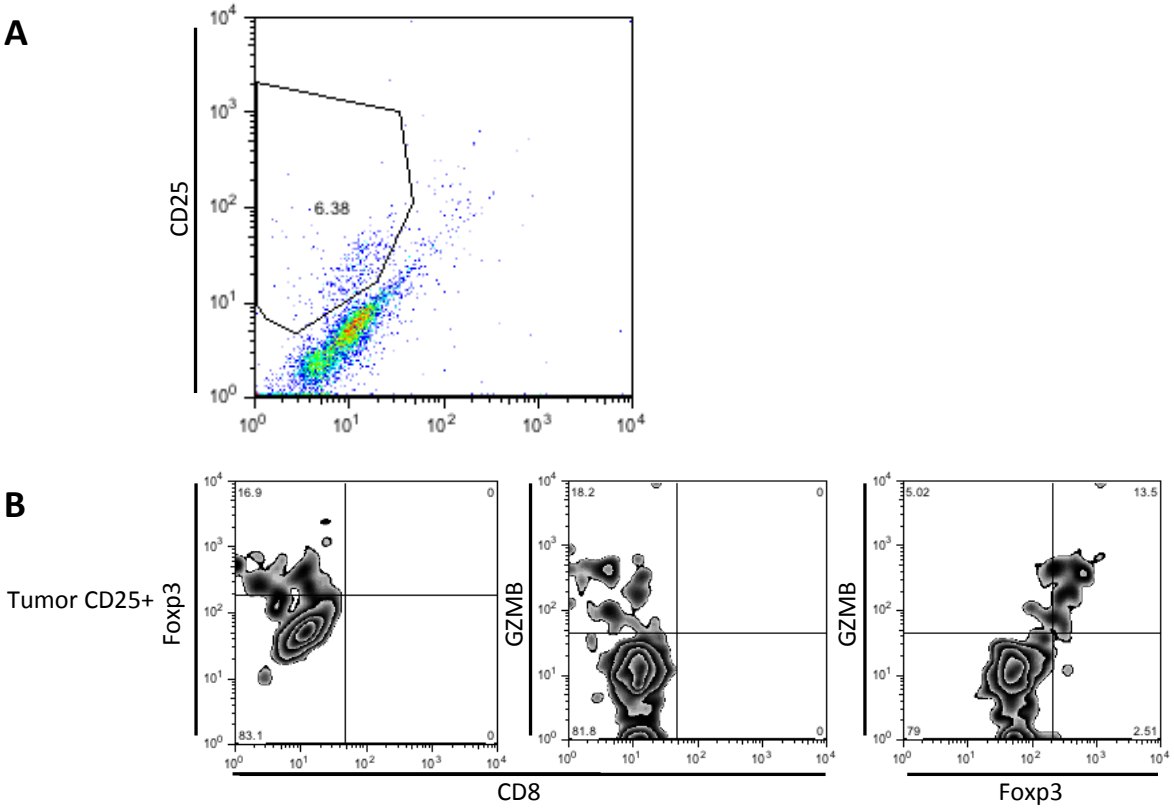
A
CD25
6.38
B
Tumor CD25+
Foxp3
16.9
83.1
CD8
GZMB
18.2
81.8
GZMB
5.02
13.5
79
2.51
Foxp3

6.2.2 Generation of Efficient CAR Transduction of CTLs and T Regulatory Cells

In order to generate Tregs that express CAR on their surface, we first developed a system of retroviral production and transduction in our laboratory. Choosing to generate a system that would be applicable to several solid tumor types, we used a CAR against VEGFR-2, an endothelial marker expressed during angiogenesis, a process essential for solid tumor growth and survival. The laboratory of Nicholas P. Restifo, MD (NCI, Bethesda, MD), generously donated plasmids for MSGV-SP6-mCD8-28BBZ (SP6), a CAR specific for the hapten 2, 4, 6-trinitrobenzenesulfonic acid, to serve as a non-specific control, and a VEGFR2-specific CAR, MSGV-DC101-mCD8-28BBz (DC101). Additionally, a plasmid containing GFP (PEAK12-GFP) was used as a control for transfection/transduction. These plasmids were co-transfected via lipofectamine 2000 along with pcL-ECO, in Platinum-E cells, and assessed for their transfection efficiency via flow cytometry. To measure DC101 expression, a chimeric peptide composed of a segment of VEGFR-2, linked to a segment of human Fc was added to cells. This peptide is bound at the VEGFR-2 domain by DC101 on the surface of cells. This was then followed with antibody specific for human Fc to the tube, to bind the second segment of the chimeric peptitde. The efficiency of transfection remained consistently around 40% for DC101 CAR, compared to >70% for GFP (Figure 18A). The transfected cells from each group were able to produce viral supernatant that could transduce splenocytes, having been activated for 18 hrs and expanded for 24 hrs, at a consistent efficiency around 70%, as assessed again by flow cytometry as early as 48 hrs post transduction (Figure 18B).

Seeking to translate this process into Tregs, virus supernatant collected from transfected Plat-E cells was used to transduce Tregs, purified from naïve spleens, that had been activated for 72 hrs with platebound anti-CD3, anti-CD28, and IL-2, and further expanded for 24 hrs in IL-2. Tregs stimulated under this condition were transduced with DC101 at an efficiency of 70% (Figure 18C), consistent with splenic populations assessed 24 hours post transduction. To be certain that transduced cells were in fact Tregs, the cells were examined post transduction for their expression of Foxp3, with 70% of cells remaining Foxp3+ (Figure 18D). Expression of DC101 and Foxp3 cannot be demonstrated in the same population, as fixing of sample cells disrupts the interaction of DC101 with the chimeric peptide used for DC101 labeling.

Figure 18. Expression of DC101 CAR in full splenic and Treg populations. (A) Transfection efficiency of PEAK12-GFP and DC101 in Plat-E producer cells. Cells were transfected for 6hrs, then allowed to grow for 48 hrs before harvesting viral supernatant, and collecting cells for flow cytometry. (B) Transduction efficiency of full splenic populations using virus produced from cells in (A). Splenocytes were stimulated for 24 hours with 2C11 supernatant (as described in Methods), then further expanded in 2% v/v IL-2 for 12 hrs. Transduction efficiency was measured 48 hrs post transduction. (C) Transduction efficiency of Tregs using virus produced from cells in (A). Tregs were stimulated for 72 hrs in α-CD3, α-CD28 and 2% v/v IL-2 (as described in Methods), then further expanded in 2% v/v IL-2 for 12 hrs. Transduction efficiency was measured 48 hrs post transduction. (D) Foxp3 expression of transduced cells in (C). Positive staining for Foxp3+ cells established from isotype controls. Double staining for Foxp3+ and DC101+ events is not possible, as the fix/perm process for intracellular staining disrupts the DC101-chimeric peptide-antibody interaction (described in results).

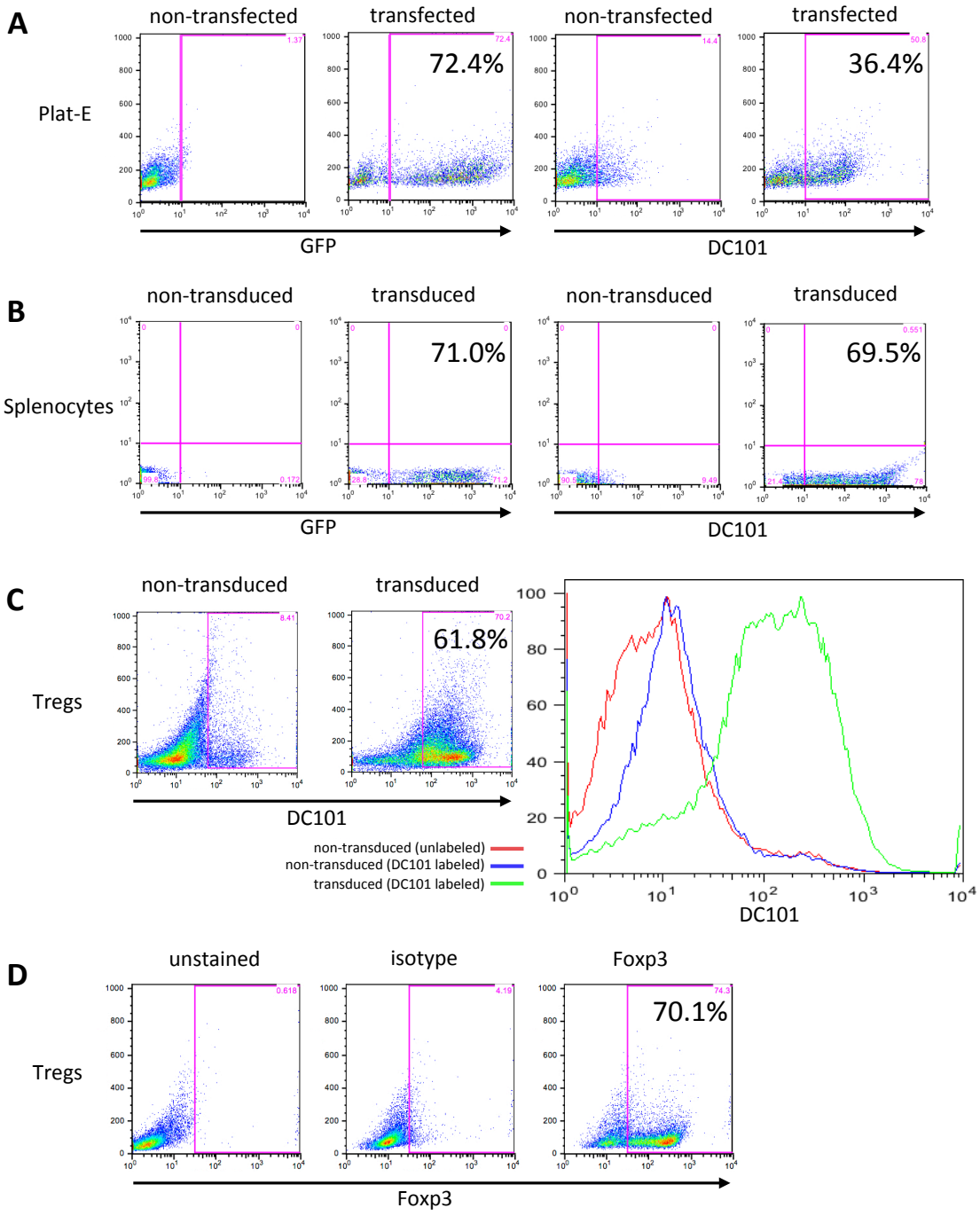
A
non-transfected
transfected
non-transfected
transfected
Plat-E
72.4%
36.4%
GFP
DC101
B
non-transduced
transduced
non-transduced
transduced
Splenocytes
71.0%
69.5%
GFP
DC101
C
non-transduced
transduced
Tregs
61.8%
DC101
non-transduced (unlabeled)
non-transduced (DC101 labeled)
transduced (DC101 labeled)
DC101
D
unstained
isotype
Foxp3
Tregs
70.1%
Foxp3

6.2.3 CAR-bearing CTLs are target specific in vitro

To determine the ability of CTLs to kill their targets specifically via CAR redirection, transduced splenocytes were subjected to standard chromium release assays. DC101 CAR transduced splenocytes were able to efficiently kill their specific VEGFR-2 expressing targets, MS1, *in vitro* (Figure 19A), whereas non-transduced, GFP or SP6 transduced control cells were not cytotoxic. Comparing redirected cytotoxicity levels against L1210, transduced and non-transduced splenocytes were able to kill at similar levels (Figure 19B), indicating that transduction did not impair cytotoxic function. However, CAR-mediated killing displayed lower levels of cytotoxicity than TCR-redirected killing, as measured through chromium release assay.

Figure 19. DC101 transduced splenocytes display VEGFR-2 specific cytotoxicity. (A) DC101 CAR-directed lytic activity of splenocytes against MS1 cell line, which express VEGFR-2, assessed via 4hr standard chromium release assay. Splenocytes expressing DC101 were generated as shown in Figure 16. Samples run in triplicate. Error bars represent SD. (B) Redirected lytic activity of transduced splenic populations from (A) against L1210 cells in 4 hr standard chromium release assay reveals no inhibition of lytic effector function from transduction process. Samples run in triplicate. Error bars represent SD.

A

MS1

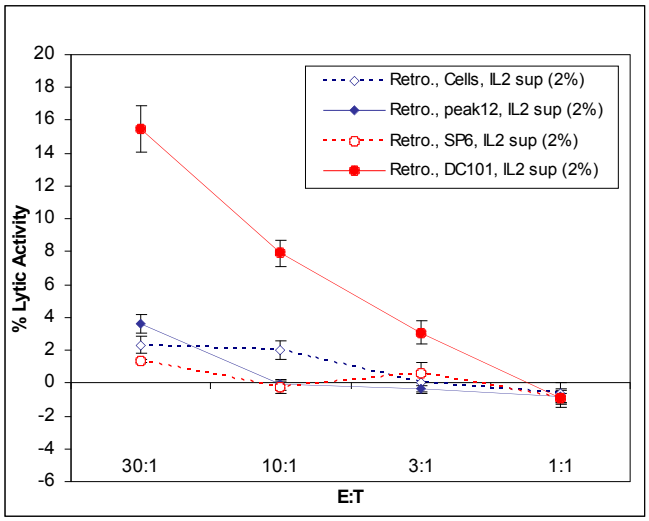
% Lytic Activity
20
18
16
14
12
10
8
6
4
2
0
-2
-4
-6
30:1
10:1
3:1
1:1
E:T
Retro., Cells, IL2 sup (2%)
Retro., peak12, IL2 sup (2%)
Retro., SP6, IL2 sup (2%)
Retro., DC101, IL2 sup (2%)

B

L1210

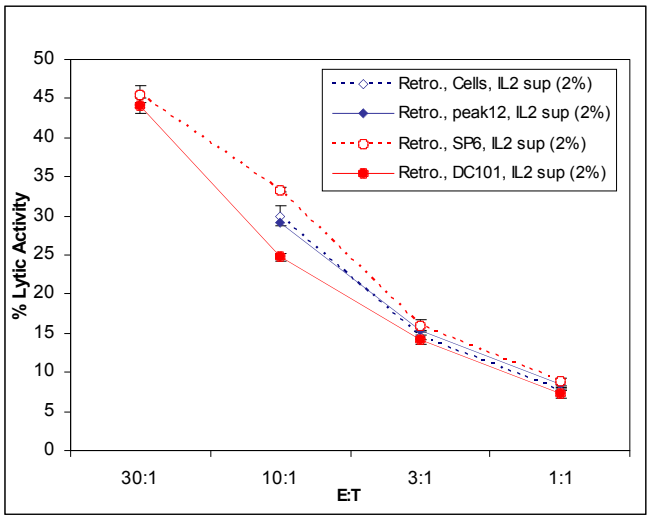
% Lytic Activity
50
45
40
35
30
25
20
15
10
5
0
30:1
10:1
3:1
1:1
E:T
Retro., Cells, IL2 sup (2%)
Retro., peak12, IL2 sup (2%)
Retro., SP6, IL2 sup (2%)
Retro., DC101, IL2 sup (2%)

6.2.4 T Regulatory Cells Demonstrate Lower Levels of Cytotoxicity Compared to CTLs in vitro

In order to investigate Treg cytotoxicity, Tregs were purified from naïve spleens, and stimulated *in vitro* via platebound anti-CD3, anti-CD28 and IL-2 for 72 hrs, then subjected to standard chromium release assay. Compared to cytotoxicity of CTLs from the same spleens, Tregs displayed significantly lower levels of cytotoxicity (Figure 20). Seeking to increase their levels of cytotoxicity, Tregs were subjected during stimulation to IFNα (Figure 21A) or IL-12 (Figure 21B), known inducers of lytic molecules (161). While these cytokines were able to increase the cytotoxicity and granzyme B levels of CTLs, they induced no change in cytotoxic effect of Tregs. In contrast to IFNα or IL-12, TGF-β1 is a known suppressor of CTL function, including cytotoxicity and proliferation. However TGF-β1 is also known to be one of the critical cytokines for induction of Treg function, and is highly abundant in the TIM of several forms of cancer. Seeking to replicate this effect of the TIM, TGF-β1 was added to CTLs and Tregs during stimulation. As anticipated, CTL proliferation and cytotoxicity was inhibited, but interestingly, had no beneficial effect on proliferation or cytotoxicity of Tregs (Figure 21C).

Figure 20. *in vitro* stimulated Tregs display lower levels of cytotoxicity than CTLs. CTLs and Tregs, stimulated in the presence of αCD3, αCD28, and 2% v/v IL-2 for 48 and 72 hrs, respectively, were assessed for their cytotoxic effector function against L1210 cells via redirected 4 hr standard chromium release assay. Figure representative of (n=4) experiments. Samples run in triplicate. Error bars represent SD. CD8+ T cells displayed significantly higher lytic activity (100:1 ***p=0.0018, 30:1 ***p=0.0012, 10:1 ***p=0.0003, 3:1 *p=0.02).

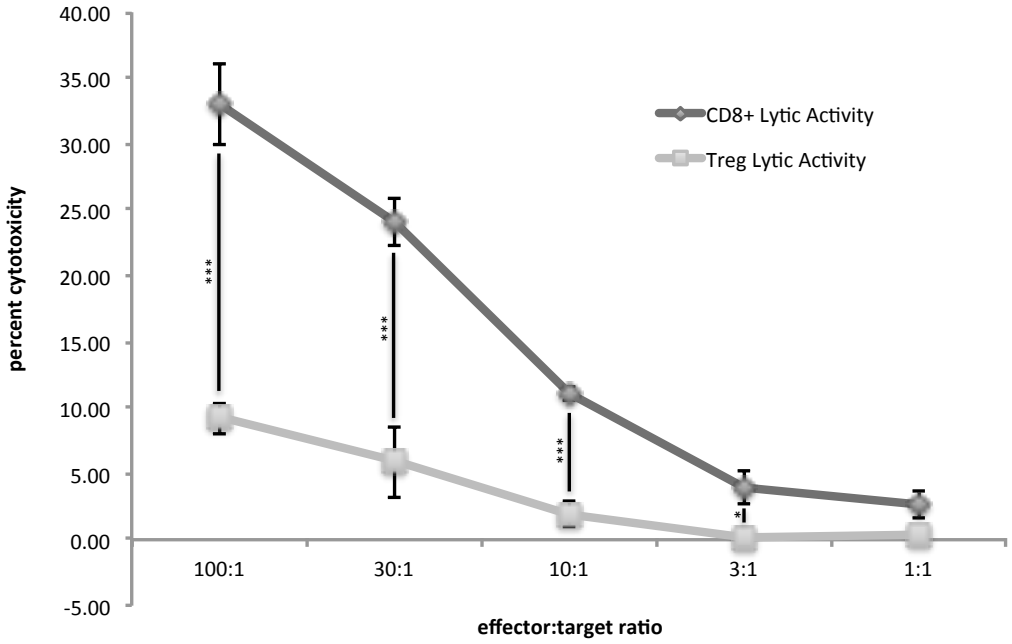
40.00
35.00
30.00
25.00
20.00
15.00
10.00
5.00
0.00
-5.00
percent cytotoxicity
CD8+ Lytic Activity
Treg Lytic Activity
***
***
***
*
100:1
30:1
10:1
3:1
1:1
effector:target ratio

Figure 21. Cytokines do not Enhance Treg Proliferation or Effector Function. Attempting to enhance Treg cytotoxic effector function, CTLs and Tregs were stimulated as mentioned previously (Figure 18), with additions of IFNα (A), IL-12 (B) and TGF-β1 (C) and assessed for proliferation and cytotoxicity. (A) CD8+ and CD4+/CD25+ cells were stimulated via α-CD3, α-CD28 and 2% v/v IL-2 for 48 or 72 hrs, respectively, with or without IFNα. These cells were counted daily to assess proliferation, expressed as a percent of the original plated amount. At 72 hrs, all populations were collected and either assessed for cytotoxicity via redirected 4 hr standard chromium release assay against L1210 cells, or kept in culture to be further expanded. Expanding T cells were then cultured in 2% v/v IL-2, with or without IFNα, and counted daily. (B) CD8+ and CD4+/CD25+ cells were stimulated as in (A), with or without IL-12. Proliferation and cytotoxicity were assessed as in (A), and expanding T cells were cultured as in (A), with or without IL-12. (C) CD8+ and CD4+/CD25+ cells were stimulated as in (A), with or without TGF-β1. Proliferation and cytotoxicity were assessed as in (A). For all standard chromium release assays, samples were run in triplicate. Error bars represent SD.

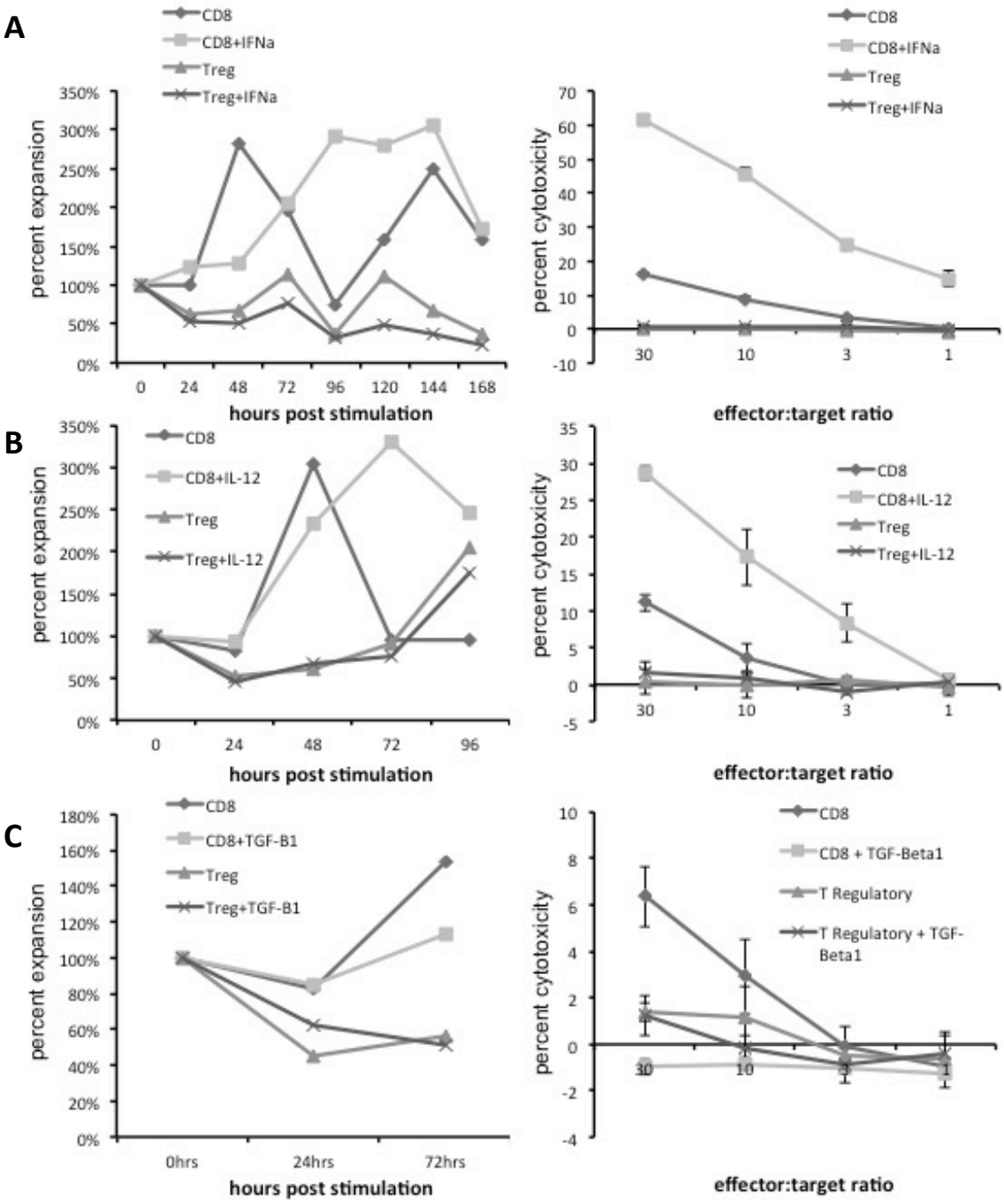
A
CD8
CD8+IFNa
Treg
Treg+IFNa
percent expansion
350%
300%
250%
200%
150%
100%
50%
0%
0
24
48
72
96
120
144
168
hours post stimulation
CD8
CD8+IFNa
Treg
Treg+IFNa
percent cytotoxicity
70
60
50
40
30
20
10
0
-10
30
10
3
1
effector:target ratio
B
CD8
CD8+IL-12
Treg
Treg+IL-12
percent expansion
350%
300%
250%
200%
150%
100%
50%
0%
0
24
48
72
96
hours post stimulation
CD8
CD8+IL-12
Treg
Treg+IL-12
percent cytotoxicity
35
30
25
20
15
10
5
0
-5
30
10
3
1
effector:target ratio
C
CD8
CD8+TGF-B1
Treg
Treg+TGF-B1
percent expansion
180%
160%
140%
120%
100%
80%
60%
40%
20%
0%
0hrs
24hrs
72hrs
hours post stimulation
CD8
CD8 + TGF-Beta1
T Regulatory
T Regulatory + TGF-Beta1
percent cytotoxicity
10
8
6
4
2
0
-2
-4
30
10
3
1
effector:target ratio

6.3 Conclusions

We show here Tregs found within rhabdomyosarcoma M3-9-M tumors express granzyme B. Additionally, we present a method of transducing Tregs, enabling their expression of CARs, based off of a system that successfully transduces splenocytes, and enables for the redirection of their cytotoxicity in a CAR-specific manner. Furthermore, we demonstrate that Tregs display lower levels of cytotoxicity than CTLs *in vitro*, and that those levels are not enhanced via cytokine induction as they are in CD8+ T cells. These findings suggests that while CTL levels of cytotoxic potency may not be inducible *in vitro* or *ex vivo*, that in a clinical model, Tregs may be able to be transduced and reintroduced to the patient, and then develop lytic molecules after adoptive transfer.

CHAPTER 7: DISCUSSION

It is well established that while the body can mount immunity to cancerous aberrant cell growth, the response is frequently suppressed or evaded by the tumor. This immune response is most frequently dependent upon cytotoxic T lymphocytes (CTLs), cells that are responsible for the targeted destruction of compromised cells within the body, in cases such as viral infection or cancer. Pediatric tumors specifically have poorly understood immune responses, due to complications presented earlier, including a lack of available patient sample studies, and few known antigens, resulting in low immunogenicity. To better understand the immune responses generated by childhood cancers, we investigated the naturally induced CTL infiltration phenotype of primary pediatric tumor samples, from patients who had yet to undergo prior therapy. While some of the cancers investigated in patient samples displayed low levels of infiltration, consistent with mouse models of tumor infiltration, others displayed no infiltration. This may be as a result of poor presentation via antigen presenting cells, or perhaps a lack of tumor specific or associated antigens. It may also be due to poor homing of CTLs to the site of the tumor, or in the case of some tumors, immune privilege. In these cases, it may be beneficial to utilize methods of increasing antigen uptake and presentation, or inducing tumor infiltration by T cells. Examples of this include introduction of chemotactic molecules, or direct administration of lymphocytes, via adoptive transfer, discussed further below.

Several cancers also generate a Tumor Immunosuppressive Microenvironment (TIM), which uses multiple mechanisms to inhibit CTL effector function. These

mechanisms, as discussed previously, include secretion of immunosuppressive cytokines, contact mediated inhibition and induction of apoptosis, downregulation of antigen presenting mechanics, and recruitment of immune regulatory cells, which further employ the same immunosuppressive mechanisms. In mice this immune effector inhibition has been proven as transient, as upon removal of the tumor infiltrating lymphocytes (TIL) function is inhibited, but can recover within hours of *ex vivo* culture, absent of immunosuppressive factors (26, 27, 43). However, this transient inhibition has not been demonstrated in human tissue before, making our findings from a human Pilocytic Astrocytoma case novel, while implicating the importance and relevance of murine models of cancer immunotherapy, including our previously unexplored rhabdomyosarcoma model.

The infiltration of CD8+ T cells in Wilms' Tumor shown here is novel, but not surprising, as other studies have partially characterized the infiltrating cell types within Wilms' Tumors (162). CD3+ T cell infiltration has been demonstrated previously, showing a 50 fold higher incidence of T cells in kidney tumor tissue, as apposed to natural kidney tissue. However there has been no analysis for individual T cell subsets, which leaves the immune response characterization lacking. Wilms' Tumors do exhibit a TAA, WT1, which is found to be upregulated not only in Wilms', but in other cancer types as well, including oral squamous cell carcinoma, leukemia, epithelial ovarian cancer, and even in brain cancers such as glioblastoma, and astrocytoma (163-165). The existence of a known TAA, and the presence of T cells within Wilms' Tumors, implicates that the body is recognizing and reacting to the cancer. However this immune response is insufficient, perhaps being shut down by factors such as Tregs, that may make up another

portion of the CD3+ cells within the TIM. Potentially associated with the T-cell infiltration observed in Wilms' tumors, these tumors are one of the most successfully treated in childhood cancer with survival well over 90% (166).

While it has long been thought that the blood brain barrier (BBB) results in the brain being seen as an immune privileged environment, recent studies have shown otherwise. It seems that in cases of malignancy, the BBB can be compromised or disrupted, allowing for immune cell infiltration, and furthermore, that resident microglia can even act as non-traditional APCs (167-171). In many cases of high-grade glioblastoma and astrocytoma, positive survival prognosis for intracranial cancer patients is associated with the presence of CD8+ T cells (172, 173). There is however, also evidence of immune suppression through increased levels of IL-10 and CTLA-4 (173). This correlates with our evidence of CD8+ infiltration, and for the recovery of CTL effector function in astrocytoma-purified TIL. Whether these TIL are specific for WT1, or some other TAA remains uncertain. It does however, prove positive that activated lymphocytes can home to the tumor site, encouraging the development of immunotherapies in the fight against brain cancers.

In cases of children with OMS, which present with Neuroblastoma, patients also present with a far more favorable outcome than those without OMS. It has long been suggested that their syndrome is the result of an autoimmune response to the developing tumor (174-176). Our findings here indicate that there is an impressive infiltration of CD8+ cells within the tumor mass, as well as the presence of other immune cell types, as compared to non-OMS cases of Neuroblastoma. This correlates with evidence that children with several different types of cancer, including Neuroblasoma, exhibit

favorable survival outcomes when associated with immune cell infiltration and especially CD8+ cells (177-179). Though OMS has not been previously defined in mice, it is important to note that with our vaccine-induced immune response, despite a rapid, specific, and complete tumor rejection, mice demonstrated no signs of OMS-like, or other autoimmune complications. While these mice have not been specifically tested for immune related adverse effects, they continue to look healthy, as they are followed for months after tumor rejection. Preliminary data from tumor rechallenge, 6 months after initial challenge and vaccination, demonstrates inhibition of tumor growth in 100% of mice so far, implicating the generation of a memory immune response, though these experiments are currently still in progress.

Several forms of tumor vaccines already exist, some with promise, and others demonstrating less success. These vaccines range from protein or antigen peptides, antigen loaded DCs, to live cell vaccines, and checkpoint blockade, as presented here. Other tumor vaccines for virally induced cancers use attenuated virus methods, such as the Human Papilloma Virus vaccine against cervical cancer, under the brand name Cervarix (159, 180). Another vaccine seeing success includes the checkpoint blocker ipilimumab, a mab against CTLA-4, branded by Bristol-Myers Squibb, which has demonstrated potent anti-tumor effects and increased patient survival in stage III human clinical trials (156-159). This led to ipilimumab receiving FDA approval in 2011 for the treatment of metastatic melanoma. Similar in nature to blocking CTLA-4, mabs against PD-1 or PD-L1 are gaining ground and undergoing clinical trials in the treatment of solid tumors and hematologic malignancies (156, 159, 160). Given the nature of immune modulators that block inhibitory signal receptors on T cells, it is reasonable to suspect

that these mab therapies would work well across several forms of cancer, and even better when immune cells are provided an antigen, such as in our whole tumor cell vaccine neuroblastoma model.

Live cell vaccines have shown some forms of application, most notably GVAX, which is designed to treat prostate cancer. GVAX uses a combination of two irradiated prostate cancer lines, one of which is more immunotolerant than the other (159, 181). These cells also secrete granulocyte-macrophage colony stimulating factor (GM-SCF), further boosting the immune response to the cellular inoculation. However, while correlative studies implicate the induction of an immune response, GVAX has failed to demonstrate a patient survival increase in clinical evaluation (159, 181, 182).

Our live cell vaccine work here differs, in that the cells are attenuated, and can be irradiated as well, to improve safety while still retaining their immunogenicity. However, the immune response that is induced is naturally driven, lacking no additional cytokine stimulation, and potent enough to drive immune dependent eradication of established tumors, via targeting of a key RAP component. While the mechanism for immunogenicity in N2a-Id2-KD cells is unknown, it may be a result of factors including improved antigen cell uptake and presentation, loss of immune-evasive or immune-suppressive mechanisms, or a combination of multiple factors (Figure 22). While Id2 is the predominant player of RAP in N2a cells, our work in other cell lines indicates that Id1 or Id3 may play a larger role in their plastic transitioning. This implies that in other lines, the attenuated-immunogenic phenotype may be achieved via KD of Id1 or Id3 instead. Conversely, the attenuated-immunogenic phenotype may not be obtainable in lines other than N2a, and research to determine this is underway. Alternatively,

determining the mechanisms of immune-evasion and/or immune-suppression, upon Id2-KD of N2a cells could lead to methods of targeting these pathways, independent of Id protein KD.

Figure 22. Schematic hypothesis of Neuro2a-Id2-KD vaccination mechanism. (A) When challenged with Neuro2a tumor cells, a naïve mouse develops a weak natural immune response. This is due to the immune suppressive and evasive properties of Neuro2a, as well as its lack of tumor specific antigens. The immune response generated is unable to clear the tumor, and the mouse eventually dies of tumor burden. (B) When naïve mice are challenged with Neuro2a, and administered Id2-KD cells after development of WT tumor, the Id2-KD cells provide a much higher level of antigen expression, through which the immune system develops a stronger, tumor-specific effector T cell response. Through co-administration of αCTLA-4 with Id2-KD cells, negative stimulation signals during T cell priming and activation are blocked, leading to an effector response able to further overcome suppression of development and degranulation.

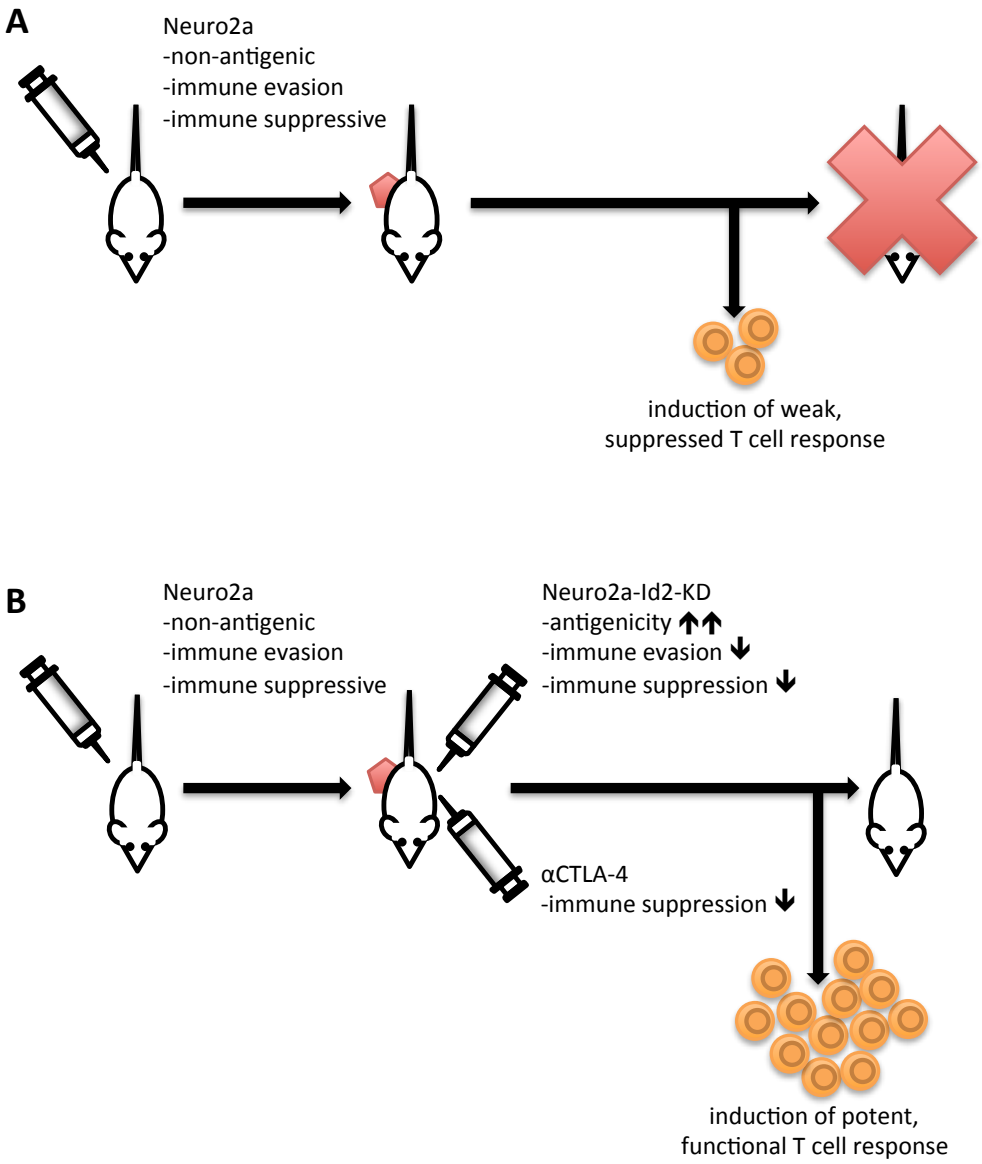
A
Neuro2a
-non-antigenic
-immune evasion
-immune suppressive
induction of weak,
suppressed T cell response
B
Neuro2a
-non-antigenic
-immune evasion
-immune suppressive
Neuro2a-Id2-KD
-antigenicity ↑↑
-immune evasion ↓
-immune suppression ↓
αCTLA-4
-immune suppression ↓
induction of potent,
functional T cell response

Adoptive cell therapies (ACT) have shown much promise in the treatment of cancer, and are in clinical use in specialized centers. These ACTs usually involve the removal of a patient's lymphocytes, followed by *ex vivo* expansion via introduction of growth factors and IL-2, and eventual reinfusion to the patient. This method has been improved upon in more recent years, with the introduction of CARs to the ACT process. The CARs, that are able to transmit the TCR activation signal upon recognition of CAR target proteins, are introduced to the patient's lymphocytes *ex vivo*, and then reintroduced to the patient. There they activate and proliferate *in vivo*, upon introduction to their CAR specific protein. CAR ACT is shown to be effective in clearing tumor burden and induction of a memory response to target antigens. Clinically, they have proven successful in the clearance of CD19 B cell malignancy, and work in murine models has proven successful when targeting solid mass tumors via angiogenic markers, such as VEGFR-2. This latter method deviates from the targeting of tumor specific antigens, by instead targeting the newly developing vasculature required for most solid tumors to survive, thereby allowing the CAR ACT to target multiple tumor types, that may or may not carry their own tumor specific antigens.

Regardless of CAR targets, there are some drawbacks to CAR ACTs. With the targeting of molecules outside the context of MHC I presentation, auto-reactivity can develop where non-cancer cells express the same proteins as the tumor cell targets. Additionally, with tumor cells being plastic as their environment dictates, loss of antigen can occur, resulting in the inability of ACT to target the tumor. It has also been observed that toxicity can be an issue, given the massive cytokine storm induced through the

activation of such a large volume of T cells. Work on resolving these toxicities and auto-reactivity will need to be addressed in the future.

While CARs aid in the ability to improve lymphocyte targeted killing of tumor cells, there are still factors within more immune-suppressive tumor types that serve to thwart their success. Cytokines like TGF-β1 and IL-10 are dominant in the TIM, as are immune regulating ligands like FasL, PD-L1, and other B7 molecules that can bind CTLA-4 on TIL. These factors come from the tumor cells themselves, as well as Tregs, that are actively recruited to the TIM. While all of these factors serve to shut down the effector function of CTLs, they contribute to the ability of Tregs to function and thrive at the same time. It also seems that factors in the TIM not yet determined, lead to the generation of lytic Tregs, which use targeted cytotoxicity to regulate effector CTLs. It has also been demonstrated that lytic Tregs can travel into tumor draining lymph nodes, to target dendritic cells for destruction, thereby preventing tumor antigen presentation to CTLs (57). Given their functionality within the TIM, we proposed and generated a system for Treg CAR ACT. While unable to induce lytic activity at the level of CTLs *in vitro*, our new findings in murine rhabdomyosarcoma, in agreement with others tumor models, demonstrate that Tregs at the site of the tumor do express granzyme B, indicating that *ex vivo* stimulation of Tregs before ACT may not be required. Furthermore, despite exhibiting lower levels of cytotoxicity, as compared to CTLs *in vitro*, the ability of Tregs to function naturally within the TIM may contribute a more effective, and longer maintained effect on reduction of tumor burden. This hypothesis will need to be evaluated in future studies.

Recent work has shown the induction of lytic Tregs in other disease states beyond cancer. Patients with chronic and acute Hepatitis C virus (HCV), as well as patients with resolved disease express high levels of Granzyme B+ Tregs (183). Furthermore, in cases of schistosome and HCV co-infection, Granzyme B becomes highly expressed in Tregs, while not shutting down CD8+ responder T cells (184). Separately, in rheumatoid arthritis patients, it has been demonstrated that Tregs specific for collagen type II antigen express Granzyme B, and significantly reduce incidence and clinical symptoms of disease, in both preventative and curative situations (185). Additionally, they are able to reduce the proliferation of antigen-specific effector CD8+ cells. In transplant studies, it is shown that Tregs are capable of suppressing effector function in CD8+ and CD4+ T effector cells, as well as CD8+ T memory cells, the effect of which could be abrogated in a perforin deficient mouse model. CD4+ T memory cells however, were still able to function, due to high levels of serine protease inhibitor-6 (Spi6), which inhibits the function of Granzyme B (186). Taken together, these data introduce new avenues for the acquisition of lytic Tregs, while remaining vague as to the disease characteristics inducing their lytic molecules.

Much less work has been done researching CAR redirection in Treg cells. One system employed the transduction of pan CD4+ T cells, with a CAR which also induced expression of Foxp3 in trans, thereby inducing the Treg phenotype (187). This method could be used in our system, to solve the dilemma of generating enough Tregs for adoptive transfer, while relying upon the TIM to induce the expression of lytic molecules. A separate method exists using adenovirus transduction, rather than lentiviral or γ-retroviral, which allows transfer of large genetic sequences up to 7kb (for comparison,

the DC101 containing plasmid used here was 7.2kb in total length) (188). Of note, is the ability to transduce lymphocytes before activating them, again allowing for the transduction of CAR to be carried out on a pan naïve CD4+ T cell population, before activating and converting them to a Treg phenotype. While this adenovirus transduction does not lead to chromosomal insertion of transferred genetic material, it could be used for preliminary studies *in vitro*, testing the ability of CARs to redirect Treg lytic function. A different study transduced human Tregs stimulated via Dynal CD3/CD28 beads, in the presence of IL-2 and Rapamycin was able to demonstrate efficient homing of anti-CD19-CAR transduced Tregs to the tumor site, where they are examined for their abilities to function efficiently in inhibition of CTL function (78). The stimulation method used however, as it contains Rapamycin, would be inhibitory to the ability of cells to generate CTL effector function. This is because Rapamycin, an inhibitor of IL-2 signaling via IL-2 receptor blockade, is shown to reduce CTL proliferation and the production of Granzyme B mRNA, and while IL-2 can be used to rescue this production, partial inhibition of degranulation still exists (189). These stimulation conditions could have masked any ability for CAR-transduced Tregs to develop lytic molecules during *in vitro* activation, and would need to be fully evaluated experimentally.

7.1 Future Studies

The confirmation of transient TIL inhibition in human patients which exhibit CTLs within their tumor mass confirms the clinical relevance of mouse models used in research. Future studies will involve continuing to evaluate the types of lymphocytes

present within human tumor masses, assessing their functional status, and overcoming their effector inhibition, to more effectively treat and overcome cancer in patients.

Hoping to prove the transient "on/off" phenomenon of inhibition in other cancers, we had harvested several different solid cancer types, however many of them proved to have little to no levels of CD8+ infiltration. Additionally, those that did exhibit levels of infiltration rarely had enough cells to investigate their functionality, within the sample size provided from the pathology department at CNMC. To build a stronger catalog of infiltration in different tumor types, immunohistochemistry staining can be preformed upon frozen tissue samples, however these samples will not serve useful for testing the functionality of the TIL within. Analysis for further lymphocyte markers such as Foxp3, CD25, CD44, CD45, CD69, along with granzyme B and Perforin, will also help elucidate the state of inhibition within each type of cancer, by revealing not only the levels of infiltration, but the activation and maturation status of TIL within. When enough freshly removed tissue presents itself, which also wields enough CTLs within, functional analysis can be further assessed via cytotoxicity and degranulation assays, and experiments to try to circumvent or overcome inhibition can be carried out using chemokines and bi-specific antibodies.

Provided here is a novel form of live tumor cell vaccine, in which tumor cells that are attenuated by targeting inhibition of RAP *in vivo*, induce a potent and specific immune response, capable of overcoming the WT form of cancer already developing within the host. The mechanism for induction of immune response however is not yet understood, and needs further investigation to understand and therefore apply to other forms of cancer.

A gene array of the Aggressive and Id2-KD forms of Neuro2a has been carried out, aiming to identify potential candidates of antigenicity and decreased immune evasion/suppression. Some of the most highly upregulated genes in both forms of Neuro2a expressed higher levels of Melanoma Antigen Gene (MAGE) than wild type (WT), though different subfamilies. However, it has been indicated that MAGE proteins are partially conserved in sequence across subfamilies. Furthermore, neuroblastoma is derived from the same neural crest stem cells as melanoma, indicating that while other Id proteins, specifically Id1 and Id3, may play a more prominent role in RAP for melanoma, targeting RAP in melanoma may be as effective in generating an immune response as it is in neuroblastoma. Regardless, identification of novel tumor specific or associated antigens in neuroblastoma can prove beneficial, and could lead to specific immunotherapy targeting methods such as CAR ACT development.

The generation of CAR bearing Tregs against VEGFR-2 presents a new approach for ACT in the treatment of immune evasive and suppressive cancers. While the methods for generation of CAR bearing Tregs has been established, and cytotoxicity of Tregs has been demonstrated *in vitro*, there are still several barriers that need to be overcome. While others have demonstrated the ability to induce production of high levels of granzyme B in Tregs *in vitro*, we were unable to do the same here. This may be due in part to minor differences in T cell stimulation, including differences in concentration with our v/v IL-2 supernatant, compared to the standardly measureable (IU) levels of IL-2 used by others in the field. Despite this complication, we have shown in rhabdomyosarcoma, that Tregs within the tumor mass do express high levels of granzyme B, consistent with work in other tumor models. This implicates that in an ACT model,

Tregs that express CAR molecules should be able to generate their own lytic molecules upon homing to the tumor site. While we have shown in a full splenic transduced population that CD4+ and CD8+ cells home to the tumor site, for Tregs specifically, this needs to be addressed in an adoptive transfer model, in which we had attempted to generate.. Unfortunately, our conditions for transduction require cells to be actively proliferating, and in our hands, the transduction process seemed to halt the proliferation of Tregs. This resulted in our inability to generate enough CAR-bearing Tregs for adoptive transfer. Work by others has shown that inhibitory cytokines within the TIM can induce the conversion of CD4+ T helper cells into Tregs (56). It may prove more efficient to generate CD4+ CAR-bearing cells for adoptive transfer, and induce their conversion to a regulatory phenotype at the tumor site, if the conversion phenomenon exists in our mouse models as well.

CHAPTER 8: BIBLIOGRAPHY

1. **Huang J, Brameshuber M, Zeng X, Xie J, Li QJ, Chien YH, Valitutti S, Davis MM.** 2013. A single peptide-major histocompatibility complex ligand triggers digital cytokine secretion in CD4(+) T cells. Immunity **39:**846-857.
2. **Irvine DJ, Purbhoo MA, Krogsgaard M, Davis MM.** 2002. Direct observation of ligand recognition by T cells. Nature **419:**845-849.
3. **Sykulev Y, Joo M, Vturina I, Tsomides TJ, Eisen HN.** 1996. Evidence that a single peptide-MHC complex on a target cell can elicit a cytolytic T cell response. Immunity **4:**565-571.
4. **Bour-Jordan H, Esensten JH, Martinez-Llordella M, Penaranda C, Stumpf M, Bluestone JA.** 2011. Intrinsic and extrinsic control of peripheral T-cell tolerance by costimulatory molecules of the CD28/ B7 family. Immunological reviews **241:**180-205.
5. **Tuosto L, Acuto O.** 1998. CD28 affects the earliest signaling events generated by TCR engagement. European journal of immunology **28:**2131-2142.
6. **Viola A, Schroeder S, Sakakibara Y, Lanzavecchia A.** 1999. T lymphocyte costimulation mediated by reorganization of membrane microdomains. Science **283:**680-682.
7. **Malek TR, Castro I.** 2010. Interleukin-2 receptor signaling: at the interface between tolerance and immunity. Immunity **33:**153-165.
8. **Gaffen SL, Liu KD.** 2004. Overview of interleukin-2 function, production and clinical applications. Cytokine **28:**109-123.

9. **Chakraborty AK, Weiss A.** 2014. Insights into the initiation of TCR signaling. Nature immunology **15:**798-807.

10. **Billadeau DD.** 2010. T cell activation at the immunological synapse: vesicles emerge for LATer signaling. Science signaling **3:**pe16.

11. **Mustelin T, Rahmouni S, Bottini N, Alonso A.** 2003. Role of protein tyrosine phosphatases in T cell activation. Immunological reviews **191:**139-147.

12. **Malissen B, Gregoire C, Malissen M, Roncagalli R.** 2014. Integrative biology of T cell activation. Nature immunology **15:**790-797.

13. **Manicassamy S, Sadim M, Ye RD, Sun Z.** 2006. Differential roles of PKC-theta in the regulation of intracellular calcium concentration in primary T cells. Journal of molecular biology **355:**347-359.

14. **Zhao Y, Lei M, Wang Z, Qiao G, Yang T, Zhang J.** 2014. TCR-induced, PKC-theta-mediated NF-kappaB activation is regulated by a caspase-8-caspase-9-caspase-3 cascade. Biochemical and biophysical research communications **450:**526-531.

15. **Lowin B, Hahne M, Mattmann C, Tschopp J.** 1994. Cytolytic T-cell cytotoxicity is mediated through perforin and Fas lytic pathways. Nature **370:**650-652.

16. **Russell JH, Ley TJ.** 2002. Lymphocyte-mediated cytotoxicity. Annual review of immunology **20:**323-370.

17. **Stinchcombe JC, Griffiths GM.** 2007. Secretory mechanisms in cell-mediated cytotoxicity. Annual review of cell and developmental biology **23:**495-517.

18. **Kupfer A, Dennert G.** 1984. Reorientation of the microtubule-organizing center and the Golgi apparatus in cloned cytotoxic lymphocytes triggered by binding to lysable target cells. Journal of immunology **133:**2762-2766.

19. **Yannelli JR, Sullivan JA, Mandell GL, Engelhard VH.** 1986. Reorientation and fusion of cytotoxic T lymphocyte granules after interaction with target cells as determined by high resolution cinemicrography. Journal of immunology **136:**377-382.

20. **Quann EJ, Merino E, Furuta T, Huse M.** 2009. Localized diacylglycerol drives the polarization of the microtubule-organizing center in T cells. Nature immunology **10:**627-635.

21. **Ma JS, Haydar TF, Radoja S.** 2008. Protein kinase C delta localizes to secretory lysosomes in CD8+ CTL and directly mediates TCR signals leading to granule exocytosis-mediated cytotoxicity. Journal of immunology **181:**4716-4722.

22. **Ma JS, Monu N, Shen DT, Mecklenbrauker I, Radoja N, Haydar TF, Leitges M, Frey AB, Vukmanovic S, Radoja S.** 2007. Protein kinase Cdelta regulates antigen receptor-induced lytic granule polarization in mouse CD8+ CTL. Journal of immunology **178:**7814-7821.

23. **Barry M, Bleackley RC.** 2002. Cytotoxic T lymphocytes: all roads lead to death. Nature reviews. Immunology **2:**401-409.

24. **Chavez-Galan L, Arenas-Del Angel MC, Zenteno E, Chavez R, Lascurain R.** 2009. Cell death mechanisms induced by cytotoxic lymphocytes. Cellular & molecular immunology **6:**15-25.

25. **Meiraz A, Garber OG, Harari S, Hassin D, Berke G.** 2009. Switch from perforin-expressing to perforin-deficient CD8(+) T cells accounts for two distinct types of effector cytotoxic T lymphocytes in vivo. Immunology **128:**69-82.

26. **Monu N, Frey AB.** 2007. Suppression of proximal T cell receptor signaling and lytic function in CD8+ tumor-infiltrating T cells. Cancer research **67:**11447-11454.

27. **Radoja S, Saio M, Schaer D, Koneru M, Vukmanovic S, Frey AB.** 2001. CD8(+) tumor-infiltrating T cells are deficient in perforin-mediated cytolytic activity due to defective microtubule-organizing center mobilization and lytic granule exocytosis. Journal of immunology **167:**5042-5051.

28. **Rosenberg SA, Spiess P, Lafreniere R.** 1986. A new approach to the adoptive immunotherapy of cancer with tumor-infiltrating lymphocytes. Science **233:**1318-1321.

29. **Rosenberg SA, Yannelli JR, Yang JC, Topalian SL, Schwartzentruber DJ, Weber JS, Parkinson DR, Seipp CA, Einhorn JH, White DE.** 1994. Treatment of patients with metastatic melanoma with autologous tumor-infiltrating lymphocytes and interleukin 2. Journal of the National Cancer Institute **86:**1159-1166.

30. **Topalian SL, Muul LM, Solomon D, Rosenberg SA.** 1987. Expansion of human tumor infiltrating lymphocytes for use in immunotherapy trials. J Immunol Methods **102:**127-141.

31. **Belldegrun A, Muul LM, Rosenberg SA.** 1988. Interleukin 2 expanded tumor-infiltrating lymphocytes in human renal cell cancer: isolation, characterization, and antitumor activity. Cancer research **48:**206-214.

32. **Spiess PJ, Yang JC, Rosenberg SA.** 1987. In vivo antitumor activity of tumor-infiltrating lymphocytes expanded in recombinant interleukin-2. Journal of the National Cancer Institute **79:**1067-1075.

33. **Kawakami Y, Rosenberg SA, Lotze MT.** 1988. Interleukin 4 promotes the growth of tumor-infiltrating lymphocytes cytotoxic for human autologous melanoma. The Journal of experimental medicine **168:**2183-2191.

34. **Rosenberg SA, Schwarz SL, Spiess PJ.** 1988. Combination immunotherapy for cancer: synergistic antitumor interactions of interleukin-2, alfa interferon, and tumor-infiltrating lymphocytes. Journal of the National Cancer Institute **80:**1393-1397.

35. **Phan GQ, Rosenberg SA.** 2013. Adoptive cell transfer for patients with metastatic melanoma: the potential and promise of cancer immunotherapy. Cancer control : journal of the Moffitt Cancer Center **20:**289-297.

36. **Stroncek DF, Berger C, Cheever MA, Childs RW, Dudley ME, Flynn P, Gattinoni L, Heath JR, Kalos M, Marincola FM, Miller JS, Mostoslavsky G, Powell DJ, Jr., Rao M, Restifo NP, Rosenberg SA, O'Shea J, Melief CJ.** 2012. New directions in cellular therapy of cancer: a summary of the summit on cellular therapy for cancer. Journal of translational medicine **10:**48.

37. **Kochenderfer JN, Rosenberg SA.** 2013. Treating B-cell cancer with T cells expressing anti-CD19 chimeric antigen receptors. Nature reviews. Clinical oncology **10:**267-276.

38. **Robbins PF, Morgan RA, Feldman SA, Yang JC, Sherry RM, Dudley ME, Wunderlich JR, Nahvi AV, Helman LJ, Mackall CL, Kammula US, Hughes MS, Restifo NP, Raffeld M, Lee CC, Levy CL, Li YF, El-Gamil M, Schwarz SL, Laurencot C, Rosenberg SA.** 2011. Tumor regression in patients with metastatic synovial cell sarcoma and melanoma using genetically engineered lymphocytes reactive with NY-ESO-1. Journal of clinical oncology : official journal of the American Society of Clinical Oncology **29:**917-924.

39. **Rabinovich GA, Gabrilovich D, Sotomayor EM.** 2007. Immunosuppressive strategies that are mediated by tumor cells. Annual review of immunology **25:**267-296.

40. **Lorenzi S, Forloni M, Cifaldi L, Antonucci C, Citti A, Boldrini R, Pezzullo M, Castellano A, Russo V, van der Bruggen P, Giacomini P, Locatelli F, Fruci D.** 2012. IRF1 and NF-kB restore MHC class I-restricted tumor antigen processing and presentation to cytotoxic T cells in aggressive neuroblastoma. PloS one **7:**e46928.

41. **Leen AM, Rooney CM, Foster AE.** 2007. Improving T cell therapy for cancer. Annual review of immunology **25:**243-265.

42. **Leach DR, Krummel MF, Allison JP.** 1996. Enhancement of antitumor immunity by CTLA-4 blockade. Science **271:**1734-1736.

43. **Vazquez-Cintron EJ, Monu NR, Burns JC, Blum R, Chen G, Lopez P, Ma J, Radoja S, Frey AB.** 2012. Protocadherin-18 is a novel differentiation marker and an inhibitory signaling receptor for CD8+ effector memory T cells. PloS one **7:**e36101.

44. **Biollaz G, Bernasconi L, Cretton C, Puntener U, Frei K, Fontana A, Suter T.** 2009. Site-specific anti-tumor immunity: differences in DC function, TGF-beta production and numbers of intratumoral Foxp3+ Treg. European journal of immunology **39:**1323-1333.

45. **Torres-Poveda K, Bahena-Roman M, Madrid-Gonzalez C, Burguete-Garcia AI, Bermudez-Morales VH, Peralta-Zaragoza O, Madrid-Marina V.** 2014. Role of IL-10 and TGF-beta1 in local immunosuppression in HPV-associated cervical neoplasia. World journal of clinical oncology **5:**753-763.

46. **Massague J, Blain SW, Lo RS.** 2000. TGFbeta signaling in growth control, cancer, and heritable disorders. Cell **103:**295-309.

47. **Yoshimura A, Wakabayashi Y, Mori T.** 2010. Cellular and molecular basis for the regulation of inflammation by TGF-beta. Journal of biochemistry **147:**781-792.

48. **Curiel TJ, Coukos G, Zou L, Alvarez X, Cheng P, Mottram P, Evdemon-Hogan M, Conejo-Garcia JR, Zhang L, Burow M, Zhu Y, Wei S, Kryczek I, Daniel B, Gordon A, Myers L, Lackner A, Disis ML, Knutson KL, Chen L, Zou W.** 2004. Specific recruitment of regulatory T cells in ovarian carcinoma fosters immune privilege and predicts reduced survival. Nature medicine **10:**942-949.

49. **Darrasse-Jeze G, Bergot AS, Durgeau A, Billiard F, Salomon BL, Cohen JL, Bellier B, Podsypanina K, Klatzmann D.** 2009. Tumor emergence is sensed by self-specific CD44hi memory Tregs that create a dominant tolerogenic environment for tumors in mice. The Journal of clinical investigation **119:**2648-2662.

50. **Ondondo B, Jones E, Godkin A, Gallimore A.** 2013. Home sweet home: the tumor microenvironment as a haven for regulatory T cells. Frontiers in immunology **4:**197.

51. **Vignali DA, Collison LW, Workman CJ.** 2008. How regulatory T cells work. Nature reviews. Immunology **8:**523-532.

52. **Tran DQ.** 2012. TGF-beta: the sword, the wand, and the shield of FOXP3(+) regulatory T cells. Journal of molecular cell biology **4:**29-37.

53. **von Boehmer H.** 2005. Mechanisms of suppression by suppressor T cells. Nature immunology **6:**338-344.

54. **Chen Q, Kim YC, Laurence A, Punkosdy GA, Shevach EM.** 2011. IL-2 controls the stability of Foxp3 expression in TGF-beta-induced Foxp3+ T cells in vivo. Journal of immunology **186:**6329-6337.

55. **Ishida Y, Agata Y, Shibahara K, Honjo T.** 1992. Induced expression of PD-1, a novel member of the immunoglobulin gene superfamily, upon programmed cell death. The EMBO journal **11:**3887-3895.

56. **Zou W.** 2006. Regulatory T cells, tumour immunity and immunotherapy. Nature reviews. Immunology **6:**295-307.

57. **Boissonnas A, Scholer-Dahirel A, Simon-Blancal V, Pace L, Valet F, Kissenpfennig A, Sparwasser T, Malissen B, Fetler L, Amigorena S.** 2010. Foxp3+ T cells induce perforin-dependent dendritic cell death in tumor-draining lymph nodes. Immunity **32:**266-278.

58. **Cao X, Cai SF, Fehniger TA, Song J, Collins LI, Piwnica-Worms DR, Ley TJ.** 2007. Granzyme B and perforin are important for regulatory T cell-mediated suppression of tumor clearance. Immunity **27:**635-646.

59. **Gondek DC, Lu LF, Quezada SA, Sakaguchi S, Noelle RJ.** 2005. Cutting edge: contact-mediated suppression by CD4+CD25+ regulatory cells involves a granzyme B-dependent, perforin-independent mechanism. Journal of immunology **174:**1783-1786.

60. **Grossman WJ, Verbsky JW, Barchet W, Colonna M, Atkinson JP, Ley TJ.** 2004. Human T regulatory cells can use the perforin pathway to cause autologous target cell death. Immunity **21:**589-601.

61. **Zhao DM, Thornton AM, DiPaolo RJ, Shevach EM.** 2006. Activated CD4+CD25+ T cells selectively kill B lymphocytes. Blood **107:**3925-3932.

62. **Lindqvist CA, Christiansson LH, Thorn I, Mangsbo S, Paul-Wetterberg G, Sundstrom C, Totterman TH, Simonsson B, Enblad G, Frisk P, Olsson-Stromberg U, Loskog AS.** 2011. Both CD4+ FoxP3+ and CD4+ FoxP3- T cells from patients with B-cell malignancy express cytolytic markers and kill autologous leukaemic B cells in vitro. Immunology **133:**296-306.

63. **Azzi J, Skartsis N, Mounayar M, Magee CN, Batal I, Ting C, Moore R, Riella LV, Ohori S, Abdoli R, Smith B, Fiorina P, Heathcote D, Bakhos T, Ashton-**

Rickardt PG, Abdi R. 2013. Serine protease inhibitor 6 plays a critical role in protecting murine granzyme B-producing regulatory T cells. Journal of immunology **191:**2319-2327.

64. **Qin FX.** 2009. Dynamic behavior and function of Foxp3+ regulatory T cells in tumor bearing host. Cellular & molecular immunology **6:**3-13.

65. **Pores-Fernando AT, Bauer RA, Wurth GA, Zweifach A.** 2005. Exocytic responses of single leukaemic human cytotoxic T lymphocytes stimulated by agents that bypass the T cell receptor. The Journal of physiology **567:**891-903.

66. **Wurth GA, Zweifach A.** 2002. Evidence that cytosolic calcium increases are not sufficient to stimulate phospholipid scrambling in human T-lymphocytes. The Biochemical journal **362:**701-708.

67. **Hadida F, Vieillard V, Autran B, Clark-Lewis I, Baggiolini M, Debre P.** 1998. HIV-specific T cell cytotoxicity mediated by RANTES via the chemokine receptor CCR3. The Journal of experimental medicine **188:**609-614.

68. **Taub DD, Ortaldo JR, Turcovski-Corrales SM, Key ML, Longo DL, Murphy WJ.** 1996. Beta chemokines costimulate lymphocyte cytolysis, proliferation, and lymphokine production. Journal of leukocyte biology **59:**81-89.

69. **Moore PA, Zhang W, Rainey GJ, Burke S, Li H, Huang L, Gorlatov S, Veri MC, Aggarwal S, Yang Y, Shah K, Jin L, Zhang S, He L, Zhang T, Ciccarone V, Koenig S, Bonvini E, Johnson S.** 2011. Application of dual affinity retargeting molecules to achieve optimal redirected T-cell killing of B-cell lymphoma. Blood **117:**4542-4551.

70. **Galluzzi L, Vacchelli E, Fridman WH, Galon J, Sautes-Fridman C, Tartour E, Zucman-Rossi J, Zitvogel L, Kroemer G.** 2012. Trial Watch: Monoclonal antibodies in cancer therapy. Oncoimmunology **1:**28-37.

71. **May C, Sapra P, Gerber HP.** 2012. Advances in bispecific biotherapeutics for the treatment of cancer. Biochemical pharmacology **84:**1105-1112.

72. **Scott AM, Wolchok JD, Old LJ.** 2012. Antibody therapy of cancer. Nature reviews. Cancer **12:**278-287.

73. **Topalian SL, Weiner GJ, Pardoll DM.** 2011. Cancer immunotherapy comes of age. Journal of clinical oncology : official journal of the American Society of Clinical Oncology **29:**4828-4836.

74. **Cruz CR, Micklethwaite KP, Savoldo B, Ramos CA, Lam S, Ku S, Diouf O, Liu E, Barrett AJ, Ito S, Shpall EJ, Krance RA, Kamble RT, Carrum G, Hosing CM, Gee AP, Mei Z, Grilley BJ, Heslop HE, Rooney CM, Brenner MK, Bollard CM, Dotti G.** 2013. Infusion of donor-derived CD19-redirected virus-specific T cells for B-cell malignancies relapsed after allogeneic stem cell transplant: a phase 1 study. Blood **122:**2965-2973.

75. **Curran KJ, Pegram HJ, Brentjens RJ.** 2012. Chimeric antigen receptors for T cell immunotherapy: current understanding and future directions. The journal of gene medicine **14:**405-415.

76. **Gross G, Waks T, Eshhar Z.** 1989. Expression of immunoglobulin-T-cell receptor chimeric molecules as functional receptors with antibody-type specificity. Proceedings of the National Academy of Sciences of the United States of America **86:**10024-10028.

77. **Kalos M, Levine BL, Porter DL, Katz S, Grupp SA, Bagg A, June CH.** 2011. T cells with chimeric antigen receptors have potent antitumor effects and can establish memory in patients with advanced leukemia. Science translational medicine **3:**95ra73.

78. **Lee JC, Hayman E, Pegram HJ, Santos E, Heller G, Sadelain M, Brentjens R.** 2011. In vivo inhibition of human CD19-targeted effector T cells by natural T regulatory cells in a xenotransplant murine model of B cell malignancy. Cancer research **71:**2871-2881.

79. **Zhang T, Wu MR, Sentman CL.** 2012. An NKp30-based chimeric antigen receptor promotes T cell effector functions and antitumor efficacy in vivo. Journal of immunology **189:**2290-2299.

80. **Hombach AA, Heiders J, Foppe M, Chmielewski M, Abken H.** 2014. OX40 costimulation by a chimeric antigen receptor abrogates CD28 and IL-2 induced IL-10 secretion by redirected CD4+T cells. OncoImmunology **1:**458-466.

81. **Chinnasamy D, Yu Z, Theoret MR, Zhao Y, Shrimali RK, Morgan RA, Feldman SA, Restifo NP, Rosenberg SA.** 2010. Gene therapy using genetically modified lymphocytes targeting VEGFR-2 inhibits the growth of vascularized syngenic tumors in mice. The Journal of clinical investigation **120:**3953-3968.

82. **Restifo NP, Dudley ME, Rosenberg SA.** 2012. Adoptive immunotherapy for cancer: harnessing the T cell response. Nature reviews. Immunology **12:**269-281.

83. **Patel NS, Muneer A, Blick C, Arya M, Harris AL.** 2009. Targeting vascular endothelial growth factor in renal cell carcinoma. Tumour biology : the journal of

the International Society for Oncodevelopmental Biology and Medicine **30:**292-299.

84. **Maliar A, Servais C, Waks T, Chmielewski M, Lavy R, Altevogt P, Abken H, Eshhar Z.** 2012. Redirected T cells that target pancreatic adenocarcinoma antigens eliminate tumors and metastases in mice. Gastroenterology **143:**1375-1384 e1371-1375.

85. **Spear P, Barber A, Rynda-Apple A, Sentman CL.** 2012. Chimeric antigen receptor T cells shape myeloid cell function within the tumor microenvironment through IFN-gamma and GM-CSF. Journal of immunology **188:**6389-6398.

86. **Galluzzi L, Vacchelli E, Eggermont A, Fridman WH, Galon J, Sautes-Fridman C, Tartour E, Zitvogel L, Kroemer G.** 2012. Trial Watch: Adoptive cell transfer immunotherapy. Oncoimmunology **1:**306-315.

87. **Kershaw MH, Westwood JA, Slaney CY, Darcy PK.** 2014. Clinical application of genetically modified T cells in cancer therapy. Clinical & translational immunology **3:**e16.

88. **Torikai H, Reik A, Liu PQ, Zhou Y, Zhang L, Maiti S, Huls H, Miller JC, Kebriaei P, Rabinovitch B, Lee DA, Champlin RE, Bonini C, Naldini L, Rebar EJ, Gregory PD, Holmes MC, Cooper LJ.** 2012. A foundation for universal T-cell based immunotherapy: T cells engineered to express a CD19-specific chimeric-antigen-receptor and eliminate expression of endogenous TCR. Blood **119:**5697-5705.

89. **Grupp SA.** 2014. Advances in T-cell therapy for ALL. Best practice & research. Clinical haematology **27:**222-228.

90. **Scheuermann RH, Racila E.** 1995. CD19 antigen in leukemia and lymphoma diagnosis and immunotherapy. Leukemia & lymphoma **18:**385-397.

91. **Wrzesinski C, Paulos CM, Kaiser A, Muranski P, Palmer DC, Gattinoni L, Yu Z, Rosenberg SA, Restifo NP.** 2010. Increased intensity lymphodepletion enhances tumor treatment efficacy of adoptively transferred tumor-specific T cells. Journal of immunotherapy **33:**1-7.

92. **Sadelain M, Brentjens R, Riviere I.** 2013. The basic principles of chimeric antigen receptor design. Cancer discovery **3:**388-398.

93. **Brentjens RJ, Riviere I, Park JH, Davila ML, Wang X, Stefanski J, Taylor C, Yeh R, Bartido S, Borquez-Ojeda O, Olszewska M, Bernal Y, Pegram H, Przybylowski M, Hollyman D, Usachenko Y, Pirraglia D, Hosey J, Santos E, Halton E, Maslak P, Scheinberg D, Jurcic J, Heaney M, Heller G, Frattini M, Sadelain M.** 2011. Safety and persistence of adoptively transferred autologous CD19-targeted T cells in patients with relapsed or chemotherapy refractory B-cell leukemias. Blood **118:**4817-4828.

94. **Kochenderfer JN, Dudley ME, Feldman SA, Wilson WH, Spaner DE, Maric I, Stetler-Stevenson M, Phan GQ, Hughes MS, Sherry RM, Yang JC, Kammula US, Devillier L, Carpenter R, Nathan DA, Morgan RA, Laurencot C, Rosenberg SA.** 2012. B-cell depletion and remissions of malignancy along with cytokine-associated toxicity in a clinical trial of anti-CD19 chimeric-antigen-receptor-transduced T cells. Blood **119:**2709-2720.

95. **Hudecek M, Schmitt TM, Baskar S, Lupo-Stanghellini MT, Nishida T, Yamamoto TN, Bleakley M, Turtle CJ, Chang WC, Greisman HA, Wood B,**

Maloney DG, Jensen MC, Rader C, Riddell SR. 2010. The B-cell tumor-associated antigen ROR1 can be targeted with T cells modified to express a ROR1-specific chimeric antigen receptor. Blood **116:**4532-4541.

96. **Lamers CH, Sleijfer S, Vulto AG, Kruit WH, Kliffen M, Debets R, Gratama JW, Stoter G, Oosterwijk E.** 2006. Treatment of metastatic renal cell carcinoma with autologous T-lymphocytes genetically retargeted against carbonic anhydrase IX: first clinical experience. Journal of clinical oncology : official journal of the American Society of Clinical Oncology **24:**e20-22.

97. **Morgan RA, Yang JC, Kitano M, Dudley ME, Laurencot CM, Rosenberg SA.** 2010. Case report of a serious adverse event following the administration of T cells transduced with a chimeric antigen receptor recognizing ERBB2. Molecular therapy : the journal of the American Society of Gene Therapy **18:**843-851.

98. **Seaman BJ, Guardiani EA, Brewer CC, Zalewski CK, King KA, Rudy S, Van Waes C, Morgan RA, Dudley ME, Yang JC, Rosenberg SA, Kim HJ.** 2012. Audiovestibular dysfunction associated with adoptive cell immunotherapy for melanoma. Otolaryngology--head and neck surgery : official journal of American Academy of Otolaryngology-Head and Neck Surgery **147:**744-749.

99. **Silver DA, Pellicer I, Fair WR, Heston WD, Cordon-Cardo C.** 1997. Prostate-specific membrane antigen expression in normal and malignant human tissues. Clinical cancer research : an official journal of the American Association for Cancer Research **3:**81-85.

100. **Di Stasi A, Tey SK, Dotti G, Fujita Y, Kennedy-Nasser A, Martinez C, Straathof K, Liu E, Durett AG, Grilley B, Liu H, Cruz CR, Savoldo B, Gee AP, Schindler J, Krance RA, Heslop HE, Spencer DM, Rooney CM, Brenner MK.** 2011. Inducible apoptosis as a safety switch for adoptive cell therapy. The New England journal of medicine **365:**1673-1683.

101. **Lupo-Stanghellini MT, Provasi E, Bondanza A, Ciceri F, Bordignon C, Bonini C.** 2010. Clinical impact of suicide gene therapy in allogeneic hematopoietic stem cell transplantation. Human gene therapy **21:**241-250.

102. **Sadelain M.** 2011. Eliminating cells gone astray. The New England journal of medicine **365:**1735-1737.

103. **Brentjens RJ, Davila ML, Riviere I, Park J, Wang X, Cowell LG, Bartido S, Stefanski J, Taylor C, Olszewska M, Borquez-Ojeda O, Qu J, Wasielewska T, He Q, Bernal Y, Rijo IV, Hedvat C, Kobos R, Curran K, Steinherz P, Jurcic J, Rosenblat T, Maslak P, Frattini M, Sadelain M.** 2013. CD19-targeted T cells rapidly induce molecular remissions in adults with chemotherapy-refractory acute lymphoblastic leukemia. Science translational medicine **5:**177ra138.

104. **Pizzo PA, Poplack DG.** 2011. Principles and practice of pediatric oncology, p. online resource (xx, 1531 p., 6th ed ed. Wolters Kluwer Health/Lippincott Williams & Wilkins,, Philadelphia.

105. **Adida C, Berrebi D, Peuchmaur M, Reyes-Mugica M, Altieri DC.** 1998. Anti-apoptosis gene, survivin, and prognosis of neuroblastoma. Lancet **351:**882-883.

106. **Islam A, Kageyama H, Hashizume K, Kaneko Y, Nakagawara A.** 2000. Role of survivin, whose gene is mapped to 17q25, in human neuroblastoma and identification of a novel dominant-negative isoform, survivin-beta/2B. Medical and pediatric oncology **35:**550-553.

107. **Paydas S, Tanriverdi K, Yavuz S, Disel U, Sahin B, Burgut R.** 2003. Survivin and aven: two distinct antiapoptotic signals in acute leukemias. Annals of oncology : official journal of the European Society for Medical Oncology / ESMO **14:**1045-1050.

108. **Coughlin CM, Vance BA, Grupp SA, Vonderheide RH.** 2004. RNA-transfected CD40-activated B cells induce functional T-cell responses against viral and tumor antigen targets: implications for pediatric immunotherapy. Blood **103:**2046-2054.

109. **Uyttenhove C, Godfraind C, Lethe B, Amar-Costesec A, Renauld JC, Gajewski TF, Duffour MT, Warnier G, Boon T, Van den Eynde BJ.** 1997. The expression of mouse gene P1A in testis does not prevent safe induction of cytolytic T cells against a P1A-encoded tumor antigen. International journal of cancer. Journal international du cancer **70:**349-356.

110. **Cheung IY, Barber D, Cheung NK.** 1998. Detection of microscopic neuroblastoma in marrow by histology, immunocytology, and reverse transcription-PCR of multiple molecular markers. Clinical cancer research : an official journal of the American Association for Cancer Research **4:**2801-2805.

111. **Cheung IY, Cheung NK.** 1997. Molecular detection of GAGE expression in peripheral blood and bone marrow: utility as a tumor marker for neuroblastoma.

Clinical cancer research : an official journal of the American Association for Cancer Research **3:**821-826.

112. **Scarcella DL, Chow CW, Gonzales MF, Economou C, Brasseur F, Ashley DM.** 1999. Expression of MAGE and GAGE in high-grade brain tumors: a potential target for specific immunotherapy and diagnostic markers. Clinical cancer research : an official journal of the American Association for Cancer Research **5:**335-341.

113. **Van den Eynde BJ, van der Bruggen P.** 1997. T cell defined tumor antigens. Current opinion in immunology **9:**684-693.

114. **Corrias MV, Scaruffi P, Occhino M, De Bernardi B, Tonini GP, Pistoia V.** 1996. Expression of MAGE-1, MAGE-3 and MART-1 genes in neuroblastoma. International journal of cancer. Journal international du cancer **69:**403-407.

115. **Ishida H, Matsumura T, Salgaller ML, Ohmizono Y, Kadono Y, Sawada T.** 1996. MAGE-1 and MAGE-3 or -6 expression in neuroblastoma-related pediatric solid tumors. International journal of cancer. Journal international du cancer **69:**375-380.

116. **Soling A, Schurr P, Berthold F.** 1999. Expression and clinical relevance of NY-ESO-1, MAGE-1 and MAGE-3 in neuroblastoma. Anticancer research **19:**2205-2209.

117. **Baets J, Pals P, Bergmans B, Foncke E, Smets K, Hauman H, Vanderwegen L, Cras P.** 2006. Opsoclonus-myoclonus syndrome: a clinicopathological confrontation. Acta neurologica Belgica **106:**142-146.

118. **Rudnick E, Khakoo Y, Antunes NL, Seeger RC, Brodeur GM, Shimada H, Gerbing RB, Stram DO, Matthay KK.** 2001. Opsoclonus-myoclonus-ataxia syndrome in neuroblastoma: clinical outcome and antineuronal antibodies-a report from the Children's Cancer Group Study. Medical and pediatric oncology **36:**612-622.

119. **Antunes NL, Khakoo Y, Matthay KK, Seeger RC, Stram DO, Gerstner E, Abrey LE, Dalmau J.** 2000. Antineuronal antibodies in patients with neuroblastoma and paraneoplastic opsoclonus-myoclonus. Journal of pediatric hematology/oncology **22:**315-320.

120. **Cooper R, Khakoo Y, Matthay KK, Lukens JN, Seeger RC, Stram DO, Gerbing RB, Nakagawa A, Shimada H.** 2001. Opsoclonus-myoclonus-ataxia syndrome in neuroblastoma: histopathologic features-a report from the Children's Cancer Group. Medical and pediatric oncology **36:**623-629.

121. **Gambini C, Conte M, Bernini G, Angelini P, Pession A, Paolucci P, Donfrancesco A, Veneselli E, Mazzocco K, Tonini GP, Raffaghello L, Dominici C, Morando A, Negri F, Favre A, De Bernardi B, Pistoia V.** 2003. Neuroblastic tumors associated with opsoclonus-myoclonus syndrome: histological, immunohistochemical and molecular features of 15 Italian cases. Virchows Archiv : an international journal of pathology **442:**555-562.

122. **Gurney JG, Ross JA, Wall DA, Bleyer WA, Severson RK, Robison LL.** 1997. Infant cancer in the U.S.: histology-specific incidence and trends, 1973 to 1992. Journal of pediatric hematology/oncology **19:**428-432.

123. **Brodeur GM.** 2003. Neuroblastoma: biological insights into a clinical enigma. Nature reviews. Cancer **3:**203-216.

124. **Chakrabarti L, Abou-Antoun T, Vukmanovic S, Sandler AD.** 2012. Reversible adaptive plasticity: a mechanism for neuroblastoma cell heterogeneity and chemo-resistance. Frontiers in oncology **2:**82.

125. **Chakrabarti L, Wang BD, Lee NH, Sandler AD.** 2013. A mechanism linking Id2-TGFbeta crosstalk to reversible adaptive plasticity in neuroblastoma. PloS one **8:**e83521.

126. **Mosse YP, Laudenslager M, Khazi D, Carlisle AJ, Winter CL, Rappaport E, Maris JM.** 2004. Germline PHOX2B mutation in hereditary neuroblastoma. American journal of human genetics **75:**727-730.

127. **Mosse YP, Laudenslager M, Longo L, Cole KA, Wood A, Attiyeh EF, Laquaglia MJ, Sennett R, Lynch JE, Perri P, Laureys G, Speleman F, Kim C, Hou C, Hakonarson H, Torkamani A, Schork NJ, Brodeur GM, Tonini GP, Rappaport E, Devoto M, Maris JM.** 2008. Identification of ALK as a major familial neuroblastoma predisposition gene. Nature **455:**930-935.

128. **Trochet D, Bourdeaut F, Janoueix-Lerosey I, Deville A, de Pontual L, Schleiermacher G, Coze C, Philip N, Frebourg T, Munnich A, Lyonnet S, Delattre O, Amiel J.** 2004. Germline mutations of the paired-like homeobox 2B (PHOX2B) gene in neuroblastoma. American journal of human genetics **74:**761-764.

129. **Kaneko Y, Kanda N, Maseki N, Nakachi K, Takeda T, Okabe I, Sakurai M.** 1990. Current urinary mass screening for catecholamine metabolites at 6 months

of age may be detecting only a small portion of high-risk neuroblastomas: a chromosome and N-myc amplification study. Journal of clinical oncology : official journal of the American Society of Clinical Oncology **8:**2005-2013.

130. **Kaneko Y, Kanda N, Maseki N, Sakurai M, Tsuchida Y, Takeda T, Okabe I, Sakurai M.** 1987. Different karyotypic patterns in early and advanced stage neuroblastomas. Cancer research **47:**311-318.

131. **Maris JM.** 2010. Recent advances in neuroblastoma. The New England journal of medicine **362:**2202-2211.

132. **Cheung NK, Kushner BH, Yeh SJ, Larson SM.** 1994. 3F8 monoclonal antibody treatment of patients with stage IV neuroblastoma: a phase II study. Progress in clinical and biological research **385:**319-328.

133. **Cheung NV, Heller G.** 1991. Chemotherapy dose intensity correlates strongly with response, median survival, and median progression-free survival in metastatic neuroblastoma. Journal of clinical oncology : official journal of the American Society of Clinical Oncology **9:**1050-1058.

134. **Kushner BH, LaQuaglia MP, Bonilla MA, Lindsley K, Rosenfield N, Yeh S, Eddy J, Gerald WL, Heller G, Cheung NK.** 1994. Highly effective induction therapy for stage 4 neuroblastoma in children over 1 year of age. Journal of clinical oncology : official journal of the American Society of Clinical Oncology **12:**2607-2613.

135. **Pearson AD, Pinkerton CR, Lewis IJ, Imeson J, Ellershaw C, Machin D, European Neuroblastoma Study G, Children's C, Leukaemia G.** 2008. High-

dose rapid and standard induction chemotherapy for patients aged over 1 year with stage 4 neuroblastoma: a randomised trial. The Lancet. Oncology **9:**247-256.

136. **Creighton CJ, Chang JC, Rosen JM.** 2010. Epithelial-mesenchymal transition (EMT) in tumor-initiating cells and its clinical implications in breast cancer. Journal of mammary gland biology and neoplasia **15:**253-260.

137. **Creighton CJ, Li X, Landis M, Dixon JM, Neumeister VM, Sjolund A, Rimm DL, Wong H, Rodriguez A, Herschkowitz JI, Fan C, Zhang X, He X, Pavlick A, Gutierrez MC, Renshaw L, Larionov AA, Faratian D, Hilsenbeck SG, Perou CM, Lewis MT, Rosen JM, Chang JC.** 2009. Residual breast cancers after conventional therapy display mesenchymal as well as tumor-initiating features. Proceedings of the National Academy of Sciences of the United States of America **106:**13820-13825.

138. **Thiery JP, Sleeman JP.** 2006. Complex networks orchestrate epithelial-mesenchymal transitions. Nature reviews. Molecular cell biology **7:**131-142.

139. **Marusyk A, Polyak K.** 2010. Tumor heterogeneity: causes and consequences. Biochimica et biophysica acta **1805:**105-117.

140. **Lonardo E, Hermann PC, Heeschen C.** 2010. Pancreatic cancer stem cells - update and future perspectives. Molecular oncology **4:**431-442.

141. **O'Brien CA, Kreso A, Jamieson CH.** 2010. Cancer stem cells and self-renewal. Clinical cancer research : an official journal of the American Association for Cancer Research **16:**3113-3120.

142. **Soroceanu L, Murase R, Limbad C, Singer E, Allison J, Adrados I, Kawamura R, Pakdel A, Fukuyo Y, Nguyen D, Khan S, Arauz R, Yount GL,**

Moore DH, Desprez PY, McAllister SD. 2013. Id-1 is a key transcriptional regulator of glioblastoma aggressiveness and a novel therapeutic target. Cancer research **73:**1559-1569.

143. **Bonavia R, Inda MM, Cavenee WK, Furnari FB.** 2011. Heterogeneity maintenance in glioblastoma: a social network. Cancer research **71:**4055-4060.

144. **Hoek KS, Eichhoff OM, Schlegel NC, Dobbeling U, Kobert N, Schaerer L, Hemmi S, Dummer R.** 2008. In vivo switching of human melanoma cells between proliferative and invasive states. Cancer research **68:**650-656.

145. **Jiang Y, Boije M, Westermark B, Uhrbom L.** 2011. PDGF-B Can sustain self-renewal and tumorigenicity of experimental glioma-derived cancer-initiating cells by preventing oligodendrocyte differentiation. Neoplasia **13:**492-503.

146. **Roesch A, Fukunaga-Kalabis M, Schmidt EC, Zabierowski SE, Brafford PA, Vultur A, Basu D, Gimotty P, Vogt T, Herlyn M.** 2010. A temporarily distinct subpopulation of slow-cycling melanoma cells is required for continuous tumor growth. Cell **141:**583-594.

147. **Saio M, Radoja S, Marino M, Frey AB.** 2001. Tumor-infiltrating macrophages induce apoptosis in activated CD8(+) T cells by a mechanism requiring cell contact and mediated by both the cell-associated form of TNF and nitric oxide. Journal of immunology **167:**5583-5593.

148. **Radoja S, Saio M, Frey AB.** 2001. CD8+ tumor-infiltrating lymphocytes are primed for Fas-mediated activation-induced cell death but are not apoptotic in situ. Journal of immunology **166:**6074-6083.

149. **Shen DT, Ma JS, Mather J, Vukmanovic S, Radoja S.** 2006. Activation of primary T lymphocytes results in lysosome development and polarized granule exocytosis in CD4+ and CD8+ subsets, whereas expression of lytic molecules confers cytotoxicity to CD8+ T cells. Journal of leukocyte biology **80:**827-837.

150. **Chan KS, Espinosa I, Chao M, Wong D, Ailles L, Diehn M, Gill H, Presti J, Jr., Chang HY, van de Rijn M, Shortliffe L, Weissman IL.** 2009. Identification, molecular characterization, clinical prognosis, and therapeutic targeting of human bladder tumor-initiating cells. Proceedings of the National Academy of Sciences of the United States of America **106:**14016-14021.

151. **Kerkar SP, Sanchez-Perez L, Yang S, Borman ZA, Muranski P, Ji Y, Chinnasamy D, Kaiser AD, Hinrichs CS, Klebanoff CA, Scott CD, Gattinoni L, Morgan RA, Rosenberg SA, Restifo NP.** 2011. Genetic engineering of murine CD8+ and CD4+ T cells for preclinical adoptive immunotherapy studies. Journal of immunotherapy **34:**343-352.

152. **Gajewski TF, Meng Y, Harlin H.** 2006. Immune suppression in the tumor microenvironment. Journal of immunotherapy **29:**233-240.

153. **Reid GS, Shan X, Coughlin CM, Lassoued W, Pawel BR, Wexler LH, Thiele CJ, Tsokos M, Pinkus JL, Pinkus GS, Grupp SA, Vonderheide RH.** 2009. Interferon-gamma-dependent infiltration of human T cells into neuroblastoma tumors in vivo. Clinical cancer research : an official journal of the American Association for Cancer Research **15:**6602-6608.

154. **Bronte V, Kasic T, Gri G, Gallana K, Borsellino G, Marigo I, Battistini L, Iafrate M, Prayer-Galetti T, Pagano F, Viola A.** 2005. Boosting antitumor

responses of T lymphocytes infiltrating human prostate cancers. The Journal of experimental medicine **201:**1257-1268.

155. **Tseng D, Volkmer JP, Willingham SB, Contreras-Trujillo H, Fathman JW, Fernhoff NB, Seita J, Inlay MA, Weiskopf K, Miyanishi M, Weissman IL.** 2013. Anti-CD47 antibody-mediated phagocytosis of cancer by macrophages primes an effective antitumor T-cell response. Proceedings of the National Academy of Sciences of the United States of America **110:**11103-11108.

156. **Grosso JF, Jure-Kunkel MN.** 2013. CTLA-4 blockade in tumor models: an overview of preclinical and translational research. Cancer immunity **13:**5.

157. **Harshman LC, Drake CG, Wargo JA, Sharma P, Bhardwaj N.** 2014. Cancer Immunotherapy Highlights from the 2014 ASCO Meeting. Cancer immunology research **2:**714-719.

158. **Hodi FS, O'Day SJ, McDermott DF, Weber RW, Sosman JA, Haanen JB, Gonzalez R, Robert C, Schadendorf D, Hassel JC, Akerley W, van den Eertwegh AJ, Lutzky J, Lorigan P, Vaubel JM, Linette GP, Hogg D, Ottensmeier CH, Lebbe C, Peschel C, Quirt I, Clark JI, Wolchok JD, Weber JS, Tian J, Yellin MJ, Nichol GM, Hoos A, Urba WJ.** 2010. Improved survival with ipilimumab in patients with metastatic melanoma. The New England journal of medicine **363:**711-723.

159. **Makkouk A, Weiner GJ.** 2015. Cancer Immunotherapy and Breaking Immune Tolerance: New Approaches to an Old Challenge. Cancer research **75:**5-10.

160. **Pardoll DM.** 2012. The blockade of immune checkpoints in cancer immunotherapy. Nature reviews. Cancer **12:**252-264.

161. **Zhang L, Kerkar SP, Yu Z, Zheng Z, Yang S, Restifo NP, Rosenberg SA, Morgan RA.** 2011. Improving adoptive T cell therapy by targeting and controlling IL-12 expression to the tumor environment. Molecular therapy : the journal of the American Society of Gene Therapy **19:**751-759.

162. **Maturu P, Overwijk WW, Hicks J, Ekmekcioglu S, Grimm EA, Huff V.** 2014. Characterization of the inflammatory microenvironment and identification of potential therapeutic targets in wilms tumors. Translational oncology **7:**484-492.

163. **Mikami T, Hada T, Chosa N, Ishisaki A, Mizuki H, Takeda Y.** 2013. Expression of Wilms' tumor 1 (WT1) in oral squamous cell carcinoma. Journal of oral pathology & medicine : official publication of the International Association of Oral Pathologists and the American Academy of Oral Pathology **42:**133-139.

164. **Schittenhelm J, Mittelbronn M, Nguyen TD, Meyermann R, Beschorner R.** 2008. WT1 expression distinguishes astrocytic tumor cells from normal and reactive astrocytes. Brain pathology **18:**344-353.

165. **Vermeij R, de Bock GH, Leffers N, Ten Hoor KA, Schulze U, Hollema H, van der Burg SH, van der Zee AG, Daemen T, Nijman HW.** 2011. Tumor-infiltrating cytotoxic T lymphocytes as independent prognostic factor in epithelial ovarian cancer with wilms tumor protein 1 overexpression. Journal of immunotherapy **34:**516-523.

166. **Raffensperger J.** 2015. Max Wilms and his tumor. Journal of pediatric surgery **50:**356-359.

167. **Alter A, Duddy M, Hebert S, Biernacki K, Prat A, Antel JP, Yong VW, Nuttall RK, Pennington CJ, Edwards DR, Bar-Or A.** 2003. Determinants of human B cell migration across brain endothelial cells. Journal of immunology **170:**4497-4505.

168. **Becher B, Prat A, Antel JP.** 2000. Brain-immune connection: immuno-regulatory properties of CNS-resident cells. Glia **29:**293-304.

169. **Prendergast CT, Anderton SM.** 2009. Immune cell entry to central nervous system--current understanding and prospective therapeutic targets. Endocrine, metabolic & immune disorders drug targets **9:**315-327.

170. **Sehgal A, Berger MS.** 2000. Basic concepts of immunology and neuroimmunology. Neurosurgical focus **9:**e1.

171. **Yang I, Han SJ, Kaur G, Crane C, Parsa AT.** 2010. The role of microglia in central nervous system immunity and glioma immunology. Journal of clinical neuroscience : official journal of the Neurosurgical Society of Australasia **17:**6-10.

172. **Donson AM, Birks DK, Schittone SA, Kleinschmidt-DeMasters BK, Sun DY, Hemenway MF, Handler MH, Waziri AE, Wang M, Foreman NK.** 2012. Increased immune gene expression and immune cell infiltration in high-grade astrocytoma distinguish long-term from short-term survivors. Journal of immunology **189:**1920-1927.

173. **Kmiecik J, Poli A, Brons NH, Waha A, Eide GE, Enger PO, Zimmer J, Chekenya M.** 2013. Elevated CD3+ and CD8+ tumor-infiltrating immune cells correlate with prolonged survival in glioblastoma patients despite integrated

immunosuppressive mechanisms in the tumor microenvironment and at the systemic level. Journal of neuroimmunology **264:**71-83.

174. **Altman AJ, Baehner RL.** 1976. Favorable prognosis for survival in children with coincident opso-myoclonus and neuroblastoma. Cancer **37:**846-852.

175. **Koh PS, Raffensperger JG, Berry S, Larsen MB, Johnstone HS, Chou P, Luck SR, Hammer M, Cohn SL.** 1994. Long-term outcome in children with opsoclonus-myoclonus and ataxia and coincident neuroblastoma. The Journal of pediatrics **125:**712-716.

176. **Russo C, Cohn SL, Petruzzi MJ, de Alarcon PA.** 1997. Long-term neurologic outcome in children with opsoclonus-myoclonus associated with neuroblastoma: a report from the Pediatric Oncology Group. Medical and pediatric oncology **28:**284-288.

177. **Carlson LM, De Geer A, Sveinbjornsson B, Orrego A, Martinsson T, Kogner P, Levitskaya J.** 2013. The microenvironment of human neuroblastoma supports the activation of tumor-associated T lymphocytes. Oncoimmunology **2:**e23618.

178. **Deschoolmeester V, Baay M, Van Marck E, Weyler J, Vermeulen P, Lardon F, Vermorken JB.** 2010. Tumor infiltrating lymphocytes: an intriguing player in the survival of colorectal cancer patients. BMC immunology **11:**19.

179. **Zhang L, Conejo-Garcia JR, Katsaros D, Gimotty PA, Massobrio M, Regnani G, Makrigiannakis A, Gray H, Schlienger K, Liebman MN, Rubin SC, Coukos G.** 2003. Intratumoral T cells, recurrence, and survival in epithelial ovarian cancer. The New England journal of medicine **348:**203-213.

180. **Mellman I, Coukos G, Dranoff G.** 2011. Cancer immunotherapy comes of age. Nature **480:**480-489.

181. **Chiang CL, Kandalaft LE, Coukos G.** 2011. Adjuvants for enhancing the immunogenicity of whole tumor cell vaccines. International reviews of immunology **30:**150-182.

182. **Browning MJ.** 2013. Antigen presenting cell/ tumor cell fusion vaccines for cancer immunotherapy. Human vaccines & immunotherapeutics **9:**1545-1548.

183. **Perrella A, D'Antonio A, Sbreglia C, Sorrentino P, Conca P, Atripaldi L, Conti P, Perrella O.** 2014. CD4+/CD25+ T cells suppress autologous CD4+/CD25- lymphocytes and secrete granzyme B during acute and chronic hepatitis C. Pathogens and disease **72:**124-130.

184. **Loffredo-Verde E, Abdel-Aziz I, Albrecht J, El-Guindy N, Yacob M, Solieman A, Protzer U, Busch DH, Layland LE, Prazeres da Costa CU.** 2015. Schistosome infection aggravates HCV-related liver disease and induces changes in the regulatory T-cell phenotype. Parasite immunology **37:**97-104.

185. **Asnagli H, Martire D, Belmonte N, Quentin J, Bastian H, Boucard-Jourdin M, Fall PB, Mausset-Bonnefont AL, Mantello-Moreau A, Rouquier S, Marchetti I, Jorgensen C, Foussat A, Louis-Plence P.** 2014. Type 1 regulatory T cells specific for collagen type II as an efficient cell-based therapy in arthritis. Arthritis research & therapy **16:**R115.

186. **Su Y, Jevnikar AM, Huang X, Lian D, Zhang Z.** 2014. Spi6 protects alloreactive CD4(+) but not CD8 (+) memory T cell from granzyme B attack by double-negative T regulatory cell. American journal of transplantation : official

journal of the American Society of Transplantation and the American Society of Transplant Surgeons **14:**580-593.

187. **Fransson M, Piras E, Burman J, Nilsson B, Essand M, Lu B, Harris RA, Magnusson PU, Brittebo E, Loskog AS.** 2012. CAR/FoxP3-engineered T regulatory cells target the CNS and suppress EAE upon intranasal delivery. Journal of neuroinflammation **9:**112.

188. **Warth SC, Heissmeyer V.** 2013. Adenoviral transduction of naive CD4 T cells to study Treg differentiation. Journal of visualized experiments : JoVE.

189. **Makrigiannis AP, Hoskin DW.** 1997. Inhibition of CTL induction by rapamycin: IL-2 rescues granzyme B and perforin expression but only partially restores cytotoxic activity. Journal of immunology **159:**4700-4707.